WCAP-10999-NP-A

WESTINGHOUSE CLASS 3

A DESCRIPTION OF THE NUCLEAR DESIGN AND ANALYSIS PROGRAMS FOR BOILING WATER REACTORS

THIS IS THE NON-PROPRIETARY VERSION OF THE NRC-ACCEPTED REPORT VERSION OF WCAP-10106

UNITED STATES
NUCLEAR REGULATORY COMMISSION
WASHINGTON, D. C. 20555

September 3, 1985

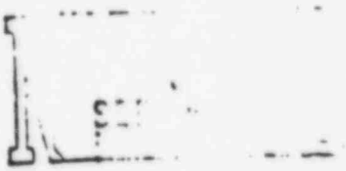

Nuclear Safety Department

Mr. E. P. Rahe, Jr., Manager
Nuclear Safety Department
Westinghouse Electric Corporation
Box 355
Pittsburgh, Pennsylvania 15230

Dear Mr. Rahe:

SUBJECT: ACCEPTANCE FOR REFERENCING OF LICENSING TOPICAL REPORT WCAP-10106 "A DESCRIPTION OF THE NUCLEAR DESIGN AND ANALYSIS PROGRAMS FOR BOILING WATER REACTORS"

We have completed our review of the subject topical report submitted by the Westinghouse Electric Corporation (Westinghouse) by letter dated June 23, 1982. We find the report to be acceptable for referencing in license applications to the extent specified and under the limitations delineated in the report and the associated NRC evaluation, which is enclosed. The evaluation defines the basis for acceptance of the report.

We do not intend to repeat our review of the matters described in the report and found acceptable when the report appears as a reference in license applications, except to assure that the material presented is applicable to the specific plant involved. Our acceptance applies only to the matters described in the report.

In accordance with procedures established in NUREG-0390, it is requested that Westinghouse publish accepted versions of this report, proprietary and non-proprietary, within three months of receipt of this letter. The accepted versions shall incorporate this letter and the enclosed evaluation between the title page and the abstract. The accepted versions shall include an -A (designating accepted) following the report identification symbol.

Should our criteria or regulations change such that our conclusions as to the acceptability of the report are invalidated, Westinghouse and/or the applicants referencing the topical report will be expected to revise and resubmit their respective documentation, or submit justification for the continued effective applicability of the topical report without revision of their respective documentation.

Sincerely,

Cecil O. Thomas

SEP 13 1985

Cecil O. Thomas, Chief
Standardization and Special
Projects Branch
Division of Licensing

Enclosure:
As stated

8509170257

ENCLOSURE

EVALUATION OF WESTINGHOUSE NUCLEAR DESIGN AND ANALYSIS PROGRAMS FOR BOILING WATER REACTORS-WCAP 10106 (TACS 48566)

1. Summary of Report

This report describes the calculational models used by Westinghouse for the nuclear design and analysis of Boiling Water Reactor (BWR) cores. The computer codes used in these calculational models were originally developed and used by ASEA-ATOM, Vasteras, Sweden and were obtained by Westinghouse under a licensee agreement with ASEA-ATOM. A detailed description of the two major codes in the nuclear design system, PHOENIX and POLCA, is presented in the report as well as descriptive overviews of the auxiliary codes. The design system is composed of the following computer codes:

PHOENIX- A two-dimensional, multi-group transport theory code used to calculate the lattice physics constants of fuel assemblies.

POLCA- A modified one-group nodal code used for the three-dimensional simulation of the nuclear and thermal-hydraulic conditions of BWR cores.

FOBUS- A Monte Carlo transport theory code used for the generation of burnable absorber neutron cross sections.

PHOEBE- A library processing code used to construct a nuclear cross section data library.

PHIPO- A linking code used to generate input for POLCA from PHOENIX output.

ANALOAD- A fuel shuffling optimization code used to generate core fuel loading patterns.

POREF- A fuel shuffling code which performs manual refueling and lays out the geometry of the refueled core.

STROD- A code used for preliminary analysis of shutdown margin.

BAREST- A code used to determine the residual burnable absorber reactivity in each fuel assembly at the end of cycle.

2. Summary of Evaluation

We have reviewed the information presented with regard to calculational methods and assumptions. The comparisons of calculations and experiment, which is a major justification made by Westinghouse for the adequacy and accuracy of the BWR analysis methodology, is being reviewed separately. A companion report, WCAP-10841, "Qualification of the PHOENIX/POLCA Nuclear Design and Analysis Programs for Boiling Water Reactors", dated June 1985 provides the relevant benchmark results.

The PHOENIX lattice physics code is used by Westinghouse for the nuclear design and analysis of BWRs. The code was developed by ASEA-ATOM for the calculation of lattice physics constants for fuel assemblies typical of those encountered in both BWR and PWR designs. Constants generated by PHOENIX are used in the three-dimensional POLCA code which simulates the neutronic and thermal-hydraulic conditions in typical BWR cores.

The code computes neutron spectra and two-group assembly averaged cross sections via a two-step procedure: 1) A 25-group nodal solution for the assembly which retains the spatial heterogeneities (based on transmission probabilities and response fluxes), followed by 2) a discrete ordinates (S_4) transport solution in up to 12-groups for the partially homogenized assembly. Burnable absorbers are treated by a perturbation technique which makes use of a Monte Carlo calculation for the absorber and its surrounding lattice environment. Branch calculations are automatically performed as functions of burnup for void,

Doppler and control rod insertions. POLCA is Westinghouse's coupled 3-D neutronics/thermal-hydraulic core simulator code intended for nuclear design and analysis of BWRs. The neutronics in POLCA utilize a modified, coarse mesh, one-group diffusion theory model. Two-group macroscopic cross-sections determined with the PHOENIX code are used and the core-reflector interface is represented with an albedo boundary condition. Feedback reactivity effects due to voids and Doppler broadening, as well as due to control rod insertion and xenon buildup are accounted for explicitly. The thermal-hydraulic model in POLCA is based on the CONDOR program, which did not form a part of the present review. The capabilities of the POLCA code include: xenon dynamics, depletion calculations, critical power ratio (CPR) and linear heat generation rate (LHGR) determination and simulation of in-core detector signals.

Based on the descriptions of the analytical methods used in the nuclear design, including those for predicting criticality, reactivity coefficients, burnup, and stability, we find the calculational models presented in WCAP-10106 acceptable.

3. Evaluation Procedure

We have reviewed the report within the guidelines provided by Section 4.3 of the Standard Review Plan. Included in our review was the description of the analytical methods used and the types of calculations which are to be performed for Westinghouse BWR licensing actions. The Core Performance Branch has been assisted by our consultants at Brookhaven National Laboratory under Technical Assistance contract FIN No. A-3407 in the review of this topical report.

4. Regulatory Position

We have reviewed the BWR methodology described in WCAP-10106 and find it to be acceptable for nuclear core design and analysis made by Westinghouse in

licensing actions including calculations of lattice physics constants and neutronic and thermal-hydraulic analyses in three dimensions. The qualification of the results obtained by the described procedures relative to measurement or other calculations is being reviewed separately and was not addressed in this review.

WCAP-10106

THIS IS THE NON-PRORIETARY VERSION OF WCAP-10106-P-A WHICH IS IDENTIFIED AS WCAP-10999-NP-A

A DESCRIPTION OF THE

NUCLEAR DESIGN AND ANALYSIS

PROGRAMS FOR BOILING WATER REACTORS

A.J. Harris
L.T. Mayhue
C.M. Mildrum

June 1982

APPROVED: P. K. Doshi
P.K. Dosni, Manager
BWR Fuel Engineering

APPROVED: R.F. Barry
R.F. Barry, Manager
BWR Fuel

APPROVED: P.W. Kramer
P.W. Kramer, Manager
NFD Engineering Department

WESTINGHOUSE ELECTRIC CORPORATION
Nuclear Fuel Division
P.O. Box 3912
Pittsburgh, Pennsylvania 15230

TABLE OF CONTENTS

TABLE OF CONTENTS (CON'T)

LIST OF FIGURES

LIST OF TABLES

ABSTRACT

The calculational models for the nuclear design and analysis of boiling water reactors in use at Westinghouse are described in this report. The calculational models described in this report form the basis of the computer programs described herein. Included in this report is a description of the lattice physics code PHOENIX, the core simulator code POLCA, and the smaller auxiliary codes which support PHOENIX and POLCA.

ACKNOWLEDGEMENTS

The computational models and computer programs described in this document were developed by ASEA-ATOM, Vasteras, Sweden and were obtained by Westinghouse Electric Corporation under a licensee agreement with ASEA-ATOM.

The authors wish to acknowledge B.H. Alsop and T.R. Freeman for their technical contributions. Appreciation is expressed to J.F. Connelley and M.M. Baker for providing programming assistance. The authors also wish to acknowledge D.W. Drawbaugh for consultation on the computational models.

1.0 INTRODUCTION

The objective of this topical report is to provide a detailed description of the calculational models in use at Westinghouse for the nuclear design and analysis of boiling water reactor (BWR) cores. These calculational models exist as a system of computer codes developed and used by ASEA-ATOM for the nuclear design and analysis of boiling water reactors. Contained in this report is a description of the computer codes comprising this comprehensive nuclear design system which provides the full range of nuclear design and analysis capabilities required.

The two major computer codes of the nuclear design system are the PHOENIX and POLCA codes. The PHOENIX code is a two-dimensional, multi-group transport theory code which is used to calculate the lattice physics constants of fuel assemblies having varying complexities. The POLCA code is a modified one-group nodal code that is used for the three dimensional simulation of the nuclear and thermal-hydraulic conditions typical of boiling water reactor cores.

In addition to providing an in-depth description of the PHOENIX and POLCA codes, this report contains a descriptive overview of the auxiliary codes which support PHOENIX and POLCA. The main auxiliary codes which are used along with PHOENIX and POLCA are FOBUS, PHOEBE, PHIPO, POREF, ANALOAD, STROD and BAREST. The FOBUS and PHOEBE codes are used in preparing the nuclear data library for PHOENIX. The PHIPO code serves as the linking code between PHOENIX and POLCA. The POREF and ANALOAD codes allow both automatic and user-selected fuel shuffling and fuel loading pattern optimization between refuelings. STROD provides a preliminary analysis of shutdown margin to scope out the most limiting conditions (e.g., time in cycle and most reactive region of core) for the shutdown margin. BAREST calculates the residual burnable absorber reactivity in each fuel assembly at the end of cycle.

Figure 1-1 shows the complete computer code system and the relationship between the individual computer codes.

The intended scope of these computational models are for the following nuclear design and analysis applications:

- Power distribution calculations
- Thermal-hydraulic calculations
- Fuel management calculations
- Control rod worth and shutdown margin calculations
- Generation of control rod pattern sequences
- Thermal margin evaluations
- Reactivity coefficients and kinetics parameters
- In-core detector simulation
- Core reactivity calculations
- Generation of process computer constants
- Generation of power to flow control lines
- Simulation of normal operation power maneuvers including load follow

In summary, the intended scope of use for these computational models includes all design-related calculations required for the nuclear design and analysis of boiling water reactors.

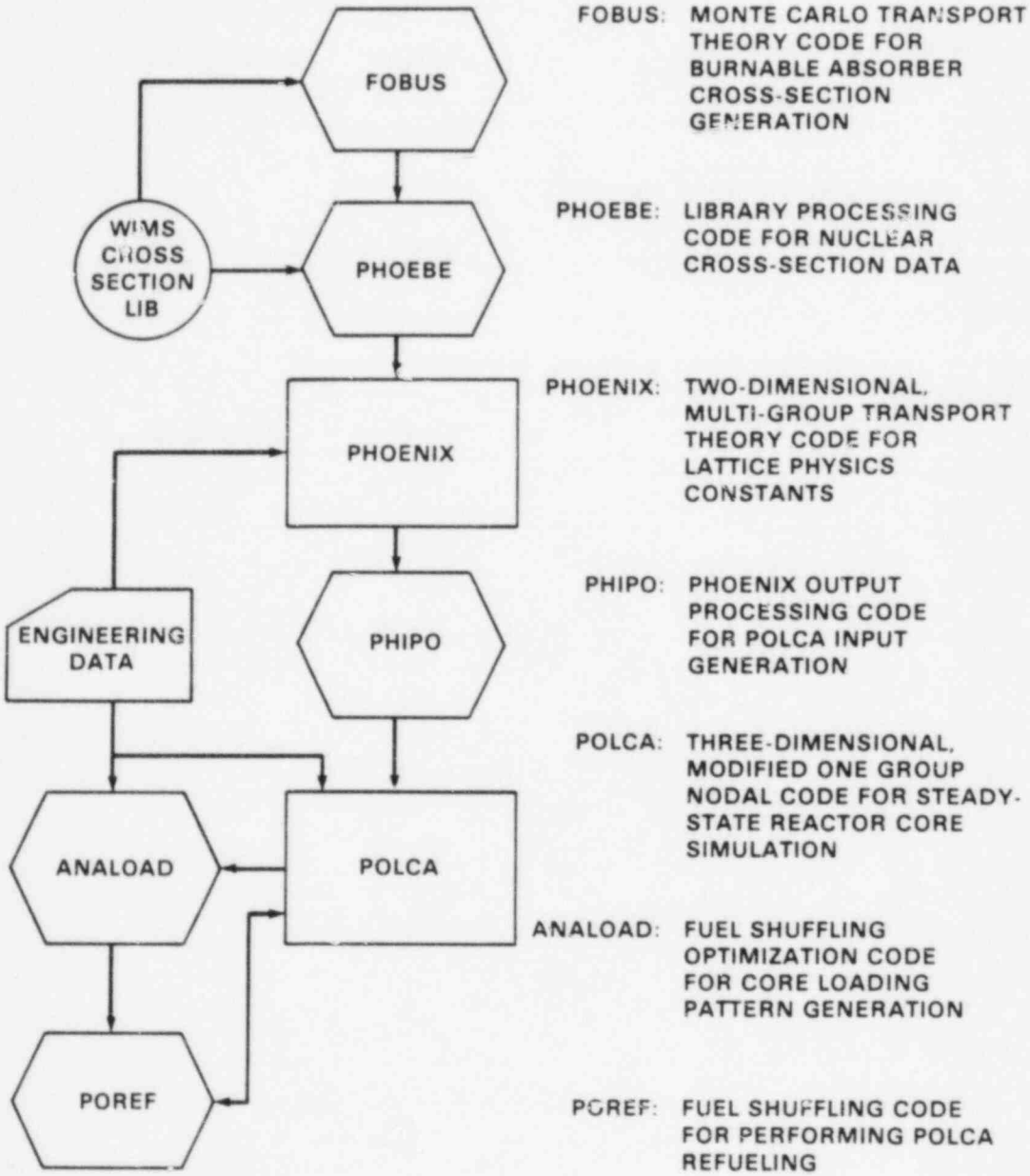

FIGURE 1-1: Westinghouse Computer Code System for Nuclear Design and Analysis of BWR Cores

2.0 PHOENIX CODE

2.1 OVERVIEW OF PHOENIX CODE

The PHOENIX computer program is a two-dimensional, multi-group transport theory code that is used for the calculation of lattice physics constants. These calculations include the calculation of reactivities, neutron spectrum and spatial power distribution, the depletion of the nuclides and burnable absorbers, fission product concentrations and the computation of neutron cross-sections. The PHOENIX code can simulate both PWR and BWR fuel assemblies. The program is capable of explicitly modelling BWR cruciform control blades containing cylindrical absorber elements, PWR cluster control rods, water gaps, burnable absorber rods or boron curtains as well as burnable absorbers integral with the fuel. Water rods, and objects present in the water gaps such as the neutron detector can also be modelled. Figures 2-1 and 2-2 illustrate typical BWR and PWR assemblies which can be modelled by PHOENIX. Figure 2-3 illustrates the pin cell types modelled by PHOENIX.

The PHOENIX code uses a 25 energy group nuclear data library which is based on a modified version of the British WIMS[1] 69 energy group library. In addition to the cross-section data, the PHOENIX library includes resonance parameters and standard tables of gadolinium microscopic cross-sections as a function of gadolinium enrichment and fraction depleted.

The solution for the detailed spatial flux and energy distribution is divided into two major steps in PHOENIX, separating to some degree the calculation for the spatial flux distribution and neutron spectrum. In the first step, a two-dimensional 25 energy group nodal solution is obtained which couples the fuel rods (pellet, clad, surrounding water), channel, water gaps and gap objects (i.e., control rod, detector, boron curtains). PHOENIX uses a method based on transmission probabilities and response fluxes which preserves the heterogeneity of the pin cells and objects. The nodal solution provides an accurate and detailed local

flux distribution which is then used to homogenize the pin cells, channel, water gaps and objects. Group collapsing to a group structure consisting of from 6 to 12 energy groups is also done.

The second step in the solution process solves for the flux distribution using a standard S_4 discrete ordinates transport theory calculation. This step is performed by a PHOENIX sub-program, SFINX,[14] and is based on the group-collapsed and homogenized cross-sections obtained from the first step in the PHOENIX flux solution. The transport fluxes are used to normalize the detailed 25 group nodal fluxes. These transport-corrected nodal fluxes are then used in PHOENIX to compute the reaction rates and power distribution and to deplete the nuclides and burnable absorbers.

The PHOENIX program provides all of the physics constants required by the three-dimensional core simulator POLCA program. The principal outputs of PHOENIX are: fuel assembly reactivity and isotopics; pin-by-pin power and flux distributions; two-group homogenized cross-sections; and, tables of detector response, local peaking factor and C-factor as a function of exposure, void fraction, burnup-averaged void and control rod presence. The C-factors are used in the minimum critical power ratio, MCPR, correlation to take into account the effect of the internal bundle power distribution on the MCPR calculated. Control rod cross-sections and xenon microscopic cross-sections are also computed.

The PHOENIX code is very user-oriented from both the input and output standpoints. The code is extremely flexible and accepts any number of energy groups, resonance absorbers, exposure steps, branch calculations, etc. Automated features have been incorporated to facilitate the calculation of void, Doppler, and control rod branches. A restart capability is also available. All output is written in an easily retrievable manner on magnetic tape for later use by PHIPO and other programs.

The subsequent sections to this report describe the methods used in PHOENIX, and Figure 2-4 gives a calculational flow diagram of the code.

2.2 NUCLEAR CROSS-SECTIONS

The nuclear data library used by PHOENIX contains microscopic cross-section data based on a 25 energy group structure. This 25 group library is largely a condensed version of the 69 group British WIMS library, adopted for use by PHOENIX and expanded with fission product data and burnable absorber tables. The 25 energy group structure contains 4 fast groups, 5 resonance groups, and 16 thermal groups. The group energy boundaries are given in Table 2-1 and 2-2 for the 69 and 25 group structures, respectively.

Each nuclide contained on the library is identified by a nuclide identification number. The microscopic cross-section set for each nuclide includes absorption, fission, nu-fission, transport, scattering matrix, fission spectrum, yields, decay constants, energy per fission, and delayed neutron fractions. For nuclides with temperature-dependent cross-sections, sets of cross-section data are available for several temperatures. Table 2-3 provides a listing of all materials available in the PHOENIX cross-section library. The temperature that the cross-sections correspond to is also indicated.

The WIMS cross section library takes its name from its use in the lattice code WIMS (Winfrith Improved Multi-group Scheme). Reference 1 describes the source of the thermal scattering matrices for H, D, graphite, O and Be. Thermal absorption cross sections for non 1/v absorbers such as U-235 and Pu-239 are based on the United Kingdom Atomic Energy Agency (UKAEA) Nuclear Data File[2]. In the fast and resonance regions, the cross sections are also derived from the UKAEA Nuclear Data File except for U-238, U-235, and Pu-239 for which the resonance data were obtained by use of the SRR code[3]. This use of the SRR code is described in sections 11 and 12 of Reference 1. The nuclides which PHOENIX treats as resonance absorber nuclides are: U-235, U-236, U-238, and Pu-239. The lethargy weighted transfer cross sections are obtained from the UKAEA Nuclear Data File by using the GALAXY code, also described and referenced in Reference 1. Two lumped pseudo fission products are used in PHOENIX to simulate those

fission products not individually traced. The first, NSFP, includes the non-saturating fission products while the second, SSFP, combines the slowly saturating fission products.

Reference 4 gives an extensive comparison between calculations using the WIMS library and experimental Winfrith[4] and Brookhaven[5] (BNL) lattices. In Reference 4 the effects of decreasing the U-238 epithermal capture cross-section and also of increasing the epithermal U-235 fission to give a capture to fission ratio, α, of 0.5 is discussed. These altered U-238 and U-235 cross sections are the basis for the recommended U-238 and U-235 cross sections used in the 69 and 25 group PHOENIX library. The revision of the U-235 cross-section takes into account the measurements of De Saussure reported in 1965 and 1966[6] who obtained a capture to fission ratio α of 0.51. In Reference 4, Figure 4 for the Winfrith lattices and Figures 5 and 6 for the BNL data compare k_{eff} calculated with and without the modified U-235 and U-238 cross-sections. The results clearly show the improved agreement with experiment using the modified cross-sections. These changes and additions are given in Reference 7. In addition the treatment of the fission products is explained in this reference.

2.3 RESONANCE CALCULATIONS

The treatment of resolved resonances uses an equivalence relation to relate the resonance integral for the heterogeneous fuel geometry of the bundle to an equivalent homogeneous (i.e.; single fuel pin) resonance integral. This relation makes use of several standard reciprocity expressions. A two-term rational approximation is also used which leads to a relation where the resonance integral for the heterogenous fuel bundle geometry can be expressed as the equivalent sum of two homogeneous resonance integrals. The equivalent homogeneous resonance integrals are then evaluated from tabulations found in the WIMS nuclear cross-section library. This section describes the equivalence relation upon which the PHOENIX resonance integral treatment is based.

The equivalence relation, developed by Stamm'ler, Blomstrand, and Weiss (Reference 9) makes use of the following standard reciprocity relations:

$$P_{bi} = \frac{4V_i \Sigma_i}{S_b} P_{ib} \qquad (2.3\text{-}1)$$

$$S_F t_{FB} = S_b t_{BF} \qquad (2.3\text{-}2)$$

$$V_i \Sigma_i P_{ij} = V_j \Sigma_j P_{ji} \qquad (2.3\text{-}3)$$

where the following definitions are used:

P_{bi}-is the probability that a neutron which enters the fuel cell isotropically through cell boundary S_b will collide in region i.

P_{ib}-is the probability that a neutron born in region i will reach the fuel cell boundary S_b without collision.

t_{FB} - is the probability that a neutron which leaves the fuel surface S_F will reach the cell boundary S_b.

t_{BF} - is the probability that a neutron which enters isotropically through S_b will reach S_F. V_i, V_j, Σ_i and Σ_j denote the volumes and total macroscopic cross-sections of region i and j, where regions i and j are arbitrary.

Using the reciprocity relations in Eq. (2.3-1) - Eq. (2.3-3), the fuel collision probability for the heterogeneous fuel array geometry, P_{FF}, can be expressed as follows:

$$P_{FF} = P_{ff} + \frac{x\,(1 - P_{ff})^2}{x\,(1 - P_{ff}) + A + B} \qquad (2.3\text{-}4)$$

where P_{ff} denotes the collision probability in the fuel for an isolated fuel rod and x is the ratio of the fuel cross-section to the escape cross-section, i.e.

$$x = \frac{4V_F\,\Sigma_F}{S_F} = \frac{\Sigma_F}{\Sigma_e} \qquad (2.3\text{-}5)$$

$$\text{where } \Sigma_e = \frac{S_F}{4V_F}$$

The constant A is given by

$$A = \frac{S_b}{S_F\,t_{FB}^2}\left\{\sum_{j \neq F} P_{bj} + t_{BF}\,(1 - t_{FB})\right\} \qquad (2.3\text{-}6)$$

The constant B corrects for the reflection of neutrons back into the fuel cells due to the water gaps. The constant B is given by

$$B = \frac{S_b}{S_F\,t_{FB}^2}\left\{\frac{f\,(1 - G)}{1 - f(1 - G)}\right\} \qquad (2.3\text{-}7)$$

Where f is the fraction of neutrons leaving the cell boundary S_b which are reflected by the water gap and G is the first-flight reflection probability across the gap.

The fraction f is purely a geometrical quantity and is equal to the ratio of the outer surface area of the fuel array at the boundary of the bundle to the total surface area of all fuel cells. For an n x m array of fuel cells, for example, the fraction f is $\frac{(m + n)}{2nm}$. If there is no water gap present, i.e. an infinite array of fuel rods, then the constant B is equal to 0.0.

A rational approximation of the form $\sum_m \frac{b_m x}{x + a_m}$ for the collision probability P_{ff} of an isolated pin is required in order to transform the heterogeneous resonance integral into an equivalent homogeneous one. Usually, the rational approximation takes the form of a single term, $P_{ff} = \frac{x}{x + a}$, first proposed by Wigner (Reference 10) who chose a to be 1.0.

In the PHOENIX resonance treatment, a more accurate two-term rational approximation is used which is one proposed by Carlvik (Reference 11). Thus the fuel collision probability for an isolated pin, P_{ff}, is approximated as

$$P_{ff} = \frac{b_1 x}{x + a_1} + \frac{b_2 x}{x + a_2} \qquad (2.3\text{-}8)$$

where the a and b constants used are those proposed by Carlvik:
$a_1=2$; $a_2=3$; $b_1 = 2$; $b_2=-1$

When this rational approximation is inserted into Eq. (2.3-4), a two term rational approximation is also obtained for the collision probability P_{FF}, of the heterogeneous fuel bundle array which takes the form

$$P_{FF} = x\left[\frac{\beta}{x + \alpha_1} + \frac{1 - \beta}{x + \alpha_2}\right] \qquad (2.3\text{-}9)$$

$$\text{with } C' = \frac{[4A + 4B + 6]}{[A + B + 1]}$$

$$\alpha_{1,\,2} = \frac{(5C + 6) \mp \sqrt{C^2 + 36C + 36}}{2(C + 1)}$$

$$\beta = \frac{C' - \alpha_1}{\alpha_2 - \alpha_1}$$

$$C = A + B$$

The transmission probabilities P_{bj} and t_{FB}, as well as the water gap reflection probability G define the constants A and B, which in turn determine C, C', α_1, α_2 and β. These probabilities are determined as part of the nodal flux coupling calculation which is discussed in Section 2.6.

With the two-term rational approximation of Eq. (2.3-9), the resonance integral (RI) for the heterogeneous geometry is transformed into a linear combination of two homogeneous integrals, i.e.;

$$RI_{HETERO} = \beta\, RI_{HOMO}\,(\Sigma_{pot} + \Sigma_m + \Sigma_{e1}) + (1 - \beta)\, RI_{HOMO}\,(\Sigma_{pot} + \Sigma_m + \Sigma_{e2}) \qquad (2.3\text{-}10)$$

Thus, the evaluation of the resonance integral for the heterogeneous array of fuel rods in the assembly reduces to the interpolation of homogeneous resonance integral tabulations in the WIMS nuclear cross-section library as a function of $(\Sigma_{pot} + \Sigma_m + \Sigma_e)$.

Having determined the resonance integrals according to Eq. (2.3-10), the resonance group cross-sections are obtained next using methods which follow closely those of the WIMS code, reported by Askew et al (Reference 1) and improved by Fayers et al (Reference 4). The intermediate Resonance (IR) method of Goldstein and Cohen (Reference 8) is

used which approximates the energy spectrum of the flux at resonance energies as being given by the following expression:

$$\phi(\mu) = \frac{\Sigma_m + \lambda \Sigma_{pot}}{\Sigma_m + \Sigma_a + \lambda(\Sigma_s + \Sigma_{pot})} \qquad (2.3\text{-}11)$$

where λ lies in the range of $0 < \lambda < 1$. Σ_m denotes the scattering macroscopic cross-section of the admixed moderator in the fuel; Σ_a, Σ_s and Σ_{pot} denote the absorption, scattering and potential scattering cross-sections of the fuel, respectively. The lethargy is denoted by μ.

Interaction between different resonance absorbers, i.e.; the mutual self-shielding of resonances is accounted for. The removal cross-section is also corrected for the flux depression that still exists within a certain range of the fuel pins at resonance energies.

In summary, the resonance treatment used in PHOENIX provides an accurate method for generating multi-group constants in the resonance region. The treatment is applicable to both finite and infinite lattices for both PWR and BWR assemblies. The method correctly takes into account the effects of both the water rods, if present, and of the water gaps on the resonance integral. The resonance treatment closely follows that used in WIMS and is actually improved over WIMS in some areas.

2.4 DANCOFF CORRECTION

The Dancoff correction is defined as the factor by which the escape probability of an isolated pin is reduced due to the presence of adjacent fuel pins. When evaluating the Dancoff correction, the assumption is normally made that the fuel pins are "black" - that is that the fuel pin absorbs all neutrons incident on the pin. Thus as $\Sigma_F \to \infty$, the fuel absorption probability approaches 1.0. The absorption probability is related to the escape probability for an isolated pin by the following well-known reciprocity relation:

$$P_{abs} = \frac{4V_F \Sigma_F}{S_F} P_{esc} \qquad (2.4\text{-}1)$$

$$= x\,(1 - P_{ff})$$

where $x = \dfrac{4V_F \Sigma_F}{S_F}$ and $P_{esc} = 1 - P_{ff}$

Thus, when $\Sigma_F = \infty$, $P_{abs} = 1.0$ and $x\,(1 - P_{ff}) = 1.0$

Eq. 2.3-5 then reduces to

$$P_{FF} = P_{ff} + (1 - P_{ff}) \left[\frac{1}{1 + A + B}\right] \qquad (2.4\text{-}2)$$

Eq. (2.4-2) can be slightly re-arranged as follows

$$1 - P_{FF} = (1 - P_{ff}) \left[1 - \frac{1}{1 + A + B}\right] \qquad (2.4\text{-}3)$$

the term $\{1 - \frac{1}{1 + A + B}\}$ is thus recognized as the Dancoff correction C.

The Dancoff factor is dependent on the transmission probabilities t_{BF}, t_{FB}, P_{bj} and the water gap reflection probability, G. These probabilities are determined during the nodal flux solution which is described in Section 2.6.

2.5 BURNABLE ABSORBER TREATMENT

The burnable absorber cross-section tables used by PHOENIX consist of pin-homogenized 25 group microscopic cross-sections which are tabulated as a function of the burnable absorber fraction remaining. These tables are generated by a separate program, FOBUS, which is described in detail in Section 4.1. FOBUS is a two-dimensional (R, Z) Monte Carlo program that computes the reactivity change and absorber depletion with exposure for discrete or integral absorbers present in the fuel assembly. The integral burnable absorber design may be in the form of discs separated by one or more absorber-free fuel pellets or it may be homogeneously loaded over the entire fuel length.

To economize on the computations, a perturbation technique is used which makes use of the Monte Carlo computation only to solve for the flux perturbation introduced by tne presence of the absorber. A simpler flux calculation is made to solve for the detailed flux distribution for the unperturbed case of a regular infinite lattice of fuel rods where the absorber is absent. An option is available as well which permits the user to input the unperturbed detailed flux distribution (from PHOENIX) in FOBUS rather than having the program calculate it. This permits the user to force normalization of the FOBUS flux spectrum to the actual flux spectrum calculated by PHOENIX at the absorber location. For gadolinium, an option is available, in addition, to let FOBUS determine the time steps for the absorber depletion calculations using a built-in empirical relation.

In the case of gadolinium as the absorber material, FOBUS only depletes the odd-numbered Gd-155 and Gd-157 isotopes which are the dominant absorber nuclides. An empirical formula is used with POLCA to correct for the reactivity penalty of the even-numbered Gd-156 and Gd-158 isotopes. At each depletion step, the multigroup absorption cross-section is computed as well as the corresponding pin-averaged fraction of initial absorber loading remaining;

$$\text{fraction remaining} = \frac{(Gd^{155} + Gd^{157})\ \text{actual}}{(Gd^{155} + Gd^{157})\ \text{initial}}.$$

This data is processed by the library service code PHOEBE which appends the data to the cross-section library used by PHOENIX.

In summary, the burnable absorber treatment consists of using FOBUS to generate the multi-group microscopic cross-sections as a function of the absorber depletion and PHOENIX to generate the neutron spectrum and reaction rate of the burnable absorber. This method provides a very reliable and accurate method of predicting the absorber worth and depletion characteristics for a wide range of burnable absorbers, including gadolinium. The absorber treatment is equally applicable to both discrete and integral absorbers where, in the latter case, the absorber may be present in the form of discs separated by non-absorber fuel pellets or may be homogeneously loaded over the entire fuel rod.

2.6 NODAL COUPLING AND HOMOGENIZATION CALCULATIONS

The determination of the detailed flux distribution by PHOENIX is divided into two major steps, separating to some degree the space and energy solutions. Figure 2-4 illustrates the solution process in PHOENIX. In the first step, a 25 group nodal solution for the flux is obtained which couples the fuel rods (pellet, clad, surrounding coolant), channel, water gaps and gap objects (control rod, detector, boron curtain). The nodal solution is based on the use of transmission probabilities and response fluxes which preserve the heterogeneity of the pin cells and objects. The detailed flux distribution from the nodal solution is then used to homogenize the pin cells, channel, water gaps and objects. A group collapsing to an energy structure consisting of from 6 to 12 groups is also done.

This section describes the nodal equations solved by PHOENIX to obtain the detailed 25 group fluxes for homogenization and group collapsing. This nodal coupling method, which was developed by Weiss and Stamm'ler (Reference 12) uses the following assumptions: 1) pin cells are square; 2) the flux angular distribution at each side of the node is isotropic (white); 3)the first-flight transmissions from one side of the node to each of the three others are equal; and 4) the source neutrons as well as the collided neutrons have no leakage preference for any side of the node. The first-flight collision probabilities, which are at the heart of the nodal coupling method and response flux formalism, are evaluated by cylindricalizing the cells and employing Carlvik's method (Reference 13).

The coupling of a given node (pin cell) N to the adjacent nodes K is accomplished by means of first-flight probabilities and partial in-currents, J_{NK}. The partial current, J_{NK}, is defined as:

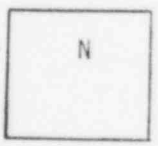

$$J_{NK} = \frac{1}{4} J_N^+ + Q_N \sum_{K' \neq K} J_{K'N} \qquad (2.6\text{-}1)$$

Square node N with its neighbors being denoted by K or K'.

J_N^+ is the outward current from node N resulting from the source term S_N, and the in-currents excluding their first-flight contributions. The second term on the RHS represents the first-flight leakage resulting from the currents entering through the other three sides, where the first-flight transmission from any side to the three others has been assumed equal i.e.,

$$Q_N = \frac{1}{3}(1 - \gamma_N) \tag{2.6-2}$$

where γ_N is the first-flight collision probability. Here the assumption has been made that a neutron, once it has collided, has forgotten through which side it has entered the node. Thus,

$$J_N^+ = R_N + (1 - \Gamma_N - 3Q_N)\sum_K J_{KN} \tag{2.6-3}$$

where R_N is the contribution from S_N, and Γ_N is the total collision probability of node N. The term $Q_N J_{KN}$ is next added to both sides of Eq. (2.6-1). The resulting equation for partial current J_{NK} becomes

$$J_{NK} + Q_N J_{KN} = \frac{1}{4} M_N \tag{2.6-4}$$

where

$$M_N = R_N + \mu_N J_N^- \tag{2.6-5}$$

Eq. (2.6-3) has been used for J_N^+ with

$$\mu_N = 1 - \Gamma_N + Q_N \tag{2.6-6}$$

and J_N^- being the total in-current into node N, i.e.,

$$J_N^- = \sum_K J_{KN} \tag{2.6-7}$$

A similar equation to Eq. (2.6-4) can be written for partial current J_{KN}. Thus

$$J_{KN} + Q_K J_{NK} = \frac{1}{4} M_K \tag{2.6-8}$$

The partial currents J_{KN} can be expressed in terms of the M_K and M_N by solving Eqs (2.6-4) and (2.6-8)

$$J_{KN} = \frac{1}{4}\left[\frac{M_K - Q_K M_N}{1 - Q_K Q_N}\right] \tag{2.6-9}$$

Substitution of Eq. (2.6-9) into Eq. (2.6-7) and then further into Eq. (2.6-5) leads to the following relation:

$$M_N \left\{1 + \frac{1}{4}\mu_N \sum_K \frac{Q_K}{1 - Q_K Q_N}\right\} - \left\{\frac{1}{4}\mu_N \sum_K \frac{M_K}{1 - Q_K Q_N}\right\} = R_N \tag{2.6-10}$$

Introducing A_{KN}, λ_N and B_N leads to the following abbreviated equation scheme for solving M_N iteratively

$$M_N = \sum_K A_{KN} M_K + B_N \tag{2.6-11}$$

where

$$\lambda_N = \left(1 + \frac{1}{4}\mu_N \sum_K \frac{Q_K}{1 - Q_K Q_N}\right)^{-1} \tag{2.6-12}$$

$$A_{KN} = \frac{1}{4}\left(\frac{\lambda_N \cdot \mu_N}{1 - Q_K Q_N}\right) \tag{2.6-13}$$

$$B_N = \lambda_N R_N \tag{2.6-14}$$

A_{KN} and B_N depend only on the nodal constants γ_N and μ_N which are related to the collision probability for node N. The term B_N is proportional to the neutron source term, R_N.

For a node at the boundary of the problem, the following relations are obtained for the partial currents at the boundary interface.

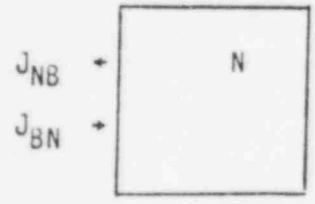

Square node N lies on the boundary, formally indexed by B

In complete analogy with Eq. (2.6-1) one obtains for the outgoing partial current J_{NB}

$$J_{NB} = \frac{1}{4} J_N^+ + Q_N \sum_{K \neq B} J_{KN} \qquad (2.6\text{-}15)$$

For J_{BN}, on the other hand, the following is obtained

$$J_{BN} = \tilde{J}_{BN} + a_B J_{NB} \qquad (2.6\text{-}16)$$

where a_B is the albedo of the boundary. $\tilde{J}_{BN}$ accounts for possible external sources beyond the boundary (in case of water gaps or a reflector, this may be the slowing-down source which gives rise to a leakage current into the system via node N). Equation (2.6-15) can be completed by adding to both sides $Q_N J_{BN}$. Rewriting also Eq. (2.6-16) then results in the following set of equations:

$$J_{NB} + Q_N J_{BN} = \frac{1}{4} M_N \qquad (2.6\text{-}17)$$

$$-a_B J_{NB} + J_{BN} = \tilde{J}_{BN}$$

Comparing Eqs. (2.6-4), (2.6-8) with Eqs. (2.6-17) shows that the boundary may formally be represented by a node for which

$$Q_B = -a_B \qquad \text{and} \qquad M_B = 4 \tilde{J}_{BN} \qquad (2.6\text{-}18)$$

Thus, Eq. (2.6-11) is solved only for the nodes N belonging to the system. Whenever a node K, in the sum on the RHS of Eq. (2.6-11), lies on the boundary it is treated as a normal node for which M_K is the M_B of Eq. (2.6-18) and where Q_B of Eq. (2.6-18) has been used to find its A_{KN}.

The flux for node N in region i is assumed to be made up of two components. The first component is the flux in region i for node N caused by the source distribution Q_{NK}, i.e.

$$X_{Ni} = \sum_{K} S_{NK} \, X^{K}_{Ni} \qquad (2.6\text{-}19)$$

where X^{K}_{Ni} is the response flux in region i of node N caused by a unit source in region K of node N. S_{NK} represents the slowing down and fission sources.

The second component of the flux is the flux caused by the in current $\bar{J}_N$ to the fuel cell which is given by $\bar{J}_N \cdot Y_{Ni}$ where Y_{Ni} is the flux in region i caused by one incident neutron on the node's circular boundary S_b.

Thus, the total flux can be expressed as follows:

$$\Phi_{Ni} = X_{Ni} + \bar{J}_N Y_{Ni} \qquad (2.6\text{-}20)$$

The iteration process first assumes a flux guess which may be, for example, the converged flux distribution from the previous depletion time step. The source term is then determined as follows for region i of node N for group g.

$$S_{Ni}(g) = \sum_{1}^{NG} \Sigma_{sNi} \, (g' \rightarrow g) \, \Phi_{Ni}(g')$$

$$+ \chi_g \sum_{1}^{NG} \nu \, \Sigma_{FNi} \, (g') \, \Phi_{Ni} \, (g') \qquad (2.6\text{-}21)$$

The first term on the RHS is the slowing down source while the second is the fission source.

Next, the leakage R_N from node N due to source S_N must be obtained. This is accomplished as follows: The total collision proabability in region J of node N, denoted Γ_{NJ}, is defined in terms of the response flux Y_{NJ} as follows

$$\Gamma_{NJ} = V_{NJ} \Sigma_{aNJ} Y_{NJ} \tag{2.6-22}$$

A reciprocity relation is used to relate Γ_{NJ} to P_{NJ}^{esc}

$$\Gamma_{NJ} = \frac{4V_{NJ} \Sigma_{aNJ}}{S_b} P_{NJ}^{esc} \tag{2.6-23}$$

$$\text{Therefore } P_{NJ}^{esc} = \frac{1}{4} S_b Y_{NJ} \tag{2.6-24}$$

Thus, the leakage from node N caused by the source S_{NJ} distribution is evaluated as follows

$$R_N = \frac{1}{4} S_b \sum_J V_{NJ} \cdot S_{NJ} \cdot Y_{NJ} \tag{2.6-25}$$

Having determined the sources S_{NJ} from the initial flux guess and R_N from Eq. (2.6-25), the next step in the solution process is to solve for B_N using Eq. (2.6-14).

The M_N terms are obtained from Eq. (2.6-11) using various acceleration techniques. Next $\bar{J}_N^-$ is determined from Eq. (2.6-5). Finally, the flux ϕ_{Ni} for node N of region i is evaluated from Eq. (2.6-20). A new source guess is obtained from the new fluxes and the iterations continue until convergence is achieved for the flux distribution.

In conclusion, the pin cell nodal method provides accurate multi-group fluxes for each micro-region of the assembly (pellet, clad, surrounding water, water gaps, etc.) for use in homogenizing the cross-sections. When transport-corrected by SFINX, which is described next, the nodal

method also provides accurate multi-group fluxes which assure the correct depletion of the nuclides and burnable absorber. The pin cell nodal method offers the distinct advantage that all pins in the assembly are treated simultaneously so that all heterogeneities such as due to the burnable absorber, multiple enrichments, water gaps and control rods are correctly taken into account. Finally, in the limit of an infinite uniform lattice, this method is consistent with the traditional calculation on a pin cell with an isotropically-reflecting boundary.

2.7 TWO-DIMENSIONAL CALCULATIONS

Prior to executing the two dimensional transport calculation, nomogenization and group collapsing is performed to obtain few group (6-12 groups) cross-sections. During this homogenization step, the channel is smeared with the water gaps. The control rod absorber pins are homogenized with the other materials of the control blade span. All homogenization is performed using flux-volume weighting.

However, a flux-volume homogenization only preserves the reaction rates and not, simultaneously, the partial currents at the surface of the homogenized regions. Consequently, the interaction between bordering regions cannot be properly described by homogenized cross-sections alone. However, the pin cell nodal calculation not only provides accurate fluxes to use for homogenizing the cross-sections, but also the partial currents between bordering regions (fuel rods, control blade, water gaps, etc.)

PHOENIX uses these partial currents to find auxiliary sources δQ, which, when introduced in the homogenized regions, restore the surface-integrated partial currents from the nodal solution. Denoting the error in the partial out-currents arising from homogenization by ∂J^{out}, one has

$$\delta Q = \frac{\Gamma_h}{\rho_h} \partial J^{out} \qquad (2.7\text{-}1)$$

where Γ_h and ρ_h are the total collision and escape probabilities of the homogenized cell.

These sources are used in the SFINX transport solution to ensure correct partial currents between the homogenized regions. The two-dimensional assembly calculation in PHOENIX is made using the SFINX program [14] which is a multi-group discrete-ordinates transport theory code. An S_4 angular quadrature is used with isotropic scattering. The S_n method is sufficiently well-known and will not be restated here. An

excellent review is given by Carlson and Lathrop in Reference 15. Comparison of the the S_4 method with higher order S_n methods and integral transport theory shows close agreement for typical fuel assembly geometries.

The conventional transport correction is used in the SFINX calculation to account for linear anisotropy. In fact, this correction is inherent in the cross-section data. The additional partial sources derived from the nodal partial currents corrects to first order any error in the partial currents between homogenized nodes resulting from the homogenization process. As boundary conditions, perfect reflection (not isotropic) or periodicity are assumed. The objects in the water gaps are included in the two-dimensional mesh so that they do not enter as boundary conditions. The mesh constructed by PHOENIX assures both reliable results and reasonable computer running time.

The standard SFINX calculation uses six energy groups. This group structure, which is shown in Table 2-4, has been carefully selected to represent as accurately as possible burnable absorber pins, the Pu-240 resonance, and control blades with either B_4C or Ag-In-Cd pins. At the user's option, the six group structure can be replaced by 2, 3, 4, 5, 7, 8, 10 or 12 groups. An extrapolation technique is used to accelerate the inner flux iteration as well as the fission source iteration. At the group to group iteration level, a looping strategy is used, in addition to the fundamental mode rebalancing, which provides rapid convergence of the group fluxes.

Following the SFINX calculation, PHOENIX expands the S_4 SFINX group fluxes back to the 25 group cross-section library structure for all of the micro regions (pellet, clad, surrounding coolant) using the detailed flux solution from the nodal calculation. Figure 2-5 gives an example of the spatial and energy condensation and expansion techniques used in PHOENIX. Thus, the nodal solution provides the fine spatial and energy detail of the flux while the SFINX calculation normalizes the nodal flux to the transport theory solution.

Since either periodic or reflective boundary conditions are used in the SFINX calculation, the flux solution obtained is representative of an infinite array of fuel assemblies. To account for the effect of leakage, a fundamental mode B1 material buckling search is made searching to a k_{eff} of 1.0. Because fast leakage is the major contributor to the net leakage, the fast-energy group structure used for the homogenized assembly is modified to include extra groups above 9 kev. Table 2-5 lists the energy group boundaries used in the B1 leakage calculation. In this calculation, a leakage flux distribution is found where $k_{eff} = 1.0$. This distribution is superimposed on the S_4 flux solution to provide the final flux distribution. This final flux distribution is then used to normalize the 25 group fine structure nodal flux. The transport (SFINX)-corrected nodal fluxes are then used to deplete each fuel and burnable absorber pin in 25 energy groups.

The SFINX calculation provides a rigorous transport theory flux solution. Combined with the detailed nodal flux solution, the nodal-transport method provides the equivalent of transport theory fine spatial and energy fluxes. This flux treatment assures that each fuel pin and burnable absorber is properly depleted and that reaction rates and reactivities are correctly computed.

2.8 CONTROL ROD TREATMENT

PHOENIX can model both BWR cruciform control rods and PWR rod cluster control rods. For the BWR cruciform rod, PHOENIX treats the control rod simultaneously with all of the other materials present in the assembly (fuel pins, water gaps, channel, etc.). In the nodal solution, PHOENIX obtains the 25 group response fluxes and transmission probabilities for each individual B_4C pin element. Homogenization and group collapsing is performed in preparation for the SFINX solution. In the homogenization step, PHOENIX combines the B_4C cladding, the metal sheet enclosing the B_4C pins and the cooling water present around the B_4C pins as a single homogeneous region surrounding each B_4C pin. The PHOENIX calculation differentiates between the hub, which is treated as a homogeneous region, and the wing of the blade where each B_4C pin is treated individually (see Figure 2-6). In the SFINX solution, additional sources given by Eq. (2.7-1) are created to preserve the anisotropic surface currents. Extra mesh lines are introduced in SFINX to model the control rod hub and individual homogenized B_4C pins. No smearing of the control rod with the water gaps is made.

The nodal-SFINX transport theory flux solution method provides a means for generating the control rod reactivity worth and group constants that is accurate, reliable and is state-of-the-art. The control rod treatment is general and can simulate both the rod cluster control rods, typically used in PWRs, and the cruciform control rods used in BWRs.

2.9 DETECTOR MODELLING

The detector is modelled in PHOENIX as an object that is placed in the narrow-narrow gap. A trace amount of U-235 is placed in the object and the U-235 reaction rate is calculated by PHOENIX. The detector response is calculated as a function of exposure and void history for typically 0,25,50 and 75% void fractions. The detector is surrounded by a stainless steel envelope sized to reproduce the actual neutron spectrum present at the active portion of the detector. The geometry used in PHOENIX for the detector is illustrated in Figure 2-7.

2.10 DEPLETION CALCULATIONS

In PHOENIX, the burnup chain equations are solved analytically by England's method described in Reference 16. The burnup calculations are applied to each individual pin cell. The basic burnup chains are decomposed into 18 linearized chains, of which 4 are heavy metal chains and the other 14 are fission product chains. These chains are shown in Table 2-6. The chains contain altogether 40 different isotopes, including some 15 heavy metal isotopes and 2 lumped fission products. The xenon concentration is always set to its equilibrium value in the depletion calculations.

The burnup calculations are performed using default burnup steps. The flux distribution is kept constant during each burnup step. If there are burnable absorbers present, the standard burnup steps are automatically modified and extra burnup steps are inserted depending on the concentration of the burnable absorber material.

Because the flux distribution is assumed to remain constant during the depletion step, inaccuracies could arise if the burnup step were too large or if rapidly depleting materials, such as gadolinium, were present. To remedy this situation, a two step "predictor-corrector" method is used. In the "predictor" step, the burnup calculation is performed with the beginning of step flux distribution to yield a set of material number densities. With this set of number densities, the PHOENIX calculation is made to obtain the flux distribution corresponding to the end of step. Using this end of step flux distribution, the "corrector" step is performed where a burnup calculation is done to yield another set of material number densities corresponding to the end of step. The final material number densities are determined as the arithmetic average of these two sets of number densities. This method permits large burnup steps even when rapidly depleting burnable absorbers, such as gadolinium, are present.

2.11 BRANCH CALCULATIONS

PHOENIX features a variety of branch calculations which are performed automatically. The branch calculations provided by PHOENIX are listed below.

a. Void Branch - The void fraction in the active coolant is automatically changed to another input specified void fraction. Cross-section for POLCA are normally run at 0,25,50 and 75% void histories with 0,25,50 and 75% void branches executed throughout the depletion. Another automated feature is the "hot clean" and "cold-clean" calculation. The "hot-clean" condition is at 0% void fraction with the coolant temperature maintained at the full power saturation temperature. The "cold-clean" condition is at 0% void fraction with the coolant at room ambient pressure and temperature conditions. Xenon is normally zeroed out in the "hot-clean" and "cold-clean" calculations. Xenon is normally set to equilibrium for the void branch calculation.

The standard output from the PHOENIX void branches is a tabulation of full power two-group cross-sections for the bundle as a function of exposure, void history and void branch as well as "hot clean" and "cold clean" cross-sections as a function of exposure and void history. These cross-section tables are prepared for POLCA by the auxiliary code, PHIPO, which is described in Section 4.3. PHIPO also fits the xenon microscopic cross-section to a polynomial of exposure and void fraction which is given by

$$\sigma_{xe}(E, VF) = (a_1 + a_2 E) \cdot (a_3 + a_4 VF + a_5 VF^2) \quad (2.11\text{-}1)$$

where E denotes exposure and VF is the void fraction.

b. Doppler Branch - Starting from the full power temperature, the fuel temperature is raised or lowered. The fuel temperature is assumed to be uniform over all fuel pins. The full power fuel temperature remains constant throughout the depletion. An effective fuel temperature is used that corrects for the fact that a single temperature is used for all fuel pins and all exposures. The Doppler branch is normally run throughout the depletion for the 50% void fraction depletion. The Doppler defect is assumed to be proportional to $\sqrt{T_{eff}}$ where T_{eff} denotes the fuel effective resonance temperature. The constant of proportionality is fit to a polynomial of exposure and void fraction of the form:

$$\frac{\Delta K}{\Delta \sqrt{T_{eff}}} = (1 + a_1 E + a_2 E^2 + a_3 E^3) \cdot (a_4 + a_5 VF) \qquad (2.11\text{-}2)$$

where E denotes exposure and VF is the void fraction. This fitting is done external to PHOENIX by the PHIPO program.

For the other void histories (0%, 25% and 75%), the Doppler calculation is only performed at beginning of life with equilibrium xenon. The burnup dependence obtained from the 50% void depletion is assumed to apply.

c. Control Branch - At specified burnups, the control blade is automatically inserted and the reactivity and cross-sections recalculated with the control blade present. Typically, the control branch is executed throughout the depletion for the 50% void history. For the remaining void histories at 0%, 25% and 75%, the control tree is only executed at beginning of life with equilibrium xenon present. The burnup dependence from the 50% void history is assumed to apply. The output from this branch calculation is a tabulation of two-group cross-sections for the fuel bundle with the control blade present which is given

as a function of exposure, void history and void branch for 0, 25, 50 and 75% void fractions. Again, the processing of the cross-section data for input to POLCA is performed by the PHIPO code.

PHOENIX permits any objects in the gaps, such as boron curtains, to be inserted or removed at any burnups and to remain for any specified burnup interval. PHOENIX also features a restart capability: At the specified restart burnup, PHOENIX dumps to magnetic tape all of the necessary information needed to reconstruct a complete input deck for that case. This deck may then be modified to perform any calculation desired at that restart burnup step.

The PHOENIX program provides the full range of branch calculations required by the POLCA 3-D nuclear-thermal/hydraulic core simulator program for the nuclear design and analysis of boiling water reactor cores. All of the branch calculations as well as the processing of the data for input to POLCA is automated. The PHOENIX program combined with POLCA and the auxiliary codes provide a computational capability that is state-of-the-art for the nuclear design and analysis of boiling water reactors.

2.12 C-FACTOR DESCRIPTION

Along with the pin-wise power distribution, PHOENIX calculates correction factors, denoted C-factors, which are used in the MCPR correlation to take into account the effect of the local power distribution on the MCPR. The C-factors are calculated as a function of exposure, void history and void branch for 0,25,50 and 75% void fraction. PHOENIX obtains a C-factor which is based on the pin-wise power distribution, peaking factor and on a dryout weight factor. The dryout factors are empirically derived from the MCPR testing conducted to develop the MCPR correlation.

2.13 INPUT/OUTPUT

The input to PHOENIX is of the free format type based on a designated "keyword" identifier. The input parameters are entered in ordered sets where the keyword identifier is used to identify each data set. PHOENIX input data does propagate from one case to another, so the only input parameters in later cases required are those which are additional or change from case to case.

Once the input has been processed, PHOENIX performs a multitude of input checks to minimize the risk of input errors. There are approximately 140 potential checks.

In the PHOENIX output, once the case input has been displayed, parameters are conveniently arranged and labelled as to be self-explanatory. Included in the output for each PHOENIX case are such physics constants as: exposure, specific power, k_∞ (both with and without the B1 buckling correction), and two group homogenized cross-section data for the fuel assembly. Also edited are the two-dimensional power, burnup, isotopic, and C-factor distributions for the bundle. In addition to these standard quantities, PHOENIX can edit, at the user's option, such quantities as reaction rates and fluxes over specified regions of the bundle.

In addition to the printed output, PHOENIX stores all of the data on magnetic tape for later processing by the PHIPO code. The PHIPO code processes the PHOENIX output files and generates the required physics data for the three-dimensional simulator code POLCA.

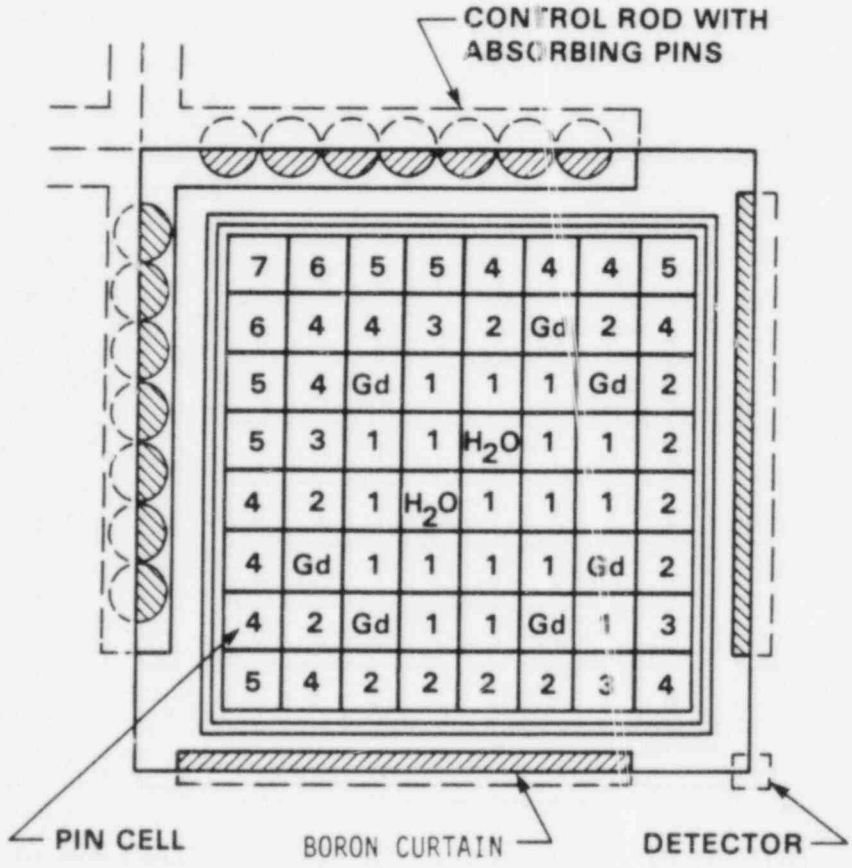

FIGURE 2-1: Typical BWR Fuel Assembly Configuration

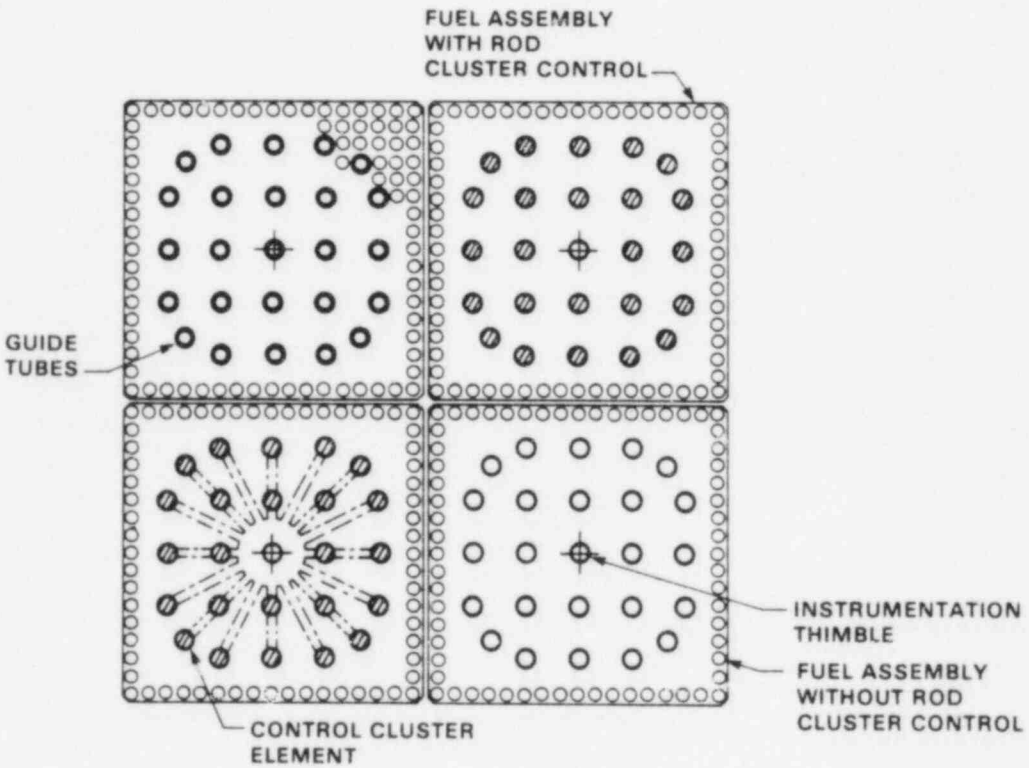

FIGURE 2-2: TYPICAL PWR FUEL ASSEMBLY CONFIGURATION

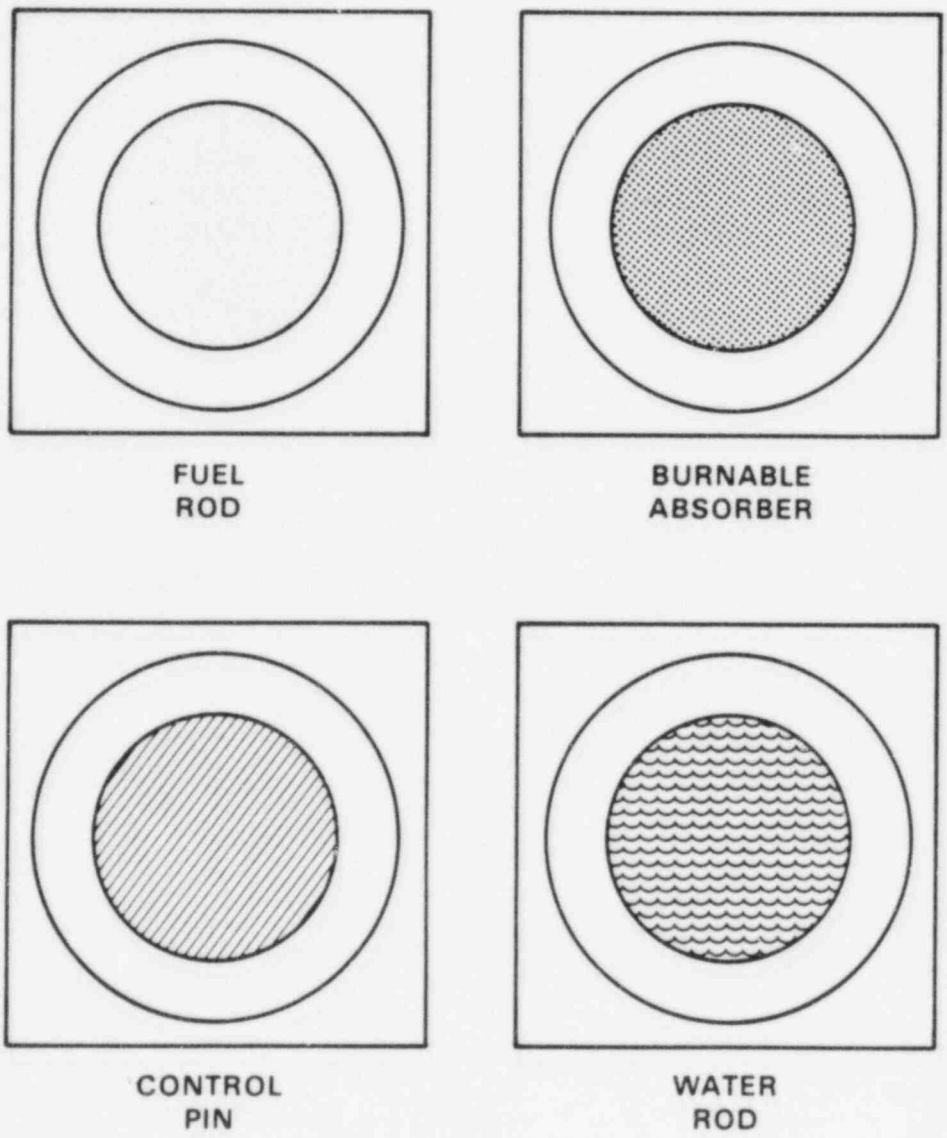

FIGURE 2-3: PHOENIX Pin Cell Types

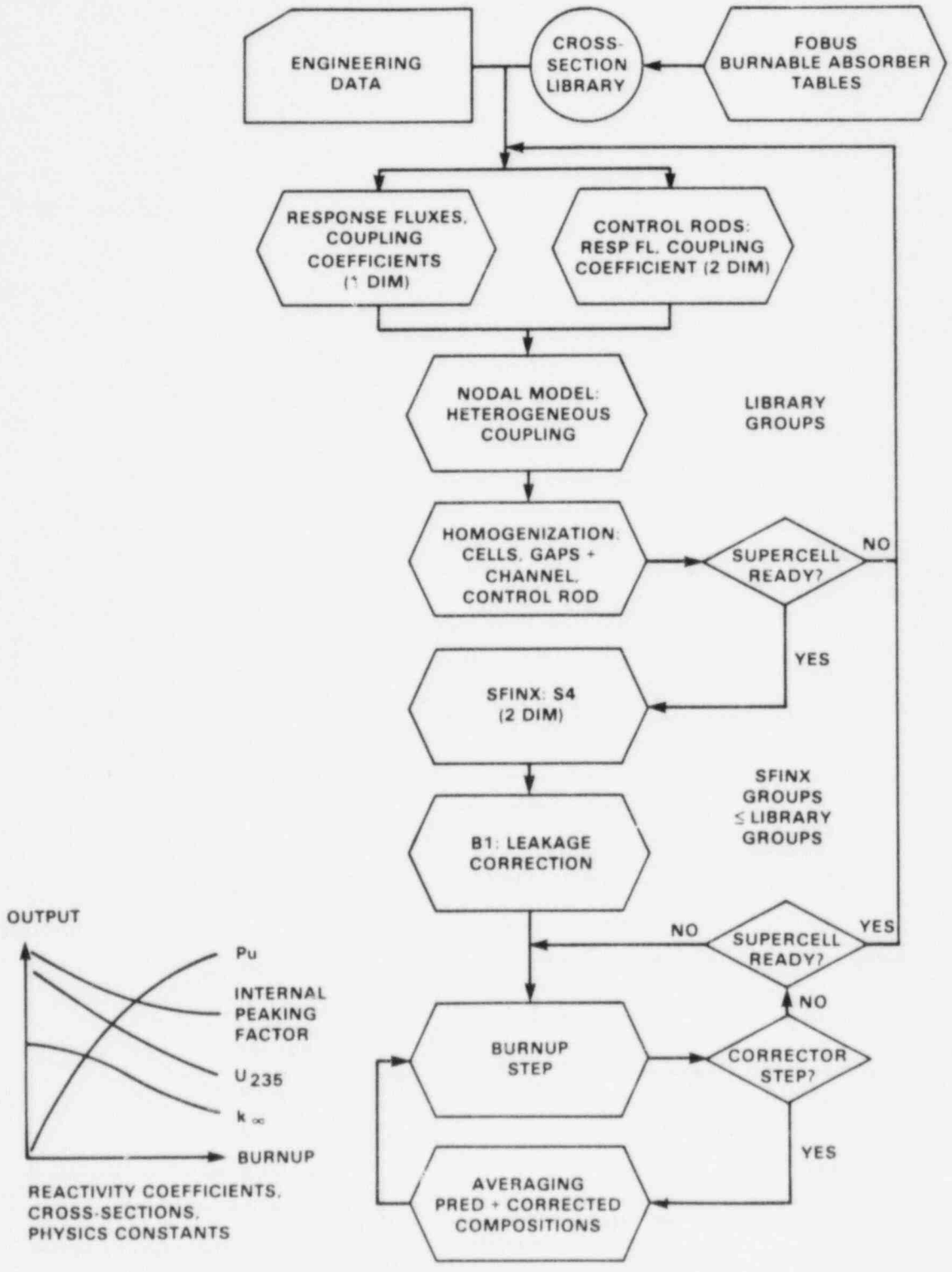

FIGURE 2-4: PHOENIX Calculational Flow Design

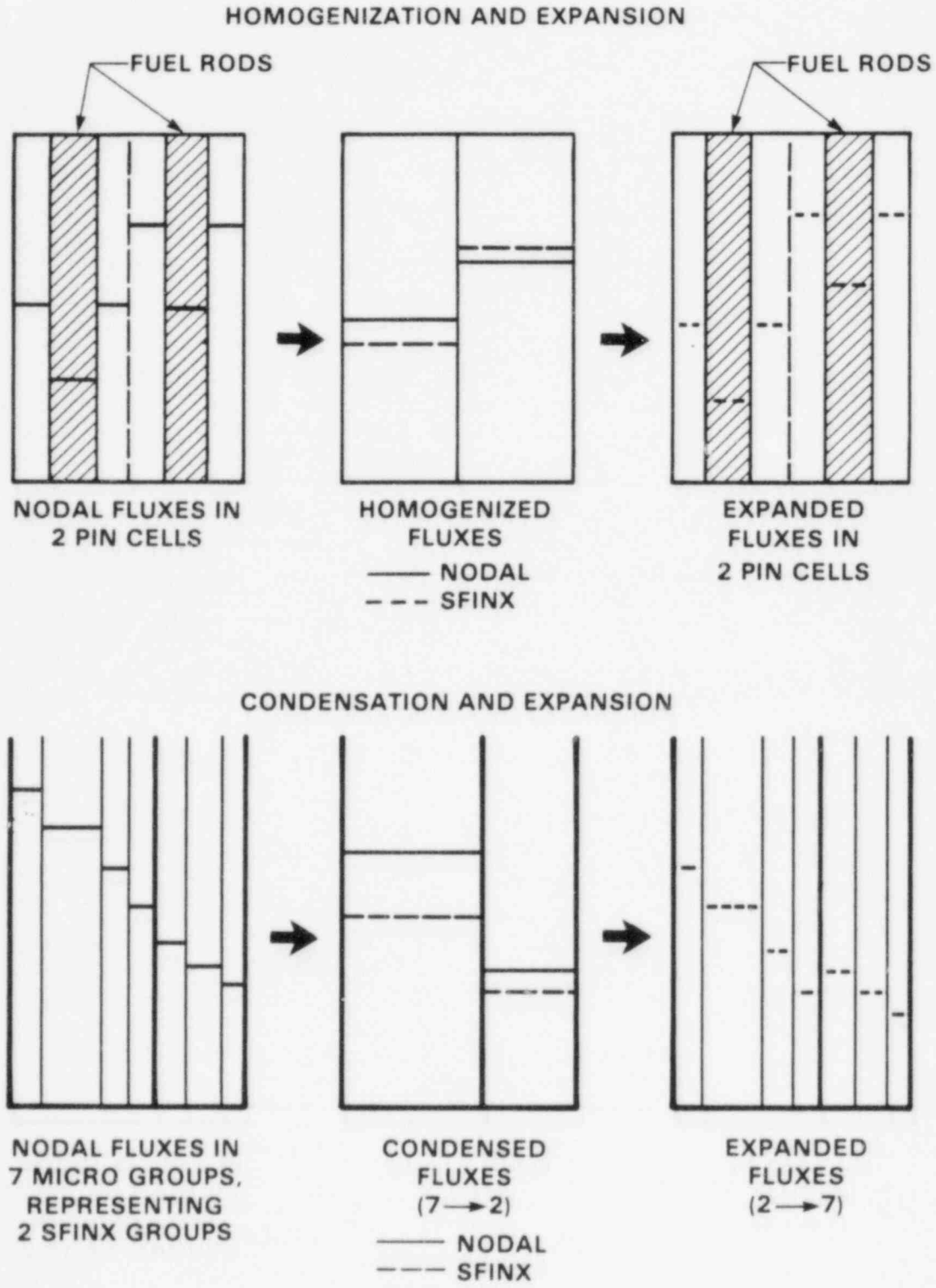

FIGURE 2-5: Spatial Homogenization And Expansion (Upper Half of Figure) And Energy Condensation And Expansion (Lower Half of Figure) Performed By PHOENIX.

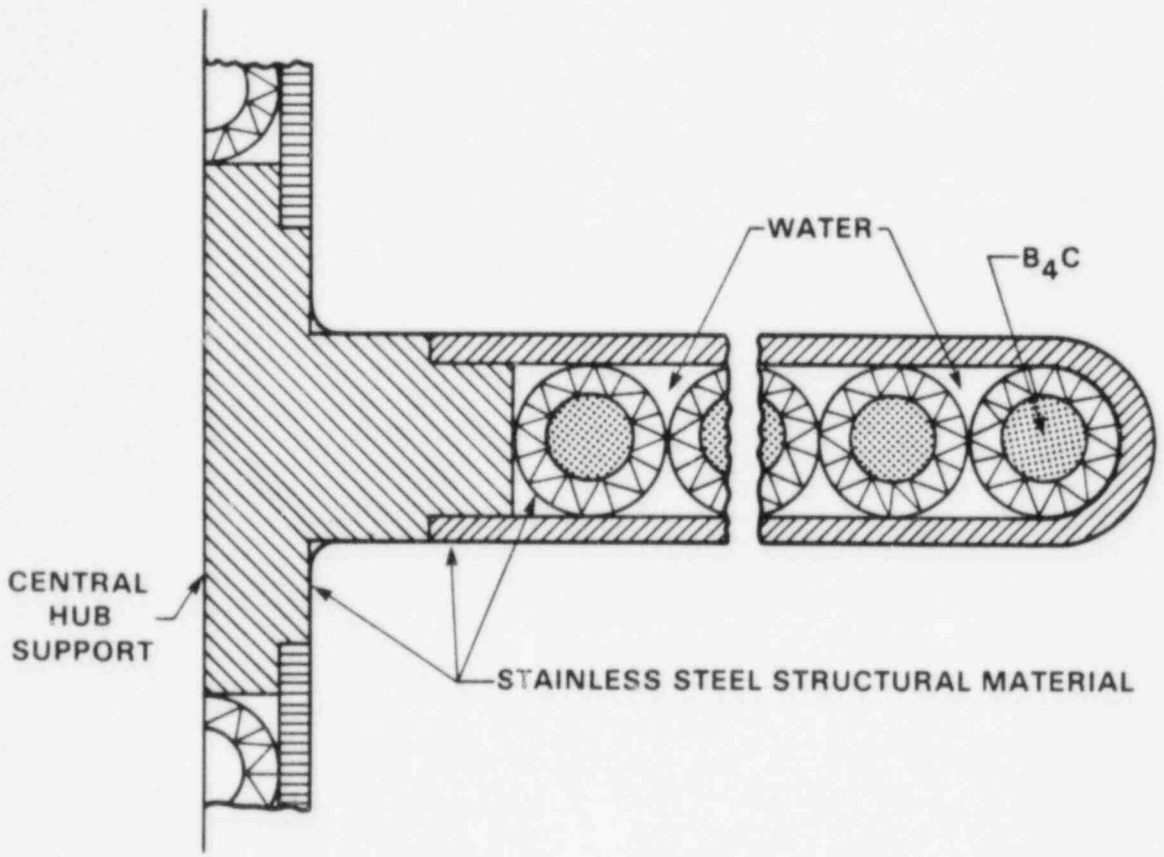

FIGURE 2-6: Typical BWR Cruciform Control Rod

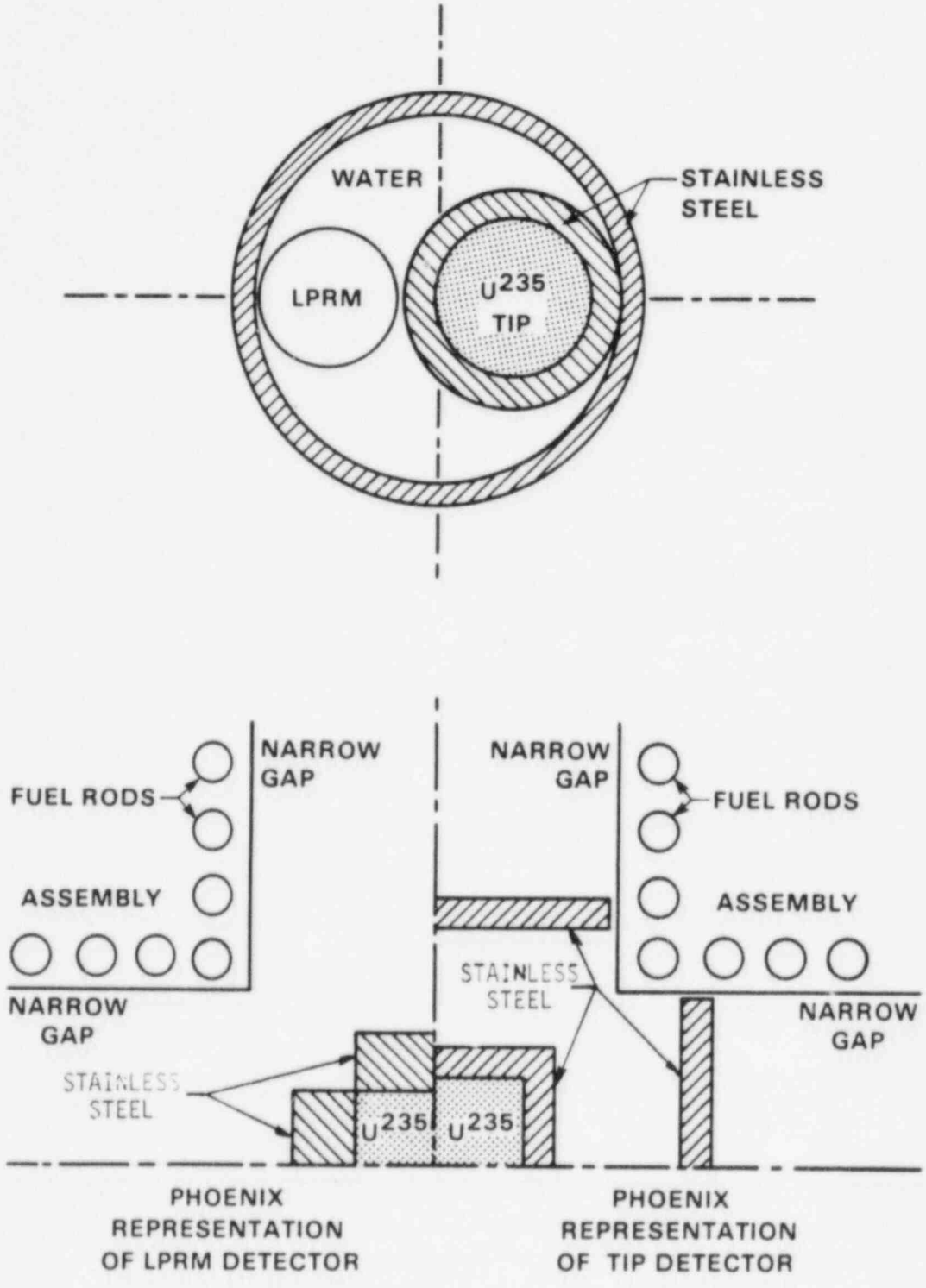

FIGURE 2-7: PHOENIX In-Core Detector Modeling

TABLE 2-1

PHOENIX 69 GROUP ENERGY BOUNDARIES

Group	Energy (MeV)			Group	Energy (eV)		
	Upper		Lower		Upper		Lower
1	10.0	-	6.0655	36	1.097	-	1.071
2	6.0655	-	3.679	37	1.071	-	1.045
3	3.679	-	2.231	38	1.045	-	1.020
4	2.231	-	1.353	39	1.020	-	0.996
5	1.353	-	0.821	40	0.996	-	0.972
6	0.821	-	0.500	41	0.972	-	0.950
7	0.500	-	0.3025	42	0.950	-	0.910
8	0.3025	-	0.183	43	0.910	-	0.850
9	0.183	-	0.1110	44	0.850	-	0.780
10	0.1110	-	0.06734	45	0.780	-	0.625
11	0.06734	-	0.04085	46	0.625	-	0.500
12	0.04085	-	0.02478	47	0.500	-	0.400
13	0.02478	-	0.01503	48	0.400	-	0.350
14	0.01503	-	0.009118	49	0.350	-	0.320
				50	0.320	-	0.300
	eV			51	0.300	-	0.280
15	9118.0	-	5530.0	52	0.280	-	0.250
16	5530.0	-	3519.1	53	0.250	-	0.220
17	3519.1	-	2239.45	54	0.220	-	0.180
18	2239.45	-	1425.1	55	0.180	-	0.140
19	1425.1	-	906.898	56	0.140	-	0.100
20	906.898	-	367.262	57	0.100	-	0.080
21	367.262	-	148.728	58	0.080	-	0.067
22	148.728	-	75.5014	59	0.067	-	0.058
23	75.5014	-	48.052	60	0.058	-	0.050
24	48.052	-	27.700	61	0.050	-	0.042
25	27.700	-	15.968	62	0.042	-	0.035
26	15.968	-	9.877	63	0.035	-	0.030
27	9.877	-	4.00	64	0.030	-	0.025
28	4.00	-	3.30	65	0.025	-	0.020
29	3.30	-	2.60	66	0.020	-	0.015
30	2.60	-	2.10	67	0.015	-	0.010
31	2.10	-	1.50	69	0.010	-	0.005
32	1.50	-	1.30	69	0.005	-	0
33	1.30	-	1.15				
34	1.15	-	1.123				
35	1.123	-	1.097				

TABLE 2-2

PHOENIX 25 GROUP ENERGY BOUNDARIES

Group	Energy (ev)		
	Upper		Lower
1	10.0 E+6	-	3.679 E+6
2	3.679 E+6	-	1.353 E+6
3	1.353 E+6	-	0.500 E+6
4	0.500 E+6	-	9118.0
5	9118.0	-	148.728
6	148.728	-	48.052
7	48.052	-	15.968
8	15.968	-	9.877
9	9.877	-	4.00
10	4.00	-	1.30
11	1.30	-	1.097
12	1.097	-	1.020
13	1.020	-	0.950
14	0.950	-	0.625
15	0.625	-	0.350
16	0.350	-	0.280
17	0.280	-	0.180
18	0.180	-	0.140
19	0.140	-	0.100
20	0.100	-	0.080
21	0.080	-	0.058
22	0.058	-	0.042
23	0.042	-	0.030
24	0.030	-	0.015
25	0.015	-	0.

TABLE 2-3

TABLE OF NUCLIDES IN PHOENIX LIBRARY

No.	Nuclide	Identification Number	Temperatures (^{o}K)
1	U-235	92235	293
2	U-236	92236	300
3	U-238	92238	293
4	Pu-239	94239	300
5	Np-237	93237	294
6	Pu-240	94240	300, 600, 1200
7	Pu-241	94241	300
8	H (Nelkin)	1001	293, 333, 373, 423, 473
9	H (Eff. width)(1)	1101	293, 450, 600
10	D (Eff. width)(1)	1102	293, 450, 600
11	B-10	5010	300
12	B	5000	300
13	N	7000	300
14	O	8000	300, 400, 700, 1100, 2000
15	Na	11000	300
16	Al	13000	293
17	Si	14000	300
18	Cr	24000	293
19	Fe	26000	293
20	Fe(2)	26100	293
21	Ni	28000	293
22	SS-347(3)	26347	293
23	Cu	29000	300
24	Zr	40000	300, 600, 1200
25	Zr-2	40302	300, 600, 1200
26	Cd	48000	300

TABLE 2-3 (Con't)

No.	Nuclide	Identification Number	Temperatures (^{o}K)
27	Pb	82000	300
28	Ag	47000	373
29	In	49000	373
30	C	6000	500
31	Be	4000	300
32	Pu-238	94238	294
33	Am-241	95241	294
34	Am-242m	95242	294
35	Am-243	95243	294
36	Cm-244	96244	294
37	Pu-242	94242	293.6
38	Kr-83	36083	293.6
39	Rh-103	45103	293.6
40	Rh-105	45105	293.6
41	Ag-109	47109	293.6
42	Xe-131	54131	293.6
43	Cs-133	55133	293.6
44	Cs-134	55134	293.6
45	Xe-135	54135	293.6
46	Cs-135	55135	293.6
47	Nd-143	60143	293.6
48	Nd-145	60145	293.6
49	Pm-147	61147	293.6
50	Sm-147	62147	293.6
51	Pm-148	61148	293.6
52	Pm-148m	61248	293.6
53	Sm-149	62149	293.6
54	Sm-150	62150	293.6
55	Sm-151	62151	293.6
56	Sm-152	62152	293.6
57	Eu-153	63153	293.6
58	Eu-154	63154	293.6

TABLE 2-3 (Con't)

No.	Nuclide	Identification Number	Temperatures (^{o}K)
59	Eu-155	63155	293.6
60	NSFP	99001	293.6
61	SSFP	99002	293.6
62	Mn	25000	293.6
63	Dy-164	66164	293.6
64	Lu-176	71176	293.6
65	Hf	72000	293.6
66	Gd-155	64155	293.6
67	Gd-157	64157	293.6
68	1/V abs	1	293.6
69	Cu 63	29063	293.6
70	Cm 242	96242	293.6

(1) The effective width model for Hydrogen and Deuterium in water (the recommended model) has been compared with more recent experimental data (1968) and shows excellent agreement see Reference 17.

(2) Nuclide 26100 ("Moxon" iron) has the same data as Nuclide 26000 except for the absorption cross-sections in Groups 21-27. These cross-sections have been adjusted to give a resonance integral 1.4 barns higher than 26000 iron data.

(3) The composition of SS-347 is:

Fe (26000) - 67.5 w/o
Ni (28000) - 11.0 w/o
Cr (24000) - 18.5 w/o
Mn (25000) - 2.0 w/o
Si (14000) - 1.0 w/o

TABLE 2-4

STANDARD SFINX ENERGY GROUP STRUCTURE

Group	Energy (ev)
1	10.0E+6 - 0.50E+6
2	0.50E+6 - 148.728
3	148.728 - 1.300
4	1.300 - 0.625
5	0.625 - 0.180
6	0.180 - 0.

TABLE 2-5

GROUP STRUCTURE FOR B1 LEAKAGE CORRECTION

Group	Energy (ev)
1	10.0E+6 - 3.679E+6
2	3.679E+6 - 2.223E+6
3	2.223E+6 - 1.353E+6
4	1.353E+6 - 0.5E+6
5	0.5E+6 - 0.183E+6
6	0.183E+6 - 148.728
7	148.728 - 1.300
8	1.300 - 0.625
9	0.625 - 0.180
10	0.180 - 0.

TABLE 2-6

PHOENIX NUCLIDE CHAINS

$U_{235} \rightarrow U_{236} \rightarrow Np_{237} \rightarrow Pu_{238}$

$U_{238} \rightarrow Pu_{239} \rightarrow Pu_{240} \rightarrow Pu_{242} \rightarrow$
$\rightarrow Am_{243} \rightarrow Cm_{244}$

$U_{238} \rightarrow Pu_{239} \rightarrow Pu_{240} \rightarrow Pu_{241} \rightarrow Am_{241} \rightarrow$
$\rightarrow Am_{242} \rightarrow Am_{243} \rightarrow Cm_{244}$

$U_{238} \rightarrow Pu_{239} \rightarrow Pu_{240} \rightarrow Pu_{241} \rightarrow Am_{241} \rightarrow$
$\rightarrow Cm_{242} \rightarrow Pu_{238}$

Fission $\rightarrow Kr_{83}$

Fission $\rightarrow Rh_{103}$

Fission $\rightarrow Rh_{105}$

Fission $\rightarrow Ag_{109}$

Fission $\rightarrow Xe_{131}$

Fission $\rightarrow Cs_{133} \rightarrow Cs_{134}$

Fission $\rightarrow Xe_{135} \rightarrow Cs_{135}$

Fission $\rightarrow Nd_{143}$

Fission $\rightarrow Nd_{145}$

Fission $\rightarrow Pm_{147} \rightarrow Sm_{147}$

TABLE 2-6 (Con't)

Fission → Pm_{147} → Pm_{148} → Sm_{149} → Sm_{150}
→ Sm_{151} → Sm_{152} → Eu_{153} → Eu_{154}
→ Eu_{155}

Fission → Pm_{147} → Pm_{148M} → Sm_{149} → Sm_{150}
→ Sm_{151} → Sm_{152} → Eu_{153} → Eu_{154}
→ Eu_{155}

Fission → NSFP (non-saturating fission product)

Fission → SSFP (slowly-saturating fission product)

3.0 POLCA CODE

3.1 OVERVIEW OF POLCA

The POLCA computer code is a modified one-group nodal code used for three dimensional simulation of the nuclear, thermal and hydraulic conditions in boiling water reactors. The POLCA code provides a tool for calculating the three dimensional power distribution in order to perform a simple but realistic simulation of different processes in a BWR. Figure 3-1 provides a calculational flow diagram of POLCA.

In POLCA the three dimensional reactor core is divided into nodes where the neutronic characteristics of each node are described by homogenized two group macroscopic cross-sections determined for each fuel assembly type in the core using the PHOENIX code. The neutron transport between nodes is calculated using a one group, coarse mesh diffusion theory method which employs an albedo treatment to represent the core-reflector interface. A thermal flux correction is used to simulate the thermal neutron transport providing a flux solution that closely approximates that of a rigorous two group calculation. The three dimensional power distribution calculated in POLCA includes the effects of the coolant flow and void distribution, the presence of control rods, as well as, reactivity effects due to Doppler and xenon.

The hydraulic calculation in POLCA is accomplished using the hydraulic program CONDOR, which has been made an integral part of POLCA, to evaluate the fluid flow through each fuel assembly. Taking into account the axial power distribution within the fuel assembly, the steam quality and void content are determined using empirical correlations. Using the fuel assembly's internal power peaking factor, the surface heat flux and dry-out margin for the peak fuel rod in each fuel bundle is calculated.

In order to accurately simulate BWR cores, emphasis has been placed in the code on providing correct representation of the thermal margins, the state of the reactor during different control processes, feedback

mechanisms, the fuel burnup and xenon distributions during the cycle, the simulation of signals from in-core neutron flux detectors, and the reactivity margins at shutdown conditions.

3.2 CORE GEOMETRY

In POLCA the fuel region of the core is divided into a large number of equal sized rectangular parallelepiped zones or nodes. Within each node the fuel composition, burnup, void content, power density, etc. are constant. However, these nodal parameters do vary from one node to another. Each node in the core is identified by a fuel type to describe its characteristics. In each radial plane the nodes are square and generally correspond to a fuel assembly's width, whereas each fuel assembly in the axial direction is divided into at most 25 axial nodes. This node division produces approximately cubic nodes with sides of approximately 6 inches in width. The neutron transport in POLCA is limited to the six nearest neighboring nodes surrounding that node (see Figure 3-2). The POLCA coordinate system is shown in Figure 3-3 where the node numbers in the I, J, and K direction, respectively, are used as coordinates.

In addition to its capability of modelling the full core geometry in three dimensions, POLCA is capable of taking advantage of radial core symmetry through appropriate boundary conditions. The code is capable of handling half and quarter core calculations assuming either reflective or rotational symmetry.

The characteristics of the core-reflector interface, both in the radial and axial direction are described in POLCA utilizing an albedo treatment to indicate the probability that a neutron leaving the core and reaching the reflector will be reflected back into the core.

3.3 NEUTRON CROSS-SECTIONS

Homogenized two group macroscopic cross-section parameters are supplied to POLCA for each fuel type in the core. For each fuel type the cross-section parameters are provided as function of burnup, void and average (burnup-averaged) void. The independent variables, burnup, void and average void have the same values for all parameters and fuel types.

The cross-section parameters are obtained from PHOENIX lattice cell calculations for each fuel assembly type in the core both with and without control rods inserted. The PHOENIX results are processed and the cross-section parameters are prepared for input to POLCA using the PHIPO code.

The macroscopic cross-section parameters required by POLCA include:

D_1, D_2, Σ_{rem}, Σ_{a1}, Σ_{a2}, Σ_{f1}, Σ_{f2}, and ν, where all parameters have the conventional definition except as noted below.

The removal cross-section, Σ_{rem}, is an averaged quantity using the upward and downward scattering cross-sections according to the following:

$$\Sigma_{rem} = \Sigma_{r1} \left(1 - \frac{\Sigma_{r2}}{\Sigma_{a2}}\right) \qquad (3.3\text{-}1)$$

The effective number of neutrons produced per fission is obtained from

$$\nu = \nu\Sigma_{f2}/\Sigma_{f2} \qquad (3.3\text{-}2)$$

POLCA determines the cross-section parameters for each node in the core using the burnup, void content, and burnup averaged void for that node. Given cross-section sets at burnup-averaged voids, V_1 and V_2, which bound the average void V in a node, the following interpolation algorithm is applied to arrive at a cross-section parameter, T, for the node with burnup B.

Given the cross-section table:

Void/Burnup	B_1	B_2
V_1	T_{00}	T_{01}
V_2	T_{10}	T_{11}

the code calculates

$$T_X = T_{00} + \left(\frac{B - B_1}{B_2 - B_1}\right) (T_{01} - T_{00})$$

$$T_Y = T_X + \left(\frac{V - V_1}{V_2 - V_1}\right) (T_{10} - T_{00})$$

$$T = T_Y + \left(\frac{B - B_1}{B_2 - B_1}\right)\left(\frac{V - V_1}{V_2 - V_1}\right) (T_{11} - T_{10} + T_{00} - T_{01}) .$$

Using then a linear interpolation between the two average voids, cross-section parameters are determined at the average void of the node.

POLCA models the reactivity effect of control rod presence through modifications to the absorption cross-sections in the adjacent fuel nodes. Values of Σ_{a1} and Σ_{a2} for fuel nodes with control rods present are provided with the cross-section tables and are determined through rodded PHOENIX calculations for each fuel type. The spectral effect of control rod presence on fuel isotopics, and therefore on fuel reactivity history, is accounted for through adjustments to the burnup void histories of nodes adjacent to control rods.

In order for POLCA to explicitly account for xenon, the microscopic absorption cross-section, σ_{xe}, for xenon is required. This quantity is supplied to the program in the form of a fitted polynomial as a function of burnup and void.

3.4 NEUTRONIC FEEDBACK MODEL

The homogenized two group cross-section parameters supplied to POLCA correspond to reference conditions used in the lattice cell calculation. POLCA therefore must modify the cross-section data to account for core conditions differing from the reference conditions. The two neutronic feedbacks modelled in POLCA are Doppler fuel temperature and xenon. POLCA accounts for fuel temperature differences from the reference temperature through modifications to k_∞. Xenon concentrations differing from equilibrium concentrations are accounted for through modification of the thermal macroscopic absorption cross-section, Σ_{a2}.

The correction to k_∞ for fuel temperature variations from the reference fuel temperature accounts for the Doppler broadening of the resonances. POLCA determines the correction to k_∞ using the following polynomial which is a function of burnup and void fraction:

$$\Delta k_\infty = (1 + K1 \cdot Bu + K2 \cdot Bu^2 + K3 \cdot Bu^3) \cdot (K4 + K5 \cdot \alpha) \cdot \{\sqrt{T} - \sqrt{T_{ref}}\} \quad (3.4\text{-}1)$$

K1 - K5	=	fitting coefficients
Bu	=	nodal burnup
α	=	nodal void fraction
T	=	fuel temperature at actual power
T_{ref}	=	fuel temperature at reference power

The xenon effect correction to the macroscopic thermal absorption cross-section for a node accounts for the actual xenon concentration being different from the equilibrium xenon concentration. The correction to the macroscopic thermal absorption cross-section is computed as:

$$\Delta\Sigma_{a2} = (N_{xe} - N_{xe}^{eq})\, \sigma_{xe} \quad (3.4\text{-}2)$$

where

N_{xe} = actual nodal xenon number density

N_{xe}^{eq} = equilibrium nodal xenon number density

σ_{xe} = microscopic thermal absorption cross-section of xenon.

The microscopic thermal absorption cross-section for xenon is evaluated using the following polynomial:

$$\sigma_{xe} = (X1 + X2 \cdot Bu) \cdot (X3 + X4 \cdot \alpha + X5 \cdot \alpha^2) \qquad (3.4\text{-}3)$$

where

X1 - X5 = fitting coefficients

Bu = nodal burnup

α = nodal void fraction.

The polynomial fitting coefficients in Eqs. (3.4-2) and (3.4-3) are generated from PHOENIX calculations using the PHIPO code.

3.5 NEUTRONIC MODEL

The three dimensional neutronics of the reactor core is described in POLCA by an effective one group nodal model. Coupling coefficients describing the inter-nodal coupling are evaluated from two group data and take into account the local spectrum mismatch effects. The following fundamental parameters are evaluated by the code for use in the solution of the nodal equations:

$$M^2 = \frac{D_1}{\Sigma_{a1} + \Sigma_{rem}} + \frac{D_2}{\Sigma_{a2}} \qquad (3.5\text{-}1)$$

$$k_\infty = \frac{\nu\Sigma_{f1}}{\Sigma_{a1} + \Sigma_{rem}} + \frac{\nu\Sigma_{f2}}{\Sigma_{a2}} \quad \frac{\Sigma_{rem}}{\Sigma_{a1} + \Sigma_{rem}} \qquad (3.5\text{-}2)$$

$$B^2 = \frac{\frac{k_\infty}{k_{eff}} - 1}{M^2} \qquad (3.5\text{-}3)$$

In POLCA the neutronic coupling in the reactor core is assumed to be primarily due to the fast neutrons which have a relatively large mean free path. In this section, unless stated otherwise, the neutron flux is assumed to be the fast (group 1) flux and its group index will be omitted.

The neutron balance for node i can be written as

$$V_i D_i B_i^2 \bar{\Phi}_i = \sum_{j=1}^{6} S_{ij} J_{ij} \qquad (3.5\text{-}4)$$

where

V_i = the nodal volume

S_{ij} = the surface between node i and one of its six neighbors j

D_i = the diffusion coefficient

B_i^2 = the material buckling

$\bar{\Phi}_i$ = the average nodal neutron flux

J_{ij} = the average net-current from node i to node j.

In order to transform Equation (3.5-4) into the POLCA nodal equations, the net-currents, J_{ij}, can be expressed in terms of the nodal fluxes utilizing the continuity condition for J_{ij} across the nodal surface S_{ij}.

$$J_{ij} = \hat{D}_i \left\{ \frac{\Phi_i - \Phi_{ij}}{h_{ij}/2} \right\} = \hat{D}_j \left\{ \frac{\Phi_{ij} - \Phi_j}{h_{ij}/2} \right\} = -J_{ji} \qquad (3.5\text{-}5)$$

where

Φ_{ij} = the average neutron flux on surface S_{ij}

Φ_i = the node "midpoint" neutron flux

$\hat{D}_i$ = the effective diffusion coefficient

h_{ij} = $[V_i/S_{ij}]$

$\hat{D}_i$ differs from the conventional diffusion coefficient because of the finite node size h_{ij}, where

$$\hat{D} = E \cdot D \qquad (3.5\text{-}6)$$

and E is a node size correction factor with $E \to 1$ as $h_{ij} \to 0$.

One can express the surface flux, Φ_{ij}, in terms of the fictitious midpoint fluxes as:

$$\Phi_{ij} = \left[\frac{\hat{D}_i \Phi_i + \hat{D}_j \Phi_j}{\hat{D}_i + \hat{D}_j} \right] \qquad (3.5\text{-}7)$$

Using this in Equation 3.5-5 yields:

$$J_{ij} = \left(\frac{2}{h_{ij}}\right)\left(\frac{\hat{D}_i\,\hat{D}_j}{\hat{D}_i + \hat{D}_j}\right)(\Phi_i - \Phi_j) \qquad (3.5\text{-}8)$$

Now according to the approximation of Borrensen[18] the coupling coefficients can be expressed as:

$$2\left(\frac{\hat{D}_i\,\hat{D}_j}{\hat{D}_i + \hat{D}_j}\right) = \sqrt{\hat{D}_i} \cdot \sqrt{\hat{D}_j} \qquad (3.5\text{-}9)$$

The average nodal flux $\bar{\Phi}$ and the node mid-point flux Φ are transformed into the new variable ϕ, defined by:

$$\phi = \sqrt{\hat{D}}\ \Phi = S\sqrt{\hat{D}}\ \bar{\Phi} \qquad (3.5\text{-}10)$$

where S is a node size correction factor relating Φ to $\bar{\Phi}$.

Then introducing Equations (3.5-8) and (3.5-9) back into Equation (3.5-4) results in the following form for the equation after dividing by the nodal volume, V_i:

$$\left[\frac{D_i B_i^2 \Phi_i}{S_i\sqrt{\hat{D}_i}}\right] = \sum_{j=1}^{6} \frac{1}{h_{ij}^2}\left(\sqrt{\hat{D}_j}\,\Phi_i - \sqrt{\hat{D}_i}\,\Phi_j\right) \qquad (3.5\text{-}11)$$

From this expression one arrives readily at the nodal equation of POLCA as:

$$\Phi_i = \frac{\sqrt{\hat{D}_i}\left(\sum_{hor} \Phi_j + r\sum_{vert} \Phi_j\right)}{\sum_{hor}\sqrt{\hat{D}_j} + r\sum_{vert}\sqrt{\hat{D}_j} - \left\{C_i\right\}\frac{k_{\infty i}}{k_{eff}} - 1\Big\}\, h_x^{\,2}\Big\}} \qquad (3.5\text{-}12)$$

where

$$C_i = \sqrt{\hat{D}_i} \cdot \left\{ M_i^2 + C_B \tau_i^2 \left[\frac{k_{\infty i}}{k_{eff}} - 1 \right] \right\}^{-1} \qquad (3.5\text{-}13)$$

with

$$C_B = 1/3$$

$$\tau^2 = \left[\frac{1}{\left\{ \frac{4}{h_x^2} \right\} + \left\{ \frac{2}{h_z^2} \right\}} \right]$$

and

$$r = \left[h_x^2 / h_z^2 \right]$$

and where "hor" and "vert" refers to the horizontal and vertical neighbors of the node.

If the neighbor node j is the reflector, ϕ_j and $\hat{D}_j$, must be redefined in order to use the nodal equation given above. Using the familiar expression for partial currents:

$$J_{ij}^{\pm} = \left[\frac{\phi_{ij}}{4} \right] \pm \left[\frac{J_{ij}}{2} \right] \qquad (3.5\text{-}14)$$

along with the following definition for the albedo $\bar{a}$:

$$\bar{a} = \left[\frac{J_{ij}^-}{J_{ij}^+} \right] \qquad (3.5\text{-}15)$$

use of the nodal equation at the reflector requires:

$$\phi_j = 0 \text{ for j=reflector}$$

and

$$\hat{D}_j = \frac{2\bar{D}}{\left(\hat{D}_i + \frac{\bar{D}}{\hat{D}_i} \right)} \quad \text{for j = reflector} \qquad (3.5\text{-}16)$$

where

$$\bar{D} = \left(\frac{h_{ij}}{4}\right)\left(\frac{1 - \bar{a}}{\bar{i} + \bar{a}}\right) \qquad (3.5\text{-}17)$$

Use of these expressions for reflector nodes allows the nodal equation to be formally extended to include the reflector in its treatment.

POLCA requires the user to input several albedo values. Albedo values used to represent the reflector in the epithermal group calculations are input for plane surfaces, inner and outer corners, and the top and bottom reflector. Several albedo values are also input to modify the results at the reflector to account for thermal neutron effects.

POLCA is primarily a one group code, assuming that the thermal flux follows the epithermal flux through the relation:

$$\Phi_2 = \left[\frac{\Sigma_{rem}}{\Sigma a_2}\right] \Phi_1$$

POLCA, however, does modify the flux solution to account for thermal neutron migration and thus obtains solutions in good agreement with rigorous two-group diffusion theory.

The translation of neutron flux in node i to power in node i is done using the following equation:

$$P_i = \frac{e}{\nu} \cdot \frac{k_\infty}{k_{eff}} \cdot C \cdot \Phi_i \qquad (3.5\text{-}19)$$

where

e = energy per fission

and

$$C = \sqrt{\hat{D}_i} \cdot \left(M^2 + \frac{1}{3} \tau^2 \left(\frac{k_\infty}{k_{eff}} - 1 \right) \right)^{-1}$$

Both node powers ard fluxes are displayed in the POLCA output.

3.6 THERMAL-HYDRAULIC MODEL

In a BWR core simulator program the thermal hydraulics model has a significant effect on the calculated core reactivity and power distribution. The neutronic and thermal hydraulic models in POLCA are coupled through the power and void interaction encompassed in the power-void iteration loop of the code. This iteration uses the three-dimensional power distribution from the neutronics calculation directly in the evaluation of the three-dimensional void distribution. An iterative procedure is utilized until consistent power and void distributions are obtained from the calculations.

The thermal hydraulic calculation in POLCA is performed using a version of the thermal hydraulic program CONDOR,[19] which has been made an integral part of POLCA. The CONDOR model is used to determine the distribution of pressure, enthalpy, temperature, coolant flow, coolant void, heat flux and critical power ratio (CPR) at steady state conditions. The CONDOR model is capable of representing the entire reactor loop including the reactor coolant pumps, circulation loops, lower core plenum, reactor core, upper core plenum, and steam separators. In practice, a simplified model is used in conjunction with POLCA. Thermal hydraulic conditions in the core are defined by the thermal reactor power, total core recirculation flow, reactor pressure, feedwater enthalpy, as well as, the three-dimensional power distribution from the neutronics calculation. The water-steam properties needed in the CONDOR model are evaluated using standard international steam table functions.[20]

In the POLCA hydraulics model the total coolant flow entering the core is known. Computing the flow through each fuel assembly (channel) is the objective of the hydraulics calculation in POLCA. The three dimensional model for the reactor core is based on a nodal mesh description similiar to that used in the neutronics model. In the

radial direction each node corresponds to a fuel assembly or flow channel, which is consistent with the nodal geometry used in the neutronics model. In the axial direction, the number of nodes may differ from that used in the neutronics model. Normally the number of nodes in the hydraulics model is reduced to shorten the computation time, without introducing any significant error in the void distribution that is calculated. The code, however, does evaluate the coolant void distribution for the axial mesh of the neutronics model using interpolation. The flow regimes which can be represented in the CONDOR model are the single-phase, subcooled boiling, and bulk-boiling states.

The calculation begins at the core inlet and continues, by node, from the inlet to outlet node for each fuel assembly channel. The pressure drop across each node is evaluated, and when integrated over the entire channel, yields the total pressure drop for the assembly. Having obtained the total pressure drop for each assembly, the core average pressure drop is computed and the assemblywise flow distribution is evaluated. The code iterates on the flow distribution through each fuel assembly until the pressure drop calculated across each assembly is equal to the core pressure drop.

Once a converged flow distribution has been obtained, the three-dimensional void distribution is calculated using the void correlation described in Reference 19. This void distribution is coupled with the power distribution in the power-void loop in POLCA. Iterations between the void and power distributions continue until both the void and power distributions have converged.

3.7 POWER-VOID ITERATION

To assure consistency between the core power distribution and coolant void distribution within POLCA a computational loop has been incorporated into the code. This consistency is necessary because in a reactor core with a negative void coefficient, a decrease (increase) of the void fraction in one region of the reactor will, generally, bring about an increase (decrease) of the power in this region. This, in turn, tends to increase (decrease) again the void fraction in the region.

The computational loop that has been incorporated into POLCA involves using the three-dimensional power distribution from the neutronics calculation in determining the void distribution using the CONDOR hydraulics model. This resulting void distribution undergoes a "void-relaxation" and then is fed back into the neutronics model for calculating a new power distribution. This iterative procedure is followed until both the power and void distribution satisfy the specified convergence criteria.

The "void-relaxation" procedure is an iteration scheme for accelerating the convergence of the coolant void distribution. The algorithm to update the void distribution between iterations is accomplished in the void relaxation method as:

$$V'_n = V_n \cdot V_{acc} + V_{n-1} \cdot (1 - V_{acc}) \qquad (3.7\text{-}1)$$

where V_n is the unaccelerated void distribution of the n^{th} iteration and

$$V_{acc} = \frac{1}{1 + W_n} \qquad (3.7\text{-}2)$$

where W_n is the void acceleration factor for iteration n.

3.8 DEPLETION MODELS

The time dependent quantities which are dealt with by POLCA can be separated, in a natural way, into two groups. The first group are those quantities with a time constant of several days. This group consists of variables such as fuel burnup, burnup void factor and control rod history. The second group are those quantities with a time constant of a few hours. In this group are variables such as the fission products, xenon and iodine. In POLCA these groups have been separated so that the xenon concentration is assumed to be in equilbrium or constant during a burnup calculation. Likewise, no change in the burnup takes place during the time that xenon is not in equilibrium.

The nodal fuel burnup, Bu, is calculated for each period of operation by the relation:

$$Bu_i(t + \Delta t) = Bu_i(t) + P_i(t) \cdot \Delta Bu \qquad (3.8\text{-}1)$$

where

P_i = normalized power density in node i
ΔBu = core burnup interval at full power

This expression assumes the power distribution in the core as constant during the time period and that the fuel density, on the average, per node is the same throughout the core. The Haling method where the power and burnup are in equilbrium at the end of cycle requires this relation of burnup to be modified according to:

$$Bu_i(t + \Delta t) = Bu_i(t) + P_i(t + \Delta t) \cdot \Delta Bu \cdot \qquad (3.8\text{-}2)$$

Since the steam content affects the neutron spectrum and thus the fuel nuclide composition, especially the plutonium concentration, the average void fraction during the burnup history of the fuel is of importance. This void history is accounted for by an effective burnup - averaged void, α, which is related to the instantaneous void, V, by:

$$\alpha_i\ (t + \Delta t) = \alpha_i(t) + \left\{\frac{V_i(t) \cdot P_i(t)}{Bu_i(t)} \cdot \Delta Bu\right\} \Big/ \left\{1 + \frac{P_i(t) \cdot \Delta Bu}{Bu_i(t)}\right\} \qquad (3.8\text{-}3)$$

Control rods will also affect the fuel composition in those parts of the core where rods have been inserted during some burnup interval. This effect is similar to that from an increased void fraction during the burnup interval. Therefore, the control rod history is treated as an "equivalent void history" contribution, $\Delta\alpha$, which is accounted for separately for each burnup interval. The contribution is added to the nodal void history prior to interpolating for the nodal cross-section parameters.

The differential equations that describe the concentration of I-135 and Xe-135 can be analytically solved when the nodal power is assumed constant during a time increment, Δt. For transient calculations, relatively long time intervals can be used since xenon feedback to power is an order of magnitude less than the effect of power on the xenon concentration. Thus, Δt can be a value up to several hours where the power in each node is assumed constant.

The concentration of the fission products Xe-135 and its precursor I-135 is defined for each node by the following equations.

$$\frac{dI(t)}{dt} = \gamma_I \Sigma_f \phi - \lambda_I I(t) \qquad (3.8\text{-}4)$$

$$\frac{dXe(t)}{dt} = \gamma_{Xe} \Sigma_f \phi + \lambda_I I(t) - \lambda_{Xe} Xe(t) - \sigma_{Xe} \phi_2 Xe(t) \qquad (3.8\text{-}5)$$

where I(t) and Xe(t) are the atom number densities of I-135 and Xe-135, λ_I, λ_{xe} their decay constants, Y_I, Y_{xe} their fission yield fractions, σ_{xe} the thermal absorption cross-section for xenon and the reaction rate $\Sigma_f\phi$ are summed over both groups using

$$\phi_2 = \phi_1 \frac{\Sigma_{rem}}{\Sigma_{a2}} \tag{3.8-6}$$

For equilibrium conditions, the derivatives are zero, which results in the following equations:

$$I(t) = \frac{Y_I \ \Sigma_f\phi}{\lambda_I} \tag{3.8-7}$$

$$Xe\ (t) = \frac{(Y_I + Y_{Xe})\ \Sigma_f\phi}{\lambda_{xe} + \sigma_{xe}\ \phi_2} \tag{3.8-8}$$

For transient cases, using a time step of Δt, the I-135 and Xe-135 concentrations are solved for by:

$$I\ (t + \Delta t) = I(t)\ EXP\ (-\lambda_I \cdot \Delta t) + \frac{Y_I \Sigma_f\phi}{\lambda_I}\ (1 - EXP\ (\lambda_I \cdot \Delta t)) \tag{3.8-9}$$

$$Xe\ (t + \Delta t) = Xe\ (t)\ EXP\ (-(\lambda_{xe} + \sigma_{xe}\ \phi_2) \cdot \Delta t) + \tag{3.8-10}$$

$$\frac{(Y_I + Y_{xe})\ \Sigma_f\phi}{(\lambda_{xe} + \sigma_{xe}\ \phi_2)} \left\{1 - EXP\left\{-(\lambda_{xe} + \sigma_{xe}\ \phi_2) \cdot \Delta t\right\}\right\} +$$

$$\frac{(\lambda_I\ I(t) - Y_I\ \Sigma_f\ \phi)}{(\lambda_{xe} + \sigma_{xe}\ \phi_2 - \lambda_I)} \left\{EXP\left\{-\lambda_I \cdot \Delta t\right\} - EXP\left\{-(\lambda_{xe} + \sigma_{xe}\ \phi_2) \cdot \Delta t\right\}\right\}$$

3.9 THERMAL LIMITS

The thermal limits of primary interest in BWR core calculations are peaking factors, linear heat generation rates and the margins to boiling transition (dry-out). Prediction of these parameters can be made from the POLCA three dimensional core calculation coupled with the lattice physics results from PHOENIX.

Peaking Factors

The peaking factors of interest in a BWR are (1) the lattice peaking factor (F_L); (2) the radial bundle peaking factor (F_R); (3) the axial assembly peaking factor (F_A); (4) the gross peaking factor (F_G); and (5) the total peaking factor (F_T). The first of these peaking factors is determined by PHOENIX for each fuel lattice configuration and is defined as the following:

$$F_L \equiv \frac{\text{Maximum rod heat flux in assembly at given elevation}}{\text{Average rod heat flux in assembly at same elevation}}$$

These numbers, F_L's, are listed directly by PHOENIX and are edited as a function of burnup, void, and fuel type by PHIPO for use in POLCA.

The radial bundle peaking factor (F_R), the axial assembly peaking factor (F_A), and the gross peaking factor (F_G) can all be obtained from the POLCA 3D calculations. Recognizing that POLCA is a nodal code with one node per assembly radially and up to 25 nodes per assembly axially, these peaking factors are defined as follows:

$$F_R \equiv \frac{\text{Axial average of node powers in assembly of interest}}{\text{Average of the axial averaged node powers of all assemblies in core}}$$

$$F_A \equiv \frac{\text{Node power at axial node of interest in assembly}}{\text{Average of all node powers in same assembly}}$$

$$F_G \equiv \frac{\text{Node power at node of interest in core}}{\text{Average node power in core}}$$

F_R and F_G are listed directly by POLCA. F_A is easily obtained from the axial nodal power edit given for each assembly.

The total peaking factor is defined as the heat flux of a particular rod of interest at an axial point of that rod compared to the heat flux averaged radially and axially over all the rods in the core. The total peaking factor can be calculated from the following expression:

$$F_T = F_L \cdot F_G \qquad (3.9\text{-}1)$$

where F_L is determined from PHOENIX calculations and F_G is calculated by POLCA. POLCA calculates the maximum total peaking factor at each node using the above equation.

LHGR and APLHGR

Two thermal parameters used in the thermal analyses of BWRs are the linear heat generation rate (LHGR) and the average planar linear heat generation rate (APLHGR).

The LHGR is defined as the power per unit length (kw/ft) produced by a fuel rod at a point of interest. Since maximum values of this parameter are of interest, POLCA calculates the maximum LHGR at each node using the following equation:

$$LHGR_i = \frac{P_i}{n_i \times h_z} \times F_{Li} \qquad (3.9\text{-}2)$$

where

P_i is the node power of the ith node

n_i is the number of rods in the assembly type corresponding to node i

h_z is the axial length of the node

F_{Li} is the lattice peaking factor for the highest power fuel rod in the fuel lattice configuration at node i

POLCA lists the values of $LHGR_i$ defined above for each node and the value and location of the maximum $LHGR_i$ for each fuel type.

APLHGR (average planar linear heat generation rate) is the LHGR for the average rod in an assembly plane of interest. APLHGR is calculated in POLCA at each node by the following equation:

$$APLHGR_i = \frac{P_i}{n_i \times h_z} \qquad (3.9\text{-}3)$$

POLCA lists APLHGR values for each node as well as the value and location of the maximum $APLHGR_i$ for each fuel type.

Critical Power Ratio

BWR fuel assemblies must be operated such that boiling transition, the transition from nucleate to film boiling, will not occur. Thermal margin to boiling transition is expressed through the critical power ratio or CPR. The CPR is defined as the ratio of the assembly power required to initiate boiling transition anywhere in the assembly to the operating power of the assembly of interest.

POLCA uses a correlation developed by ASEA-ATOM, termed the AA-74 correlation, which predicts boiling transition assembly powers using assembly cross-section average flow parameters. CPR values are then calculated by ratioing the boiling transition powers and the operating assembly powers. At present, the AA-74 correlation has been verified for the ASEA-ATOM 8x8 bundle design. Modifications to the correlation will be made to enable CPR evaluation of reload fuel.

3.10 SPECIAL FEATURES

POLCA has several special features available to the user including the option to determine simulated detector signals, perform cold reactivity calculations, and to adjust flow or power to obtain predetermined reactivity levels. In addition auxiliary codes exist to aid the user in preparing input for POLCA, performing manual and automatic refueling, optimizing preliminary loading patterns, estimating shutdown margin, and determining residual burnable absorber worth.

1. Simulated In-Core Detector Signals

An important result of the POLCA calculation for use in comparing POLCA results to measurements is the simulation of the signals from the 100 to 150 neutron flux detectors in the core. These detector signals supply the most important and the most accessible information concerning the actual power distribution in the reactor core. The actual detector signal is, in the first approximation, proportional to the neutron flux in the detector position.

Because POLCA does not supply sufficient details about the neutron flux, the detector signals must be calculated with the help of the power distribution in the surroundings of the detector. The detector reading can be considered to be proportional to the power in the adjacent nodes of the horizontal plane of the detector. The absolute reading is not of utmost importance due to the intercalibration of the detectors. What is important and is calculated is the relative signal intensity.

The constants of proportionality between the power and detector signal, K_i, are determined by PHOENIX and supplied to POLCA as function of burnup, void and fuel type. There also is a very strong dependency to control rods inserted in the vicinity of the detectors. The control rod

effect depends on the distance of the control rod to the detector. For this reason, correction factors, KSS_i, are used. The exact position of the detector must be represented in PHOENIX to generate the K_i and KSS_i tables.

The average detector reading is calculated in POLCA as:

$$D = \frac{1}{N} \sum_{i=1}^{N} \frac{P_i}{K_i \times KSS_i} \qquad (3.10\text{-}1)$$

where

P_i = the power in node i

N = the number of nodes that are represented by the detector.

In POLCA the detectors can be placed at any arbitrary location in the vertical direction. The calculated detector signals are linearly weighted using the nodal powers above and below the detector position. The simulated detector signals are determined for both the traveling in-core probes (TIP) and the local power range monitors (LPRM).

2. Cold Reactivity Calculations

POLCA can perform calculations at temperatures below the hot full power operating temperature. The user must input the cross-section table set corresponding to the temperature at which he wants the calculation done. The calculation is then performed in the same manner as a "hot" POLCA calculation.

3. Flow and Power Searches

POLCA has the capability of automatically varying pump speed (flow) or power to maintain a previously determined reactivity level. If the user wishes to maintain constant power then POLCA will automatically adjust

pump speed to maintain reactivity. Similarly, if the user desires to keep flow constant, power is adjusted to maintain reactivity. POLCA assumes the following equation relates reactivity to flow and power:

$$dk_{eff} = \left[\frac{\partial K_{eff}}{\partial W}\right]_P dW + \left[\frac{\partial K_{eff}}{\partial P}\right]_W dP = \left(\frac{dW}{W}\right) C_1 + \left(\frac{dP}{P}\right) C_2 \qquad (3.10\text{-}2)$$

where W and P are the core flow and power, respectively, and C_1 and C_2 are constants determined by POLCA.

3.11 INPUT/OUTPUT

The majority of the input to POLCA is of the free format type based on a designated "keyword" identifier. The input parameters are divided into several groups, in such a way that closely related data have been assigned to the same group. The groups of data include: geometric data, lattice cell data in the form of parameter tables, control rod data, neutron detector data, and thermal-hydraulic data.

The calculational results are generally displayed in self-explanatory tables and diagrams. Most of the three dimensional distributions can be written to magnetic tape for subsequent use either as a precondition for another POLCA calculation or for use by the various auxiliary programs.

The parameters which are output by POLCA include global values of reactivity, core pressure drop and flow through the core. The three dimensional distributions which are available as output include power, burnup, flux, coolant flow, iodine and xenon concentrations. Other useful parameters output are thermal margins (CPR, LHGR, APLHGR), and predicted detector signals for both the traveling incore probes (TIP) and local power range monitors (LPRM).

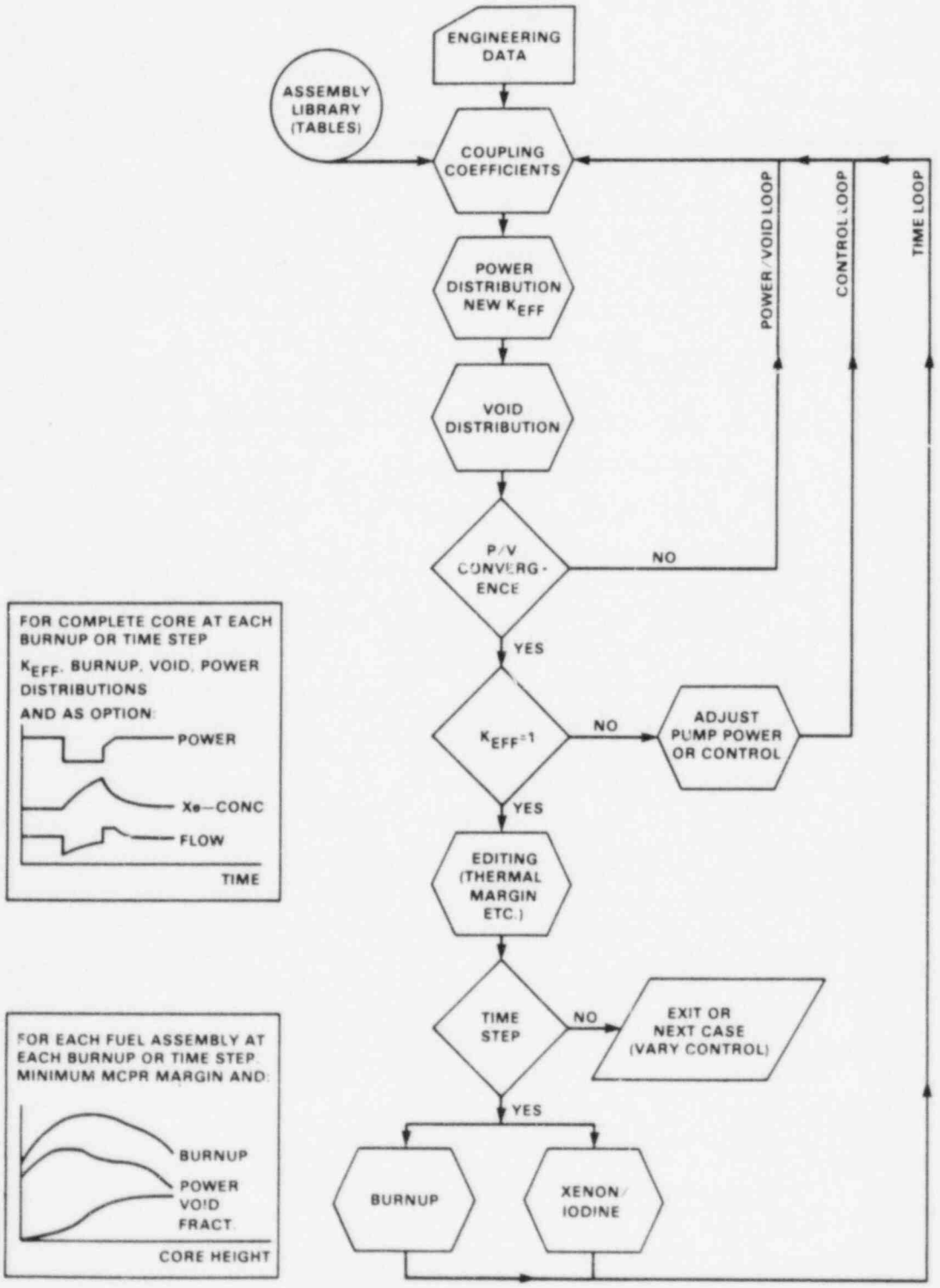

FIGURE 3-1: POLCA Calculational Flow Design

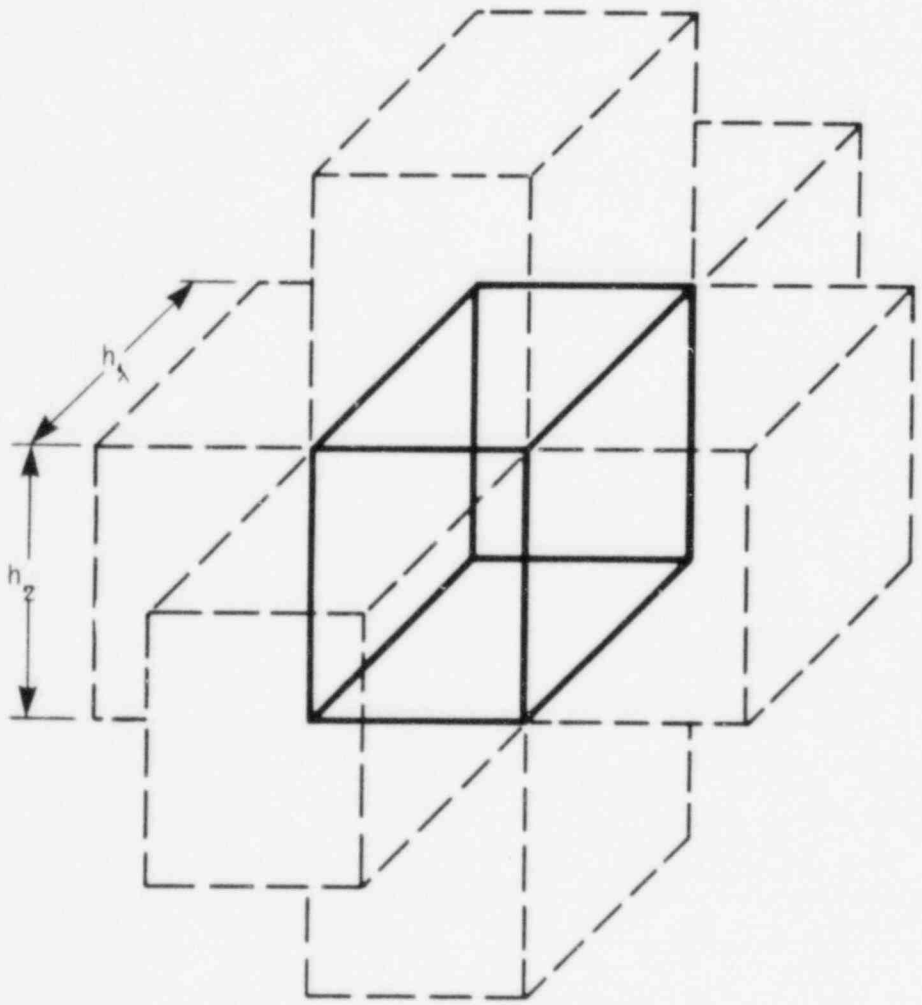

FIGURE 3-2: POLCA Nodal Geometry Of Six Nearest Neighbor Nodes

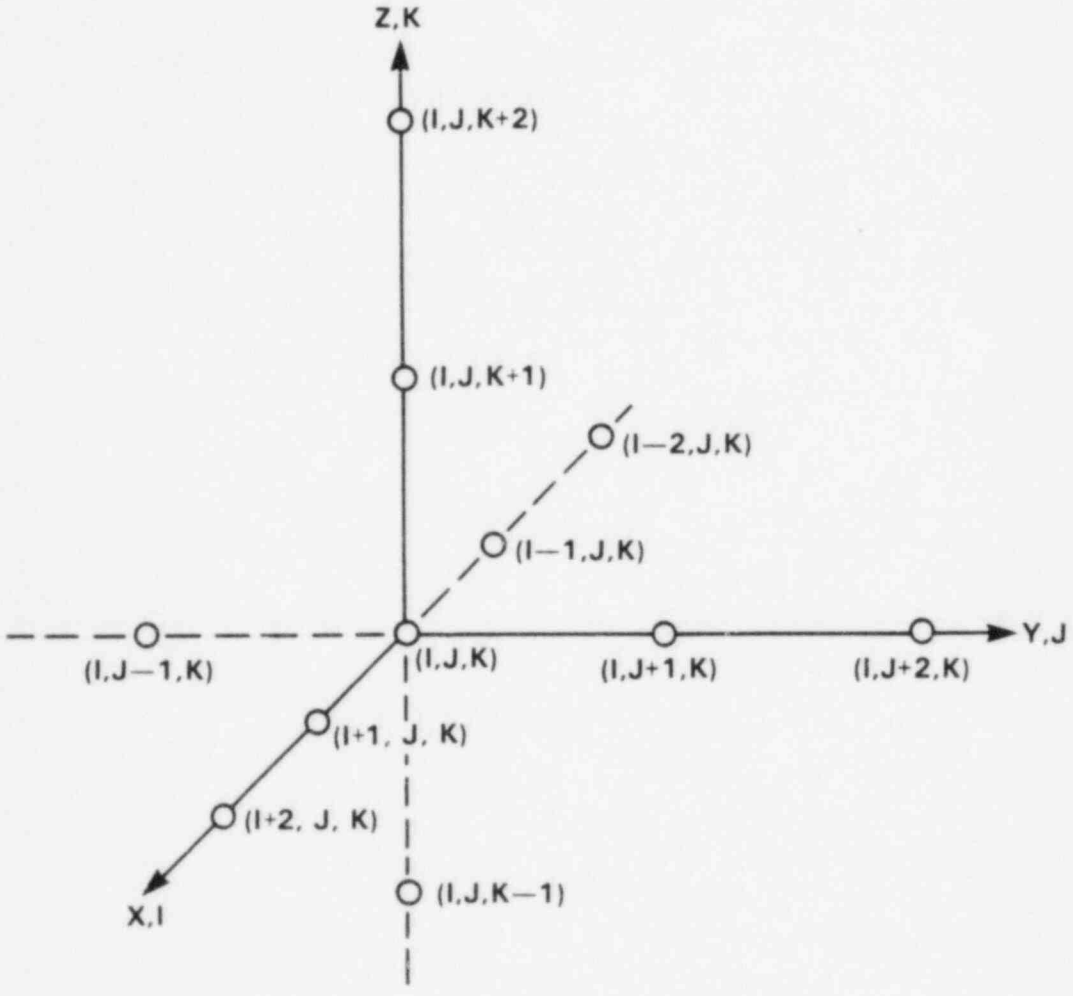

FIGURE 3-3: POLCA Coordinate System

4.0 AUXILIARY CODES

4.1 FOBUS

FOBUS is a Monte Carlo transport theory program that calculates the burnable absorber microscopic cross-sections as a function of the depletion of the absorber. These cross-sections are added to the PHOENIX cross-section library by the PHOEBE processing program. The program is two dimensional in (R,Z) geometry and can accommodate up to 25 energy groups. FOBUS can model both discrete and integral absorbers. The integral absorber may be homogeneously distributed over the entire fuel column or can be in the form of discs separated by one or more absorber-free fuel pellets. FOBUS can use up to 195 regions to model the absorber pin consisting of up to 15 radial zones and 13 axial segments.

The Monte Carlo calculation is only used to determine the perturbation on the flux distribution and reactivity that results when the absorber is introduced. A simpler and faster flux solution is obtained for the unperturbed case where the absorber is absent. FOBUS assumes a 3x3 fuel array (See Figure 4-1) for its geometry - the absorber is taken to be at the central pin location. Isotropic (white) boundary conditions are assumed at the boundary of the 3x3 fuel pin geometry. FOBUS first solves for the flux distribution with the absorber absent using the multigroup PHOENIX macroscopic cross-sections input for each pin region (pellet, cladding, and surrounding coolant). At the user's option, the unperturbed average neutron spectrum can be input and FOBUS will re-normalize the calculated spectrum to the input spectrum. Thus, FOBUS permits the user to input the actual spectrum present at the absorber location in the bundle. This spectrum could be that calculated by PHOENIX, for example. The anisotropy of the unperturbed flux, ϕ_0, is described by a P-3 expansion of the scattering cross-section which preserves both the isotropic flux and the current in the z direction.

The flux perturbation, $\tilde{\phi}$, resulting from the introduction of the absorber in a volume V, can be proven to be made up exclusively of neutrons produced by the surface source at the absorber boundary where the source Q_S is defined as

$$Q_S = \phi_o (E, \vec{\Omega}, \vec{r}) \cdot (\vec{\Omega} \cdot \vec{n}) \qquad (4.1\text{-}1)$$

ϕ_o represents the unperturbed angular flux directed inward toward the absorber at the surface and $\vec{n}$ is a unit surface vector normal to the absorber surface. The flux perturbation, $\tilde{\phi}$, is equal to $\phi - \phi_o$ outside of the absorber region and is equal to ϕ inside the absorber where ϕ_o represents the unperturbed flux before the introduction of the absorber and ϕ is the flux distribution after the insertion of the absorber. The fission source distribution is assumed to remain unchanged with the introduction of the absorber.

Prior to calculating the flux perturbation $\tilde{\phi}$, FOBUS simplifies the geometry to include only the single cylindrical absorber pin surrounded by a circular buffer region. A flux-volume weighting of all materials making up the non-absorber fuel pins in the 3x3 fuel array is performed using the unperturbed flux distribution. The Monte Carlo calculation is then made for the single absorber pin and buffer cylindrical cell using the neutron source spatial distribution determined according to Eq. (4.1-1). An isotropic (white) boundary condition is applied at the buffer boundary. FOBUS selects the rays for the Monte Carlo source neutrons in a manner that assures good statistics. The energy distribution of the neutron source is specified by the user in the input.

Since up to 195 regions are used in FOBUS to represent the absorber pins the distribution of the absorption and depletion of the nuclides in the absorber pin is determined with high accuracy. The basic output of FOBUS is a tabulation of the multigroup (up to 25 energy groups) microscopic absorption cross-sections as a function of the pin-averaged fraction of the absorber remaining. This data is processed by the

PHOEBE program which adds the cross-section to the PHOENIX cross-section library. In the case of gadolinium as the burnable absorber, FOBUS only depletes the odd-numbered Gd-155 and Gd-157 isotopes which are the pre-dominant absorbers. An empirical correction is used with POLCA to correct for the residual reactivity penalty due to the even-numbered Gd-156 and Gd-158 isotopes. In the specific case of gadolinium, the user may elect to have FOBUS determine the time steps to use for the absorber depletion calculation. An empirical relation is used by FOBUS to determine the step size. This relation is dependent on the gadolinium initial loading and concentration.

4.2 PHOEBE

PHOEBE is a library processing program to construct or modify a nuclear cross-section data library for use by the PHOENIX code. The nuclear data library produced by PHOEBE is specifically designed for use with the lattice physics code PHOENIX. Like most other libraries being used by lattice cell codes, the energy range (10 Mev to 0.0 ev) is discretized to a 25 energy group structure. However, the library used by PHOENIX differs from most libraries in that the data is stored in a random access mode, such that each single data entry is directly accessible by PHOENIX, therefore minimizing the file manipulations (rewinding, backspacing, record skipping) between data accesses. The library is also different in that the data is not stored by element but rather by energy group. This is done to improve computer resource utilization.

The main function of the PHOEBE code is to create a nuclear data library file in a format acceptable to PHOENIX. There are two main sources for the nuclear data that is processed by PHOEBE in creating the PHOENIX library. The major source of the nuclear data is the WIMS nuclear cross-section library. For each nuclide, a microscopic cross-section set is accepted containing absorption, fission, nu-fission, transport, scattering matrix, fission spectrum, yields, decay constants, energy per fission and delayed neutron fractions. Also included are the tabulations of resonance integrals as a function of the potential scattering cross-sections and temperature. The other source of nuclear cross-section data is the two-dimensional Monte Carlo program FOBUS. From FOBUS comes microscopic cross-sections for the burnable absorber materials as a function of the fraction of burnable absorber remaining. The nuclear cross-section data accepted by PHOEBE is in card image format where a keyword identifer is used to identify each individual data set.

The PHOEBE program is also capable of modifying a PHOENIX library previously created by PHOEBE. The program allows selective changes to be made to existing data on the library, as well as, to add or delete

nuclides from the PHOENIX library. The library produced by PHOEBE contains identifying information such as the date the library was created, the number of energy groups, and a list of all nuclides on the library. The cross-section and resonance data stored on the library is divided into two groups, the group independent and group dependent data. The group independent data includes addressing information, temperatures, potential scattering cross-sections, etc. The group dependent data includes the cross-section sets, smooth resonance data, and the resonance integral tables.

4.3 PHIPO

PHIPO is the linking code between PHOENIX and POLCA. PHIPO reads PHOENIX magnetic output tapes and from these generates input for POLCA including controlled and uncontrolled cross-section tables, xenon cross-section coefficients, internal peaking factor tables, Doppler feedback constants, detector constants, and C-factors.

POLCA requires cross-section tables as a function of burnup void (void fraction used in depletion calculation), void-tree void (branch case void fraction), and burnup. POLCA cross-section tables are constructed by running a series of PHOENIX depletions for each fuel type. Each PHOENIX series has several different burnup void cases with an equal number of void-tree voids (branch cases) run for each burnup void. PHIPO reads the magnetic output tape of a PHOENIX series and constructs the cross-section tables for the fuel type corresponding to the series in POLCA format. The POLCA cross-section tables constructed by PHIPO can be input as cards or POLCA can read them from tape. Normally, a POLCA cross-section table will have four burnup voids (typically, 0, 25, 50 and 75% void) with four void tree voids at 9 or 10 burnup steps for each fuel type.

Since POLCA treats xenon explicitly, POLCA requires as input the microscopic absorption cross-sections for xenon. PHIPO reads the xenon microscopic absorption cross-sections from PHOENIX as a function of burnup and void fraction. It then calculates coefficients to fit these xenon microscopic cross-sections as a function of burnup and void fraction. These coefficients are output in a format which is then read by POLCA. A set of xenon coefficients is generated for each fuel type.

The Doppler correction effect is accounted for in POLCA by an adjustment to k_∞ for fuel temperature differences from that used in the PHOENIX cross-section table calculations. Generally, the void effect on the Doppler coefficients is determined by calculations done at beginning of assembly life with equilibrium xenon at four different void fractions (0%, 25%, 50% and 75%). The burnup variation on the Doppler

coefficients is determined by PHIPO from PHOENIX branch calculations with a fuel temperature different than that in the cross-section table at about 10 depletion steps in a 50% burnup void fraction PHOENIX depletion calculation. PHIPO, after determining the fitting coefficients for the correlation puts these in a form that POLCA can read as input. The Doppler fitting coefficients are calculated for each fuel type.

POLCA models the effect of control rods by using Σ_{a1} and Σ_{a2} values corresponding to controlled fuel of the fuel type being modeled. Other cross-section parameters are taken from uncontrolled fuel of the same fuel type. PHIPO sets up tables of Σ_{a1} and Σ_{a2} for controlled fuel from PHOENIX branch calculations performed with control rods modeled. Normal practice for the PHOENIX control branch calculation is the same as that used in Doppler branch calculations. The void dependence is determined by control branches run at the beginning of assembly life depletion steps (equilibrium xenon) at four void fractions (0%, 25%, 50%, 75%). The burnup effect is determined from control branches done at about 10 depletion steps in a 50% burnup void PHOENIX depletion calculation. The tables of Σ_{a1} and Σ_{a2} are thus a function of fuel type, burnup, and void and are set up by PHIPO in a form acceptable to POLCA.

PHIPO handles cold cross-sections and rodded cross-sections in the same manner as hot cross-sections are handled. These are also set up in cross-section table sets as a function of burnup void, burnup, and fuel type in a format consistant with POLCA requirements.

PHIPO reads internal peaking factors for each assembly type and arranges them in tables as a function of burnup and burnup void consistent with POLCA input requirements. The same is done for the C-factors used in the CPR correlation to take into account the effect of the bundle internal power distribution on the critical power ratio.

An important part of the POLCA calculation is a simulation of neutron flux detector signals in the core. The detector constants are calculated by PHIPO from the fission rates in the detector which PHIPO reads from PHOENIX calculations in which the detector was modeled explicitly. All fission rates are normalized to the 1 MWD/MTU, 0% void burnup step of a user-chosen fuel type. The detector constants, K_i, at other void and burnup steps and for other fuel types are then calculated consistent with this normalization.

PHIPO tabulates the detector constants as a function of void and burnup in format consistent with POLCA input requirements.

4.4 POREF

POREF is a POLCA auxiliary code which performs manual refueling, and lays out the geometry of the refueled core for use in POLCA. POREF reads POLCA output tapes from the previous cycle POLCA depletion extracting burnups, void histories, control rod histories, and fuel types which are used in the refueled core. POREF has the capability to read two POLCA tapes - one from the previous cycle and one from another cycle to permit assembly reinsertion. POREF can be run in quarter, half, or full core configurations.

In addition to the information from the POLCA output tapes, POREF requires the composition and location of the feed assemblies. The user must also input all the burned assembly moves, the locations of reinserted assemblies and those assemblies which are to be removed from the core.

As output, POREF writes a magnetic tape containing the assembly locations, fuel types, burnup, void histories, and control rod histories for the refueled core. From the tape, POLCA can construct a complete data set for the refueled core.

4.5 ANALOAD

ANALOAD is a POLCA auxiliary code which allows automatic refueling from one cycle to another and will perform an optimization on the refueled core to meet user specified requirements. ANALOAD is run in two steps and forms part of a sequence with POLCA and POREF. This sequence is illustrated in Figure 4-2.

The first ANALOAD step takes as input the end-of-cycle (EOC) POLCA output tape from the previous cycle. The user inputs to ANALOAD the number and composition of the feed assemblies to be placed in the next cycle. In addition, the user provides a radial target reactivity distribution for the code to use as a basis for choosing assembly positions in the refueled core. ANALOAD then positions the feed assemblies in a pre-arranged pattern which the user has selected. Burned assemblies are graded according to reactivity and placed in the core in locations which are consistent with the target reactivity distribution. The code discharges as many assemblies as are loaded in the feed batch, choosing for discharge the assemblies with the lowest reactivity.

The output of a step 1 ANALOAD run is a set of input cards to the POREF code containing the necessary information to perform the refueling as determined by ANALOAD using the previous cycle EOC POLCA output. The user then runs POREF and then POLCA to establish a POLCA model for the next cycle. The user can use this model or, at his option, use ANALOAD to optimize the loading pattern as determined by the first step ANALOAD.

Optimization of the refueled core is performed by using ANALOAD in the second step mode, operating on the refuelled core obtained from the first step ANALOAD sequence. ANALOAD optimizes the refueled core to meet user-chosen values of three parameters: (1) peaking factor, (2) shutdown margin; and (3) EOC reactivity. ANALOAD makes fuel shuffling changes based on perturbation analyses on these optimization parameters. ANALOAD then modifies the POREF deck output from the step 1 ANALOAD sequence to reflect the new shuffle. POREF and POLCA are then run in sequence to complete the development of the optimized POLCA model. ANALOAD can be run in quarter, half or full core configurations.

4.6 STROD and BAREST

Two other auxiliary codes to POLCA are STROD and BAREST. The purpose of the STROD code is to give an easily reviewed preliminary analysis of shutdown margin. The code requires that the k_∞ distribution of the core be known. The analysis is then performed by a local homogenization of fuel around withdrawn control rods with the aid of predetermined weight factors. POLCA is then run examining the most reactive areas of the core, as indicated by STROD, to finalize the shutdown margin calculation.

BAREST is used to determine the detailed distribution of burnable absorber remaining in the core during the operating cycle. BAREST reads the POLCA dump tape and determines the residual reactivity worth of Gd-155 and Gd-157 for each node. The program can also be used to make a detailed study of other reactivity differences dependent on fuel type such as a change in enrichment.

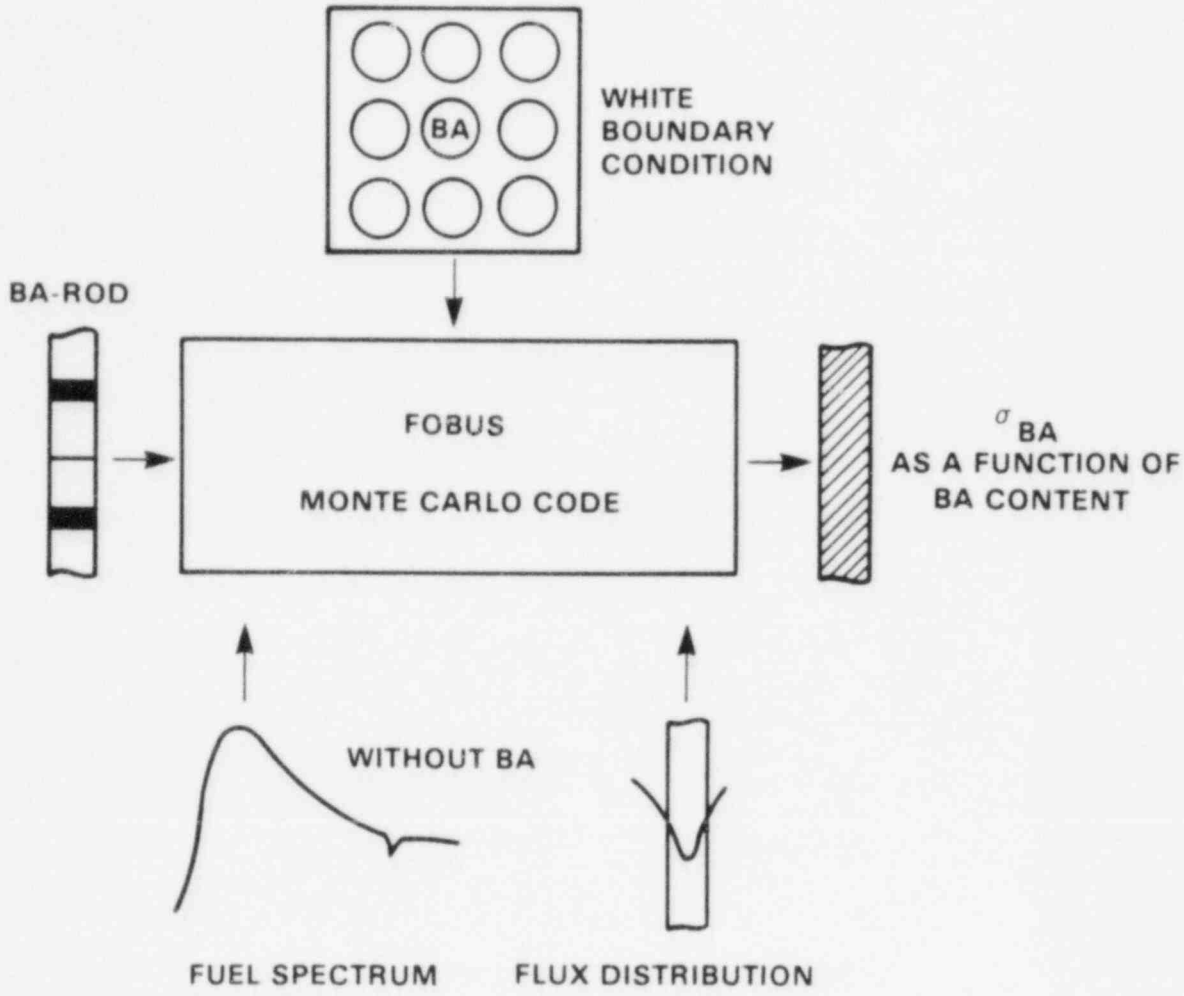

FIGURE 4-1: FOBUS Code

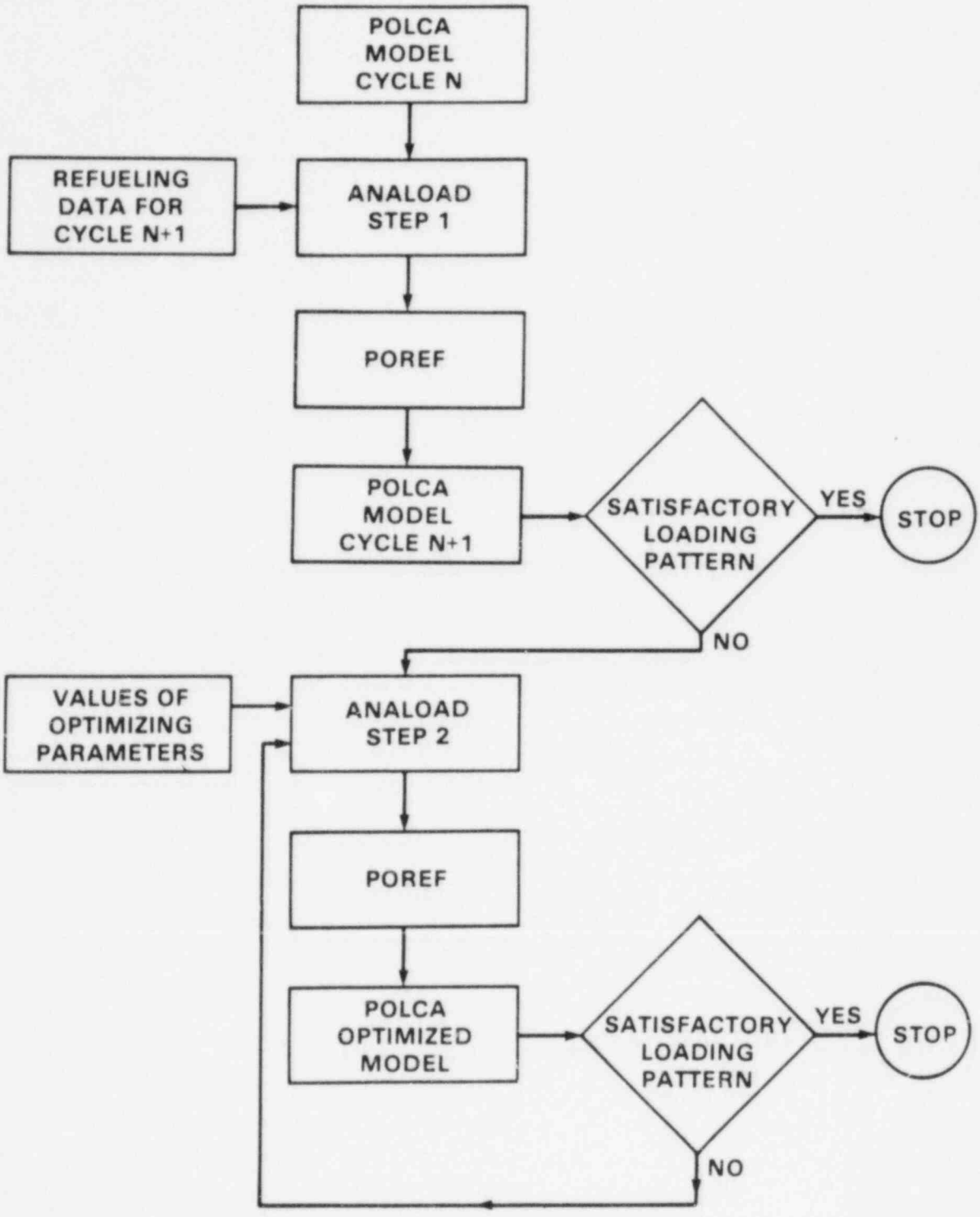

FIGURE 4-2: POLCA Sequence For Refueling

5.0 CONCLUSIONS

The calculational models used in the nuclear design and analysis of boiling water reactor cores have been described in this report. The major areas addressed are the lattice physics code PHOENIX in Section 2, and the nuclear and thermal-hydraulic core simulator code POLCA in Section 3. Section 4 addresses the auxiliary codes wnich support the PHOENIX and POLCA codes.

PHOENIX is a state-of-the-art computer code capable of accurately calculating the lattice physics behavior of BWR and PWR fuel assemblies and providing all constants required in modelling BWR assemblies in the three-dimensional core simulator code POLCA. The use of the multigroup nodal calculations at the pin cell level combined with the S_4 two-dimensional transport theory SFINX calculation for the assembly provides accurate and detailed multigroup flux distributions, reaction rates, and macroscopic cross-sections. PHOENIX uses accurate and advanced models for resonance absorption effects, burnable absorbers, control rods, and in-core neutron flux detectors. To fulfill its role in the generation of constants for POLCA, PHOENIX provides a full range of calculations including fuel and burnable absorber depletion, as well as, branch calculations as a function of void, fuel temperatures and the control rod presence.

POLCA is a three-dimensional code capable of accurately simulating the nuclear, thermal and hydraulic conditions in BWRs. Use of a modified one group nodal method for the neutronics coupled with the integral CONDOR calculation for the thermal-hydraulics provides realistic simulation of all important phenomena in a BWR that must be correctly modelled by a simulator code. POLCA permits an accurate evaluation of the thermal margins and the state of the reactor for varying power and flow conditions. POLCA correctly simulates all important reactivity effects including fuel depletion, xenon distribution effects, fuel and coolant temperature effects, void distribution effects, and the influence of control rods. POLCA also accurately simulates the signals from the in-core flux detectors.

The auxiliary codes facilitate the use of PHOENIX and POLCA. Capabilities provided by these auxiliary codes include: a) preparation of the nuclear data library for PHOENIX; b) data transfer between PHOENIX and POLCA; and c) fuel shuffling and loading pattern optimization for refueling.

From the discussions and descriptions included in this report, it is clear that the nuclear design code system represents state-of-the-art methodology that provides the full range of nuclear design and analysis capabilities required for the analysis and design of boiling water reactor cores, including the following applications:

- Power distribution calculations
- Thermal-hydraulic calculations
- Fuel management calculations
- Control rod worth and shutdown margin calculations
- Generation of control rod pattern sequences
- Thermal margin evaluations
- Reactivity coefficients and kinetics parameters
- In-core detector simulation
- Core reactivity calculations
- Generation of process computer constants
- Generation of power to flow control lines
- Simulation of normal operation power maneuvers including load follow

6.0 REFERENCES

1. Askew, J. R., F. J. Fayers, and P.B. Kemshell, "A General Description of the Lattice Code WIMS," Journal of British Nuclear Energy Society, 5, pp. 564-584 (1966).

2. Story, J. S., et al., "Evaluation, Storage and Processing of Nuclear Data for Reactor Calculations," in Proceedings of the Third International Conference on the Peaceful Uses of Atomic Energy, Geneva, 1964, Vol. 2, pp. 168-176, United Nations, New York, (1965).

3. Brissenden, R. J. and C. Durston, "The Calculation of Neutron Spectra in the Doppler Region," in Proc. of the Conference on the Application of Computing Methods to Reactor Problems, pp. 51-76, ANL-7050, (August 1965).

4. Fayers, F. J., P. B. Kemshell, M. J. Terry, "An Evaluation of Some Uncertainties in the Comparison Between Theory and Experiment for Regular Light Water Lattices," Journal of British Nuclear Energy Society, 6, pp. 161-181 (1967).

5. Hellens, R. L. and G. Price, "Reactor Physics Data for Water Moderated Lattices of Slightly Enriched Uranium," Reactor Technology-Selected-Reviews," p. 529, USAEC Division of Technical Information (1965).

6. De Saussure, G., et. al, "Measurement of the U^{235} Capture-to-Fission-Ratio, α, for Incident Neutron Energies from 3.25 eV to Neutron 1.8 keV," Nucl Sci. Eng. 23, p. 45 (1965).

7. Taubman, C. J., "The WIMS 69 - Group Library Tape 166259," AEEW-M-1324 (July 1975).

8. Goldstein, R., and E. R. Cohen, "Theory of Resonance Absorption of Neutrons," Nuclear Science and Engineering, 13, pp. 132-140 (1962).

9. Stamm'ler R. J. J., J. Blomstrand and Z. J. Weiss, "Equivalence Relations for Resonance Integral Calculations," J Nuclear Energy 27, pp. 885-888 (1973).

10. Wigner, E. P., E. Creutz, H. Jupnik and T. Snyder, "Resonance Absorption of Neutrons by Spheres," J. Appl. Phys. 26, pp. 260-270 (1955).

11. Carlvik, I., "A Simplified Treatment of Spectrum Hardening in a Fuel Rod Caused by Selective Absorption," AB Atomenergi (Internal Report), RFR-174, Stockholm (1962).

12. Weiss, Z., and R. Stamm'ler, "Nodal Coupling of Heterogeneous Pin Cells," Trans Am. Nucl. Soc. 26, p. 223-224 (1977).

13. Carlvik, I., "A Method for Calculating Collision Probabilities in General Cylindrical Geometry and Applications to Flux Distributions and Dancoff Factors," in Proc. of the Third International Conf. on the Peaceful Uses of Atomic Energy, Geneva, 1964, Vol. 2, pp. 225-233, United Nations, New York, (1965).

14. Stamm'ler R. J., "Methods Used in the Design of Fuel Assemblies - 2D Sn Calculations," in Numerical Reactor Calculations-IAEA, Proc. Series No. 307, pp. 3-49, Vienna, IAEA, (1972).

15. Carlson, B. G. and K. D. Lathrop, "Transport Theory-The Method of Discrete Ordinates," in Computing Methods in Reactor Physics, pp. 171-266, Gordon and Breach, New York, (1968).

16. England, T. R., "CINDER-A One Point Depletion and Fission Product Program," WAPD-TM-334, (August 1962).

17. Butland, A. T. D. and C. T. Chudley, "Examination of Thermal Neutron Scattering Models for Light and Heavy Water by Comparison with Diffusion and Cross-Section Data," J. Br. Nucl. Energy Soc., 13, pp. 99-114 (1974).

18. Borresen, S., " Simplified Coarse-Mesh, Three-Dimensional Diffusion Scheme for Calculating the Gross Power Distribution in a Boiling Water Reactor," Nucl. Sci. Eng. 44, pp. 37-43, (1971).

19. Olson, C. A., "CONDOR-A Thermal-Hydraulic Performance Code for Boiling Water Reactors," WCAP-10108, (June 1982).

20. Schmidt, E., Properties of Water and Steam in SI-units, Springer-Verlag, New York, (1969).

RESPONSES TO NRC QUESTIONS

Note: The document has been revised to correct the typographical errors identified in the NRC questions 4, 14 and 23, relating to the PHOENIX program.

QUESTIONS ON WESTINGHOUSE NUCLEAR DESIGN PROGRAMS
FOR BOILING WATER REACTORS - WCAP 10106

PHOENIX Program

1. Question

What is the impact of neglecting resonance absorption in Pu-240, Pu-241, and Pu-242 on calculations of reactivity vs. burnup as well as Doppler coefficients?

Answer

In Section 2.2 (p. 2-3) of the topical, the statement is made that PHOENIX treats only U-235, U-236, U-238, and Pu-239 as resonance absorber nuclides. What is intended by that is that these isotopes occur in sufficient concentrations that resonance spatial self-shielding must be accounted for. For the remaining resonance absorbers, such as Pu-240, Pu-241 and Pu-242, the infinite dilution resonance integral (RI) data is taken directly from the library. For U-235, U-236, U-238 and Pu-239, the resonance integral (RI) data is given in the cross-section library as a function of resonance fuel temperature and background scattering cross-section, σ_p (e.g., potential scattering cross-section per absorber atom). A two-term rational approximation is made which leads to an equivalence relation for the heterogeneous case RI. Thus, the heterogeneous case RI is transformed into a linear combination of two homogeneous RI's. The homogeneous RI's are then interpolated from the RI library at the appropriate effective background cross-sections. Interpolation in the RI tables is linear in $\sqrt{\sigma_p}$. The remaining resonance absorbers, such as Pu-240, Pu-241 and Pu-242, are present in low enough concentrations that the infinite dilution RI data can be used. The large 1.056 eV Pu-240 resonance is treated explicitly by the fine group division of the WIMS 69 group library. This library has 12 energy groups in the range from 0.78 eV to 1.3 eV where the total microscopic

cross-section of Pu-240 is greater than 1000 barns. The 25 group WIMS library used for standard PHOENIX calculations is derived by condensation of the 69 group constants.

2. Question

Are the temperatures in Table 2-3 for C, Ag, and In correct?

Answer

Table 2-3 indicates a temperature of 373°K for Ag and In and 500°K for C. These temperatures are correct. The cross-sections for Ag and In were generated at a higher temperature than the room temperature of 293.6°K used for most other elements in the WIMS library since these elements are normally used as control rod absorber materials and the neutron absorption in the control rod will lead to a higher temperature for the absorber vs. its surrounding coolant. The carbon cross-sections are available at the single temperature of 500°K in the version of WIMS currently used by Westinghouse. However, the U.K, Atomic Energy Authority has released a newer version of WIMS (Ref 1) where it has added additional carbon cross sections at a total of 14 temperatures using a Butland improved thermal scattering model. In this library, carbon cross-sections are tabulated at: 293, 313, 400, 500, 600, 655, 700, 900, 1100, 1300, 1600, 2000, 2500, and 3273°K.

3. Question

Table 2-3 implies that U-235, U-238, and Pu-239 do not have temperature dependent data. Please explain.

Answer

Resonance integral (RI) tables as a function of background scattering cross-section are available at the following temperatures for each nuclide:

U-235 resonance tables at 300°K
U-236 resonance tables at 300°K
U-238 resonance tables at 300, 600, 900°K
Pu-239 resonance tables at 300, 900°K

For U-238 and Pu-239, linear interpolation in $\sqrt{T}$ is made where T represents the fuel effective resonance temperature. The U-235 and U-236 resonance integrals are not nearly as sensitive to resonance broadening. The U-235 resonances are generally very broad and therefore are not sensitive to Doppler broadening. Equally important, the U-235 resonances include both fission as well as absorption and Doppler broadening affects both to the same degree such that any changes to the fission and absorption integrals tend to cancel out. The same is not true for U-238, for example, where the resonances only involve absorption. Since U-236 is present only in small concentrations, its resonance integral closely approximates the infinite dilution integral. For the case of infinite dilution, the RI is not affected by Doppler broadening since: a) there is no flux depression under the resonances and b) it has been shown that the area under a resonance does not change with temperature (see Bell & Glasstone Chp 8.1d, for example).

4. Question

Are the equations (2.3-8) and (2.3-11) correct? It appears there may be typographical errors.

Answer

Equation 2.3-8 has a typographical error. It should read:

$$Pff = \frac{b_1 \cdot x}{x + a_1} + \frac{b_2 \cdot x}{x + a_2}$$

Equation 2.3-11 is correct as it stands. Equation 2.3-11 has used the narrow resonance approximation for the admixed moderator scattering term given by Σm. Equation 2.3-11 was given for illustrative purposes only. Refer to equation (1) of the Appendix, attached at the end of this letter, for the exact flux equation used in the WIMS resonance treatment.

A further point of clarification should be made. The resonance treatment in WIMS does not make the Intermediate Resonance (IR) approximation of Goldstein and Cohen for the principal resonance absorbers U-238, U-235 and Pu-239, but, rather, only uses the λ factor formalism of that method. The resonance integral tables in WIMS for U-238, U-235 and Pu-239 are based on accurate solutions of the slowing down equation given below:

$$\Sigma t\,(\mu)\,\phi\,(\mu) = \sum_i \left[\int_{\mu-\Delta_i}^{\mu} \Sigma_{si}\,(\mu')\,\phi\,(\mu')\,\frac{\exp\,(\mu' - \mu)}{1 - \alpha_i}\,d\mu' \right]$$

The right hand term of the equation represents the slowing down source at lethargy μ summed over all isotopes in the mixture. $\phi(\mu)$ denotes the flux at lethargy μ.

The resonance integrals for U-235, U-238 and Pu-239 in the WIMS library have been calculated using point energy cross-sections determined from the multi-level, multi-channel formulation (Ref. 2) contained in the GENEX (Ref. 3) code. Both s and p-wave neutron contributions are included with a statistical treatment for defining resonances in the unresolved region. These cross-sections have then been used in the SDR slowing down code (Ref. 3) to obtain a shielded neutron energy spectrum defined by some 120,000 energy points. The SDR calculations were made for a range of homogeneous mixtures of the resonance absorber with hydrogen as the

moderator for a range of effective fuel temperatures. The resonance integrals (RI) thus calculated were then tabulated in WIMS as a function of the background cross-section, σ_b, given by:

$$\sigma_b = \lambda\sigma_p + \left(\frac{N_H}{N}\right) \sigma_{pH}$$

where λ is the Goldstein and Cohen Intermediate Resonance method λ factor; σ_p is the potential scattering cross-section of the resonance absorber; N_H/N is the ratio of hydrogen to absorber nuclide concentration and σ_{ph} is the potential scattering cross-section of hydrogen.

For hydrogen, the λ factor is 1.0. For isotopes other than hydrogen, the λ factor was derived by comparing the accurate solutions to the slowing down equation above for, on the one hand, mixtures of U-238 and pure hydrogen and, on the other, mixtures where part of the hydrogen was replaced with another given isotope. A "hydrogen-equivalent" λ factor for the given isotope was then deduced from such comparisons. This method is described in Reference 4. When using the tabulations to find the RI in a given mixture, PHOENIX evaluates the background cross-section as follows for interpolation in the RI tables:

$$\sigma_b = \sum_i \left(\frac{Ni}{N}\right) \lambda_i \sigma_{pi}$$

where the summation is made over all isotopes i in the mixture.

5. Question

For which nuclides is temperature dependent resonance absorption/fission considered? At what temperatures is data for these nuclides stored and how is the data used in the calculation (e.g., interpolation, closest value)?

Answer

See answer to question 3 in the PHOENIX section.

6. Question

How is the U-238 temperature dependent resonance integral normalized to measured data?

Answer

Reference 5 gives an extensive comparison between calculations using the WIMS library and experimental Winfrith [5] and Brookhaven [6] lattices. In Reference 5, the effects of decreasing the U-238 epithermal capture cross-section and also increasing the epithermal U-235 fission cross-section to give a capture to fission ratio α of 0.5 was studied. These altered U-238 and U-235 cross sections are the basis of the recommended U-238 and U-235 cross sections in the WIMS 69 group and 25 group libraries. The revision of the U-235 cross section took account of the measurements of de Saussure reported in 1965 and 1966[7] who obtained a capture to fission ratio α of 0.51. For U-235, the absorption resonance integral (RI) was unchanged. The fission RI was increased to $(RI)_{fission} + 0.0948 \cdot RI_{absorption}$. For U-238, the U-238 cross-section was uniformly reduced by 0.2 barns at all energies to correct for the previous ~7% overprediction of the U-238 RI. It is believed that the U-238 resonance shapes provided too much capture in the tails of the resonances. The 0.2 barn cross-section reduction corrects for this. Figure 4 in Reference 5, for the Winfrith lattices, and

Figures 5 and 6 for the BNL data compare Keff calculated with and without the modified U-235 and U-238 cross sections with the measured Keff of 1.0. The results clearly show the improved agreement with experiments using the modified cross sections.

The PHOENIX and POLCA programs have been extensively benchmarked by Westinghouse against U.S. BWR plant measurements and results of higher-order method calculations. This benchmarking includes comparison of hot and cold critical reactivities, core power distributions, TIP and gamma scan comparisons, comparison of reactivities for a number of UO_2 critical lattices, comparison of isotopics against Yankee Core V measured isotopics and comparison to KENO-IV Monte Carlo calculations. This benchmarking is complemented by the wealth of experience that ASEA-ATOM has gained using these programs in the design of the Swedish BWR plants over the last decade. All of the benchmarking results confirm the accuracy and reliability of the PHOENIX and POLCA programs, including PHOENIX's treatment of resonance absorption. All of the benchmarking results will be provided in a topical report which is planned to be submitted to the NRC in the second quarter of 1984.

7. Question

How is mutual self-shielding of resonances accounted for?

Answer

Since the discussion of mutual self-shielding of resonances is lengthy, it is provided as an Appendix at the end of this transmittal.

8. Question

Explain the basis for the temperature used in Doppler broadening (i.e., actual or effective). If an effective temperature, what is it based on?

Answer

The fuel temperature that is used for Doppler broadening calculations is an effective resonance temperature. This effective resonance temperature reproduces the correct Doppler broadened resonance capture in the PHOENIX program. The effective temperature weights the radial temperature profile across the fuel pellet, with an empirically - derived radial temperature weighting function. The radial temperature distribution is calculated using the BWR version of the PAD fuel rod design code (Ref. 8) and the LASER code[9] for the radial power distribution calculation. The radial temperature weighting function was derived by comparison to Monte Carlo calculations at the effective temperature over a wide range of fuel pellet physical temperature distributions for both steady-state and transient heat generation rate distributions. An additional weighting factor corrects for the fact that the same effective fuel temperature is used uniformly for all fuel pins in the bundle.

9. Question

How are Gd isotopes other than 155 and 157 treated in PHOENIX and FOBUS?

Answer

PHOENIX and FOBUS only deplete the odd-numbered Gd-155 and Gd-157 isotopes which are the dominant absorber nuclides. The even-numbered isotopes of gadolinium are not treated in PHOENIX and FOBUS. Rather, an empirical formula is used to correct for the reactivity penalty associated with the even-numbered isotopes. Based on the number of gadolinium-bearing fuel rods and w/o Gd_2O_3 loaded, the even-numbered gadolinium isotopes reactivity penalty can be computed for each bundle design. Among changes that are planned for PHOENIX and FOBUS for the future, however, is the incorporation of the complete gadolinium depletion chain from Gd-154 to Gd-158. This will replace the empirical formula discussed above.

10. Question

Does FOBUS deplete fuel isotopes both in the buffer zone and in the burnable absorber rod?

Answer

The purpose of FOBUS is to generate 25 group burnable absorber microscopic absorption cross-sections as a function of the depletion of the absorber. In the case of gadolinium, this means 25 group cross-sections for Gd-155 and for Gd-157. These cross-sections are input to PHOENIX which performs a 25 group flux and reaction rate calculation simultaneously for all fuel and absorber pins in the assembly. Thus, the effect of the depletion of the fuel on the neutron spectrum at the absorber pin locations and on the absorber depletion characteristics is primarily accounted for in the PHOENIX calculation.

The FOBUS program does not deplete the fuel either in the buffer or in the absorber. FOBUS does allow the absorber-free fuel cross-sections to be input by the user. FOBUS then calculates the unperturbed flux (e.g., without burnable absorber present) based on those cross-sections. Alternatively, the unperturbed flux spectrum can be input. The normal procedure for generating absorber pin microscopic cross-sections is to input the PHOENIX-edited 25 group cross-sections smeared over those fuel pins immediately adjacent to the absorber pin in the assembly and to do like-wise for the flux spectrum. The FOBUS flux calculation is then forced to agree with the PHOENIX input spectrum. By performing manual restart calculations in FOBUS, the input flux spectrum and absorber-free fuel cross-sections can be changed during the course of the absorber pin depletion to reflect the influence of fuel burnup. While the influence of fuel burnup is accounted for in the calculation of the microscopic

cross-sections, it should be remarked that sensitivity calculations to flux spectrum have shown that while the individual group microscopic cross-sections can be affected somewhat, there is negligible change observed in the overall gadolinium worth or pin-wise power distribution when these cross-sections are input to PHOENIX.

11. Question

How is the case of two adjacent Gd bearing rods treated?

Answer

The treatment of two adjacent gadolinium (Gd) bearing rods which typically would be diagonally adjacent rods is treated in FOBUS in the same manner as the case of an isolated Gd rod. In FOBUS, the Gd pin is centered in a 3x3 pin array of absorber-free fuel pins and the Monte Carlo flux and reaction rate calculation performed to obtain the 25 group microscopic cross-sections for input to PHOENIX. In PHOENIX, a 25 group nodal flux distribution is solved simultaneously for every fuel pin, channel and object in the assembly. This nodal flux solution is corrected for by a coarser-group transport calculation (see answer to Question 16 below for more details). Thus, it is the PHOENIX calculation and not the FOBUS calculation that is relied upon to account for all influences on the gadolinium-bearing pins, including the influence of adjacent Gd pins. Since the nodal flux is solved in PHOENIX as a single matrix for the entire assembly, each gadolinium pin "sees" the influence of all other fuel pins in the assembly, both Gd and non-Gd bearing rods; all objects such as the control blade; the channel and water gaps.

12. Question

What is the standard approach used to determine the flux for the unperturbed case in FOBUS-input or calculated? How are differences in the spatial representation in FOBUS and PHOENIX accounted for if input is from the latter?

Answer

As discussed in the answer to Question 10, the standard method is to input the 25 group fluxes from PHOENIX and normalize the FOBUS flux calculation to the input spectrum. The input flux should be representative of the flux at the fuel pins immediately surrounding the absorber pin. This assures that the FOBUS calculation uses a realistic flux that reflects the conditions directly at the absorber pin, and takes into account all features surrounding the absorber pin, such as the possible presence of adjacent water rods.

13. Question

Comment on the adequacy of the assumption that the fission source distribution does not change with the introduction of the absorber.

Answer

The FOBUS calculation is based on the use of a reciprocity relation that states that the flux change caused by the introduction of an absorber into a region V is equivalent to that flux produced by an incoming boundary source equal to the surface-perpendicular, inward-directed angular flux calculated for the unperturbed (absorber-free) condition. This is what is expressed by Equation 4.1-1 in the topical.

In order to arrive at that reciprocity relation, the assumption of a flat fission source distribution outside of the absorber pin must be made. This approximation is a good one since the introduction of the absorber in a fuel pin primarily depresses the power in that pin alone without causing any strong spatial disturbance of the fission source in the remaining fuel rods of the assembly. The introduction of the absorber also results in a large change to the flux spectrum in that pin but has much less of an effect on the remaining absorber-free pins in the assembly since the gadolinium loading is normally limited to a small number of fuel rods (6-9 is typical) in the assembly. Thus, the approximation that the source distribution remains unchanged outside of the absorber pin itself, which is the assumption made in arriving at the reciprocity relation, is a good one. Furthermore, the 25 group treatment in FOBUS and PHOENIX is fine enough in energy that such assumptions do not lead to any significant error in the prediction of absorber reaction rates in PHOENIX. It is primarily in the PHOENIX calculation that all important spectrum and spatial heterogeneities are "caught".

The PHOENIX and POLCA programs have been extensively benchmarked against U.S. BWR plant measurements for reactivity, power distributions, gamma scan measurements and Traversing Incore Probe (TIP) measurements. These benchmarking results consistently confirm the reliability of both PHOENIX and POLCA, including the treatment of burnable absorbers by these programs. These benchmarking results will be provided to the NRC in a topical report which is planned to be submitted in the second quarter of 1984. It should also be pointed out that the codes are also based on a wealth of Swedish BWR plant experience since these codes have been used routinely by ASEA-ATOM for the past decade in the design of Swedish plants-this experience extending to date to include at least 54 reactor cycles of operation. The gadolinium treatment of PHOENIX was also benchmarked to high temperature critical experiments performed in the Studsvik KRITZ facility (Ref. 10). These critical experiments consisted of 4x4 arrays of BWR-type assemblies containing an 8x8 lattice of fuel rods with up to 7 gadolinia rods per assembly. Comparisons were made for fission rate distributions and reactivity. Excellent agreement was obtained.

14. Question

Equation (2.6-10) appears to contain typographical errors.

Answer

All equations in Section 2.6 of the topical have been reviewed and were found to be correct and free of typographical errors, including Equation 2.6-10. The only slight inconsistency in Equation 2.6-10 appears to be μ_N which is designated by the Greek symbol μ in Equation 2.6-10 while in Equation 2.6-6, where it is defined, it resembles more the standard alphabet letter u. The two are intended to be identical, however.

15. Question

How are boundary conditions for the assembly problem obtained when non-zero current conditions are used?

Answer

The PHOENIX program assumes either periodic or reflective (exact reflection-not white or albedo reflection) boundary conditions on all sides of the assembly. While the boundary referred to on p. 2-16 in the discussion of the PHOENIX nodal solution process is admittedly not clearly defined, it refers to the boundary of the fuel pin array and not to the boundary of the assembly. The discussion was included to show that changes to the nodal equations are required in PHOENIX to handle the outer row of fuel pins on each side of the assembly, since these fuel nodes are not surrounded by other fuel nodes on all four sides. As is illustrated on p. 2-16 of the topical,the fuel nodes on the outer edge of the fuel pin array do not have to be handled separately from the interior fuel nodes. That is, they obey the same nodal matrix equation given by 2.6-11 on p. 2-15 if the effective transmission probability from the outer face of each

outer edge fuel cell to the interior three faces identified by Q_B, is re-defined as being represented by the albedo from that boundary face of the node-denoted by a_B in Equation 2.6-18. The albedo for each outer edge fuel pin is evaluated according to:

$$a_B = 1 - \sum_{i=1}^{m} \Sigma_{ri} V_i Y_i \qquad \text{Eq. (1)}$$

where: Σ_{ri} denotes the removal cross-section for region i
V_i is the volume of region i
Y_i is the neutron current response flux for region i

The summation in Equation (1) above is done over all regions i outside of the fuel pin array which, as shown in the illustration below, would normally include any coolant not included in the pin array, the channel, water gap, control blade (if present), etc.

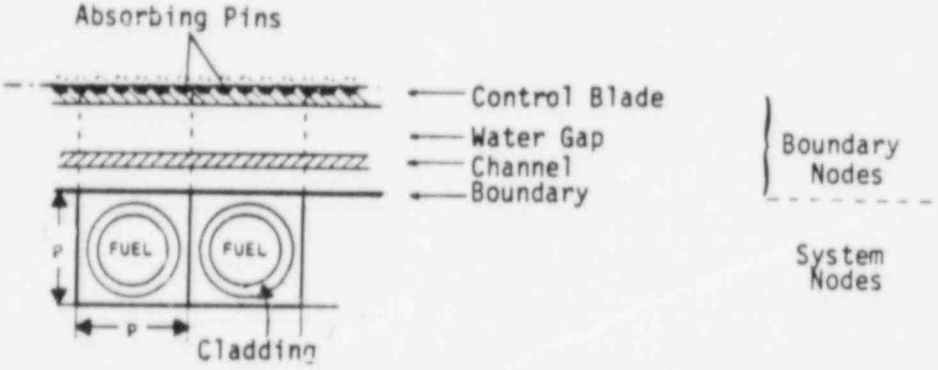

Boundary Nodes in a BWR assembly with a control blade in the gap

The evaluation of the current response fluxes Y_i as well as the source response fluxes X_i referred to in Equation 2.6-19 and 2.6-20 of the topical and used in Equation (1) above is based on Carlvik's treatment of collision probabilities in cylindical geometry - for nodes comprising the fuel pin array (Refs. 11-13); and standard slab geometry solution (Ref. 14) - for nodes outside of the fuel pin array.

16. Question

Given that the pin cell nodal method provides accurate multi-group fluxes for each micro-region of the assembly and the inter-nodal partial currents from this calculation are imposed as "truth" to be matched by the SFINX S_n module, what is the need for this latter calculation? It seems that all the data needed to homogenize the assembly are available following the 25-group nodal calculation.

Answer

The objective of the nodal calculation in PHOENIX is to provide the pin-cell coupling for all fuel pins and other details of the assembly (water gap, channel, etc.). The nodal calculation provides the energy detail for the flux (25 group) and spatial detail within each fuel cell (flux in pellet, clad, coolant, etc.) The nodal flux solution is not considered to be the most accurate flux solution that can be obtained, especially near absorber pins and near the water gap interface where strong heterogeneities exist. A more rigorous flux solution is obtained by performing the SFINX S_N calculation which is based on transport theory. Thus, the cell-average flux distribution is taken from the SFINX result which is for a coarser number of energy groups. The nodal flux solution provides the fine energy detail within each broad SFINX group and provides the fine spatial detail within each fuel cell. The nodal flux is normalized to the SFINX cell average flux level.

The auxiliary source terms δQ which are used in SFINX are not intended to force the SFINX calculation to reproduce the partial currents from the nodal solution. Otherwise, as is suggested by the question, there is no reason to perform the SFINX calculation in the first place. The additional source terms defined by Equation 2.7-1 are intended to correct for the fact that the flux solution for the homogenized cell problem does not preserve the partial currents at the cell boundaries from the fine mesh solution upon which the homogenization is based. The additional

source terms are introduced in the homogenized cell problem to assure that the partial currents are preserved. In PHOENIX, the auxiliary source terms per unit volume, $\delta Q/V$, are generated in the course of the nodal calculation. They are evaluated using the following expression:

$$\frac{\delta Q}{V} = f_H \cdot \hat{\phi} \quad \text{with } f_H = \frac{4\bar{\Sigma}_R}{S}\left(\frac{\delta \bar{J}}{\bar{\phi}}\right) \qquad \text{Eq. (1)}$$

$$\text{and } \delta \bar{J} = \bar{J} - \bar{J}_{HOM}$$

$\bar{\Sigma}_R$ denotes the cell average removal cross-section, S is the surface area of the cell. $\delta \bar{J}$ is the difference between the true partial in-current, $\bar{J}$, and that obtained from the homogenized cell problem $\bar{J}_{HOM}$. $\bar{\phi}$ is the cell average flux from the nodal calculation while $\hat{\phi}$ is the cell average flux from the SFINX S_N calculation. The auxiliary source terms are derived from the fine mesh and homogenized cell nodal solution which provide $\delta \bar{J}$ and $\bar{\phi}$ from which f_H can be evaluated using Eq. (1). These auxiliary source terms only assure that the partial currents in the fine mesh nodal solution are preserved in the homogenized cell nodal solution. The approximation is made that the source correction terms are approximately the same for the SFINX calculation. Thus, it is assumed that these source terms, based on comparison of fine to homogenized cell nodal solutions, when introduced in the SFINX homogenized cell calculation leads to a flux solution that preserves the partial currents that one would obtain with a fine mesh SFINX (not nodal) calculation. Since a fine mesh SFINX calculation for each cell is not made, the homogenization correction based on the fine mesh nodal solution must be used instead. Thus, there is no attempt to force the SFINX solution to agree with the nodal solution for the partial currents, which would be self-defeating, but rather, the homogenization correction from the nodal calculation is assumed to remain valid for the SFINX calculation as well.

17. Question

Figure 2-4 indicating that SFINX group $\leq$ library groups appears incorrect since the text implies a maximum of 12 groups for SFINX calculations. Please clarify.

Answer

A maximum of twelve (12) energy groups can be used in the SFINX calculation. The library groups in the statement "SFINX Groups $\leq$ Library Groups" refers to the 12 SFINX energy groups and not to the WIMS 25 group cross-section library. The statement intends to point out that the SFINX calculations can be run in less than the maximum of 12 energy groups permitted in SFINX, such as in 2, 3, 4, 5, 6, 7, 8, or 10 energy groups. The normal group structure used for SFINX calculations is 6 energy groups. For each group structure, the group energy boundaries are built-in and are included as part of the SFINX library data.

18. Question

Justify the representations for LPRMs and TIPs as shown in Figure 2-7, particularly with regard to the tube surrounding both detectors. What void is used for the channel?

Answer

The PHOENIX two-dimensional physics lattice code is used to generate the detector relative signal as a function of exposure, void history and instantaneous void. This data is then input to the POLCA 3-D core simulator program in tabular form as a function of the above listed parameters. The detector model in PHOENIX is as shown in Figure 2-7 of the topical (WCAP-10106). The stainless steel cladding for the TIP detector, as well as the stainless steel clad of the instrumentation tube

assembly are squared-off in the PHOENIX model. However, the dimensions and adjusted density used for the stainless steel are chosen to:
1) preserve the volume of water inside the instrumentation tube;
2) preserve the coolant volume displaced by the instrumentation tube and;
3) the actual amount of stainless steel present in the instrumentation tube cladding. The water inside the instrumentation tube as well as the narrow gap coolant immediately surrounding the instrumentation tube are assumed to be non-boiling. The effect of any boiling can be accounted for through sub-factors that make up the detector correction term C_i in Equation (1) in the response to Question 19 in the PHOENIX section. The burnup void and instantaneous void fractions assumed in the channel are normally 0%, 25%, 50%, and 75% void. The position of the detector relative to the assembly in the PHOENIX model also matches the actual nominal position of the detector. Thus, the PHOENIX model preserves all important features of the detector in order to assure an accurate simulation.

The best evidence of the reliability of the model is the excellent agreement obtained between simultaneous measurements of TIP distributions and bundle gamma scans. Such comparison will be provided as part of the benchmarking topical to be submitted in the second quarter of 1984.

19. Question

How is the influence of neighboring assemblies and possible control rod orientations relative to the detector location accounted for in the calculation of detector response?

Answer

The detector signal is proportional to the neutron flux at the detector. For fission chamber detectors, the detector signal is taken to be proportional to the power level in the four nodes (usually) surrounding

the detector. A node as defined here normally has a square transverse dimension equal to the assembly pitch with a height typically six inches in length. Thus, the detector signal, D, is evaluated by the following expression:

$$D = \sum_{i=1}^{4} P_i \cdot F_i \cdot C_i \qquad \text{Eq. (1)}$$

where P_i denotes the nodal power level of the immediately adjacent nodes and F_i denotes the detector constant for each node. The factor C_i is a correction factor. The detector constant F_i is the ratio of the relative detector signal divided by the bundle power and is calculated in the 2-D PHOENIX lattice code for each fuel type as a function of exposure, void history, and instantaneous void for the uncontrolled state. These detector constants are provided to the POLCA 3-D core simulator program in tabular form. POLCA interpolates on the detector constant to the appropriate exposure, void and void history for each of the four adjacent fuel nodes and performs the summation indicated by Equation (1) above.

The last term in Equation (1), denoted C_i, is a correction term which includes a number of sub-factors including three which correct for control

[redacted] + (a,c)

Control Rod Correction Factor; SS_i

[ ] + (a,c)

In case there is only one control rod next to the detector such as in the example above, then the correction factors SS_i are related to $SSFACT_i$ by:

[ ] + (a,c)

Skewed Void Drag Factor: $DRAG_i$

[ ]+ (a,c)

[ ] + (a,c)

Control Rod History Factor; $SHCORR_i$

[ ] + (a,c)

20. Question

How do the results from the "predictor-corrector" averaging process for typical burnup steps compare to results from depletion with small, appropriately sized burnup time increments?

Answer

Two cases are provided to illustrate the accuracy of the predictor-corrector method. The first in Table 1 compares the bundle average infinite multiplication factor k_∞ based on PHOENIX lattice calculations between fine and coarse depletion steps for an 8x8 fuel

assembly with 4 gadolinia rods of 4.0 w/o Gd_2O_3. The depletion was made at full power at 50% void fraction for the uncontrolled condition.

[ ] + (a,c)

TABLE 1

COMPARISON OF REACTIVITY RESULTS FROM PHOENIX LATTICE
CALCULATION USING STANDARD AND FINE BURNUP
STEPS - HOT FULL POWER AT 50% VOID FRACTION
FOR UNCONTROLLED CONDITION

Case 1 - 8x8 assembly with 4 rods of 4.0 w/o Gd_2O_3

Burnup (MWD/MTU)	Standard Burnup Steps	k_∞ Results*	Fine Burnup Steps	k_∞ Results**	k_∞ Difference (standard-fine steps) (pcm)
[					] + (a,c)

0954L:6/840206

TABLE 2

COMPARISON OF REACTIVITY RESULTS FROM PHOENIX LATTICE
CALCULATION USING FINE AND COARSE
BURNUP STEPS - HOT FULL POWER AT 40% VOID
FRACTION FOR UNCONTROLLED CONDITION

Case 2 - QUAD+ assembly without Gadolinium

Burnup (MWD/MTU)	Standard Burnup* Steps k_∞ Results	Fine Burnup** Steps k_∞ Results	k_∞ Difference (standard-fine steps) (pcm)
[			] +(a,c)

0954L:6/840206

21. Question

How do the results from the 18-chain, 40-isotope depletions compare to results from a full CINDER-type approach for typical and maximum burnup situations?

Answer

Calculations have not been made comparing the PHOENIX depletion algorithm against full CINDER depletion results. The basis for confidence in the PHOENIX treatment is based on the following considerations:

a) The linearized chains treat individually all of the principal uranium and plutonium isotopes.

b) The depletion chains treat individually all important fission product isotopes, with these isotopes contributing $\simeq$ 90% of the total fission product reactivity worth .

c) The PHOENIX and POLCA programs have been extensively benchmarked against plant operating data for hot and cold critical reactivities, core power distributions, TIP and gamma scan (both bundle and rodwise scans) distributions. The excellent results obtained uniformly for all comparisons, particularly the absence of reactivity anomalies, provides the basis for confidence in the PHOENIX depletion calculation.

d) PHOENIX has been benchmarked for isotopics against the Yankee Core V measured isotopic data. Very good results were consistently obtained with the accuracy judged to be comparable to the industry standard for licensed lattice physics programs. All benchmarking results for PHOENIX and POLCA will be included in a topical report to be submitted to the NRC in the second quarter of 1984.

e) The PHOENIX and POLCA programs are based on a wealth of Swedish BWR experience. These programs have been used routinely by ASEA-Atom for the past decade in the design of Swedish BWR plants - the experience to date extending to over 54 reactor cycles of operation. This plant operating experience is complimented by: 1) a series of critical lattice measurements using gadolinia absorber rods and typical 8x8 fuel bundle designs in the KRITZ facility at Studsvik; and b) destructive and non-destructive examinations of partially-depleted gadolinia absorber rods in the Oskarshamm 1 BWR reactor.

The excellent results obtained from the benchmarking by Westinghouse to domestic operating plant data and higher order calculations, to which must be added the equally excellent agreement that has been observed by ASEA-Atom in Swedish BWR's provides the basis for confidence in the use of PHOENIX for depletion calculation.

22. Question

Comment on the adequacy of only a linear dependence on void fraction for Doppler feedback?

Answer

A linear approximation for the Doppler reactivity feedback with void fraction provides an excellent fit. An example is given here. PHOENIX lattice calculations were performed at 0, 25, 50, and 75% void at 0 MWD/MTU where, at each void, the fuel temperature was changed from the reference of 929°K to a temperature of 1321°K. The calculations were performed for the QUAD+ assembly with a bundle average enrichment of 3.09 w/o U-235 loaded with 8 gadolinia rods of 5.0 w/o Gd_2O_3 each. Table 1 below provides the reactivity results and tabulates $\Delta k/\Delta(\sqrt{T_{eff}})$ as well.

TABLE 1

K_- Results

Void Fraction	$T_1 = 929°K$	$T_2 = 1321°K$	$\Delta k_-/(\sqrt{T_2} - \sqrt{T_1})$
[			] + (a,c)

0954L:6/840206

23. Is the reference to FOBUS as a three-dimensional program on p. 4-4 incorrect?

Answer

The FOBUS program is, in fact, a three-dimensional Monte Carlo program. FOBUS, which stands for (FOil BurnUp Scheme) was developed to handle both absorber discs separated by absorber-free pellet(s) or homogeneous absorbers. While the program does solve for the flux and reaction rates in 3-D, the geometry representation flexibility of the code has been constrained to cylindrical (R, Z) geometry. Annular geometry has also been forced in the selection of the neutron ray distribution for the source neutrons. Since the geometry representation is limited to two-dimensional (R, Z) problems, it may be more appropriate to refer to the code as a two-dimensional (R, Z) program since it doesn't feature the full flexibility of a 3-D program.

POLCA Program

1. Question

Describe and justify the thermal flux correction used to simulate thermal neutron transport.

Answer

Thermal neutron transport is determined in POLCA through calculation of a spectrum index R defined as:

$$R = \frac{\bar{\phi}_2}{\bar{\phi}_1} \qquad (1)$$

For the case of an infinite homogeneous medium the spectrum index is given by:

$$R_\infty = \frac{\Sigma_r}{\Sigma_{a2}} \qquad (2)$$

R can be related to R_∞ by the following equation:

$$R = R_\infty (1+\Delta R) \qquad (3)$$

Since as a rule $\Delta R << 1$, the following approximation can be used for the thermal and epithermal fluxes:

$$\phi_1 \simeq S_1 \bar{\phi}_1$$

$$\phi_2 \simeq R_- S_1 \bar{\phi}_1 \qquad (4)$$

Where, as defined in the topical report:

$\bar{\phi}_1$ is the average nodal epithermal flux

S_1 is the node size correction factor relating the average flux to the midpoint flux

ϕ_1, ϕ_2 are the midpoint epithermal and thermal fluxes, respectively.

Substituting equations 1) and 4) into the two group neutron balance equations and using Börreson's factorization along with the assumption that neutron streaming between nodes is dependent only on the mean nodal fluxes in the same group, two equations result: one for epithermal neutrons and one for thermal neutrons. The epithermal equation is equation 3.5-12 as given in the topical report. This equation is:

$$\phi_i = \frac{\sqrt{\hat{D}_{1i}}\left(\sum_{hor} \phi_j + r \sum_{vert} \phi_j\right)}{\sum_{hor}\sqrt{\hat{D}_{1,i}} + r \sum_{vert}\sqrt{\hat{D}_{1j}} - \left\{C_i\left\{\frac{k_{\infty i}}{k_{eff}} - 1\right\} h_x{}^2\right\}} \qquad (5)$$

Where the index "1" is used to clarify that the epithermal parameter is used and other parameters are as defined in the topical.

The thermal neutron equation, using the following definition:

$$\phi_1^{as} = \sqrt{\hat{D}_2}\,\phi_1^{as} = \sqrt{\hat{D}_2}\,R_-\,\phi_1 \qquad (6)$$

[ ] + (a,c)

Where Σ'_j means the summation is over the six neighboring nodes. An expression similar to this is used for peripheral nodes.

Equation (5) is the POLCA nodal equation from which the epithermal flux is calculated. The thermal flux is found from equations (1), (2), (3), and (7).

The basis for confidence in the thermal flux modelling in POLCA is based on two considerations: 1) the sophistication of the thermal flux modelling; and 2) the excellent benchmarking results obtained with POLCA. This program has been extensively benchmarked against domestic BWR plant operating data for hot and cold critical reactivities, core power distributions and thermal margins to fuel thermal limits, TIP and gamma scan measurements. The excellent results obtained uniformly for all comparisons provide the basis for confidence in the thermal flux treatment in POLCA.

The POLCA program is founded as well on a wealth of Swedish BWR plant experience. This program has been used by ASEA-ATOM as the principal nuclear design code in the design of Swedish BWR plants for the past decade, and has been integrated into the process computer as the heart of the software program. The design experience of ASEA-ATOM with this program extends to date to over 54 reactor cycles of plant operation.

The excellent results from the Westinghouse benchmarking combined with the equally excellent results obtained by ASEA-ATOM in Swedish BWR plants provides the basis for confidence in the use of POLCA for nuclear design calculations and in the reliability and accuracy of the thermal flux treatment in that program. All benchmarking results with POLCA will be provided in a topical report to be submitted to the NRC in the second quarter of 1984.

2. Question

Provide an estimate for the errors introduced by neglecting the effects of control rods on all parameters other than the fast and thermal absorption cross-sections.

Answer

The effects of the control rods on cross-sections other than the fast and thermal absorption cross-sections, Σ_{a1} and Σ_{a2}, are not neglected. The rodded Σ_{a1} and Σ_{a2} cross-sections are effective absorption cross-sections that preserve the reactivity change ΔK_∞ from unrodded to rodded. With the infinite multiplication factor k_∞ given by:

$$k_\infty = \frac{\nu\Sigma_{f1}}{\Sigma_{a1} + \Sigma_{rem}} + \left(\frac{\Sigma_{rem}}{\Sigma_{a1} + \Sigma_{rem}}\right) \cdot \frac{\nu\Sigma_{f2}}{\Sigma_{a2}}$$

where standard terminology has been used, an effective rodded Σ_{a1} and Σ_{a2} are found which preserve the ΔK_∞ change-unrodded to rodded-when used in conjunction with the unrodded fission and removal cross-sections $\nu\Sigma_{f1,2}$ and Σ_{rem}. By preserving the reactivity change, this method consequently does not introduce errors of any significance.

3. Question

Provide the bases for the assumed dependence of σ_{xe} on burnup and void fraction. What is the dependence, if any, of σ_{xe} on the xenon number density?

Answer

The microscopic absorption cross-section of xenon, σ_{xe} is fitted as a function of exposure, E, and void fraction, VF, according to the following expression:

$$\sigma_{xe}(E,VF) = (a_1 + a_2 \cdot E) \cdot (a_3 + a_4 \cdot VF + a_5 \cdot VF^2) \qquad \text{Eq. (1)}$$

This provides an excellent fit as is demonstrated by the following example.

Using the PHOENIX lattice code, assembly depletions were carried out at four void fractions: 0, 25%, 50%, and 75% void. The calculations were made for the QUAD+ assembly design with a bundle active fuel enrichment of 3.09 w/o U-235 with eight gadolinia rods of 5.0 w/o Gd_2O_3. Table 1 provides a comparison between the as-calculated bundle average xenon microscopic absorption cross-section σ_{a2} (left-column) and the fit result (middle column) and also gives the percentage difference between the two (right column). The fit used Equation (1) above with the following fitting coefficients:

[redacted] +

(a,c)

Table 1 indicates that the fitting expression for σ_{a2} given by

[redacted] + It should be (a,c)

noted that the bundle cross-sections provided by PHOENIX for the POLCA 3-D simulator program already include exactly the equilibrium xenon contribution. The absorption cross-section σ_{a2} given by Equation (1) is only used to correct the cross-sections for deviations from the equilibrium concentration. Thus, a larger fitting error can, in principle, be tolerated than if σ_{a2} was being used to determine the entire xenon contribution to the bundle absorption cross-section.

The xenon thermal absorption cross-section σ_{a2} has very little dependence on the xenon number density itself. To illustrate this, the bundle average xenon σ_{a2} is compared in Table 2 below where, in the first case, the cross-section was evaluated with no xenon present and, in the second, with equilibrium xenon present. The comparison corresponds to 0 MWD/MTU for the QUAD+ assembly design described above and was made at the following four void fractions: 0%, 25%, 50%, and 75% void.

Table 2

Void Fraction	Xenon σ_{a2} with No Xenon Present ($\times 10^{-18}$ cm^2)	Xenon σ_{a2} with Equilibrium Xenon ($\times 10^{-18}$ cm^2)	Difference (Percentage)
[redacted]			

+ (a,c)

TABLE 1

RESULTS FOR 0% VOID FRACTION

BURNUP (MWD/MTU)	Calculated Xenon σ_{a2} ($\times 10^{-18}$ cm^2)	Fit Result for Xenon σ_{a2} ($\times 10^{-18}$ cm^2)	Difference $(\frac{\text{calc-fit}}{\text{fit}}) \times 100\%$
[			] + (a,c)

RESULTS FOR 25% VOID FRACTION

BURNUP (MWD/MTU)	
[	] + (a,c)

TABLE 1 (Cont.)

RESULTS FOR 50% VOID FRACTION

BURNUP (MWD/MTU)	Calculated Xenon σ_{a2} ($\times 10^{-18}$ cm^2)	Fit Result for Xenon σ_{a2} ($\times 10^{-18}$ cm^2)	Difference $(\frac{\text{calc-fit}}{\text{fit}}) \times 100\%$
[			] + (a,c)

RESULTS FOR 75% VOID FRACTION

BURNUP (MWD/MTU)			
[			] + (a,c)

4. Question

Is the thermal-hydraulics model in POLCA a non-homogeneous, non-equilibrium model?

Answer

The thermal hydraulic portion of the POLCA code is the CONDOR code[15]. The void model in the CONDOR code is a nonequilibrium homogeneous model. There is no explicit equation to calculate void generation. Nonhomogeneous effects are accounted for in the void model. However, void generation effects are implicitly considered in the void model. This void model is described in the next paragraph (from Section 4 of Reference 15).

The void generation in two-phase flow boiling channel can be divided into three regions as illustrated in Figure 4.1 of Ref. 15. Region I consists of voids traveling in a narrow bubble layer close to the wall. Region II starts at the point Z_o where the bubbles are detached into the subcooled core and Region III starts at the point Z_1 where the bulk temperature reaches the saturation temperature and thermodynamic equilibrium is attained. The void fraction model in CONDOR: 1) neglects the void fraction in Region I, 2) uses the Levy model[16] to predict the void departure point in Region II and, 3) in Region III uses a model based on the formulation of Zuber[17] with coefficients adjusted to give agreement with test data.

In the void models, slip correlations are not explicitly used but rather are implicitly included within the void model. The effect of coolant superheat is also implicitly accounted for within the void model.

The void-quality model used in the CONDOR code was developed using two sets of experiments on 36 rod bundles. The first set consisted of data from a 36 rod Marviken full scale test assembly (Test FT-36B) and the

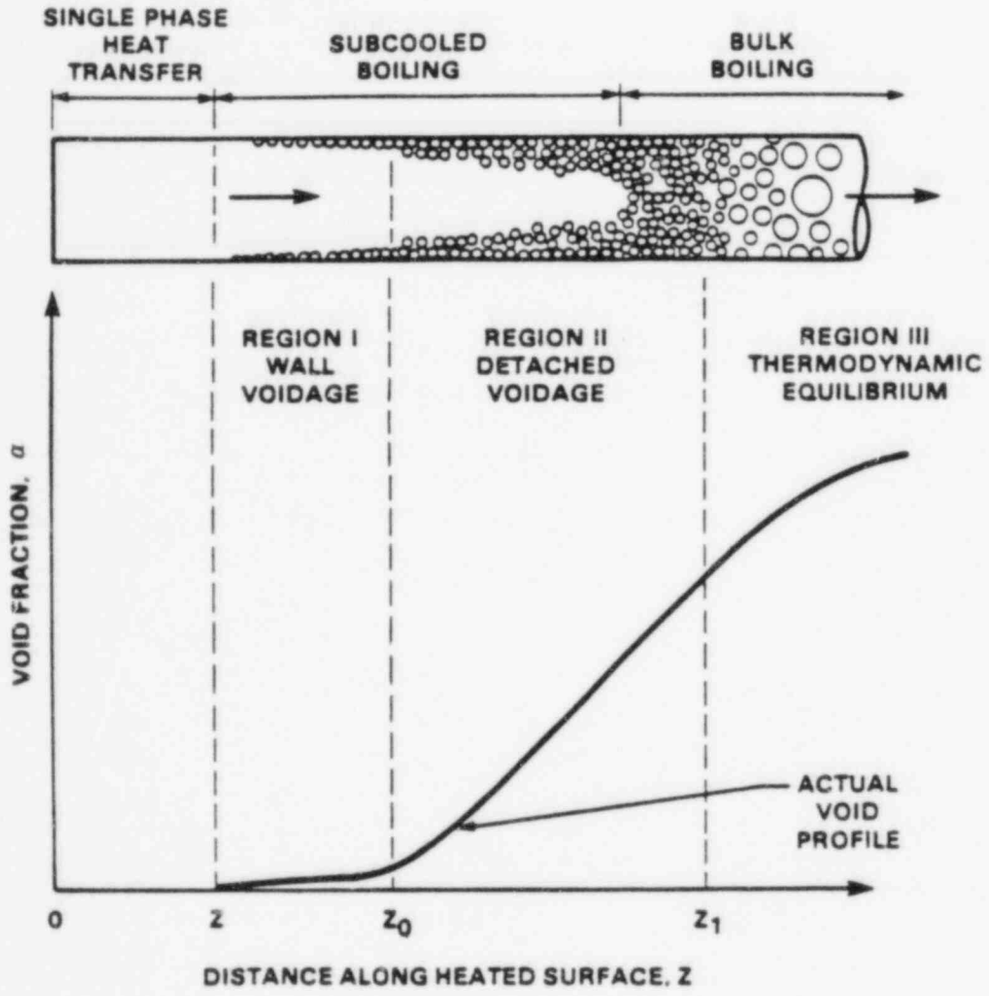

Figure 4.1 Two Phase Flow Boiling Regions

second set consisted of data from a 36 rod BWR type cluster (6x6 square array - Test OF36). Both of these tests were conducted in the FRIGG BWR test loop in Sweden.

The void-quality model was later compared to three other sets of void measurements. The first was from a full scale BHWR 36 rod cluster (Test FT-36C). The second was from a full scale simulation of an Oskarshamn-1 (ASEA-ATOM BWR plant) fuel assembly consisting of 64 rods in an 8x8 rectangular array using a radially-symmetric power distribution (Test OF-64). The third test again used a full scale simulation of an Oskarshamn-1 fuel assembly consisting of 64 rods, this time using a radially skewed power distribution (Test OF-64B). These last three tests were also from the FRIGG testing program. A comparison of the void quality model to the data described above showed excellent agreement between the measurements and the model predictions.

The entire CONDOR code[15], including all of the thermal hydraulic models, is presently under separate review by the NRC. The approved version of this code will be used as the thermal hydraulics model in POLCA.

5. Question

Describe the slip correlations used, if any.

Answer

See Response to Question 4 above in the POLCA Section.

6. Question

Describe the boiling and non-boiling heat transfer correlations used.

Answer

The Dittus-Boelter[18] correlation is used for non-boiling heat transfer. The Thom[19] correlation is used for boiling heat transfer.

7. Question

How is coolant superheat accounted for?

Answer

See Response to Question 4 above in the POLCA Section.

8. Question

Describe the void generation model used in POLCA.

Answer

See Response to Question 4 above in the POLCA Section.

9. Question

Describe the fuel rod heat transfer model and the nodalization used.

Answer

The POLCA program does not perform any fuel temperature calculations as such. Fuel temperatures are introduced into POLCA in tabular form to calculate the reactivity effect due to Doppler broadening. These fuel temperatures are effective resonance temperatures which include a spatial weighting of the radial temperature distribution within the pellet with the spatial flux distribution calculated at resonance energies. This is discussed further in the response to Question 8 on the PHOENIX program. The fuel temperature distribution is calculated by the PAD program as modified for BWR design applications (Ref. 8). The following paragraph, excerpted from Reference 8 summarizes the heat transfer model used.

The PAD 3.3 code uses the Dittus-Boelter correlation for forced convection heat transfer. The Thom correlation is used for fully developed nucleate boiling where crud is unimportant and the Tong correlation is used for fully developed nucleate boiling considering a crudded surface. These correlations appropriately predict, for the PAD closed channel analysis, the bulk coolant temperature effects of a BWR fuel rod.

10. Question

Supply the functional form of the AA-74 correlation for CPR, and available data for verification of the correlation.

Answer

[ ] + (a,c)

REFERENCES

1. Halsall, M. J., "LWR-WIMS, A Computer Code for Light Water Reactor Lattice Calculations," UKAEA-AEEW-R 1498, June 1982.

2. James, M. F. "Recommended Formulae and Formats for a Resonance Parameter Library," AEEW-R621, 1968.

3. Brissenden, R. J., Durston, C. "A User's Guide to GENEX, SDR, and Related Computer Codes," AEEW-R622 1968.

4. Aldous, A. C. "Numerical Studies of the Hydrogen Equivalent of Some Structural Materials in their Effect on U-238 Resonance Capture," UKAEA Report AEEW-M 860, Winfrith (1969), England.

5. Fayers, F. J., P. B. Kemshell, M. J. Terry, "An Evaluation of Some Uncertainties in the Comparison Between Theory and Experiment for Regular Light Water Lattices," Journal of the British Nuclear Society 6 p161 (1967).

6. Hellens, R. L. and G. Price, "Reactor Physics Data for Water Moderated Lattices of Slightly Enriched Uranium," Reactor Technology-Selected-Reviews, p529, USAEC Division of Technical Information, 1965.

7. de Saussure, G. et. al, "Measurement of the U^{235} Capture to Fission Ratio α for Neutron Energies from 3.25 eV to 1.8 KeV," Nuclear Sci. Engr. 23, 45 (1965) and G. de Saussure, et al., "Measurement of the Neutron Capture and Fission Cross Sections and Their Ratio, α, for U^{233}, U^{235}, and Pu^{239}," Paper CN 23/48, IAEA Conference on Nuclear Data, Paris 1966.

8. Ewing, J. H., Smith W. L., "Improved Analytical Models Used in Westinghouse Fuel Rod Design Computations/Application for BWR Fuel Analysis," WCAP-8720, Addenda 3 (P), January 1983.

REFERENCES

9. Supplemental information of fuel design transmitted from R. Salvatori, Westinghouse NES, to D. Knuth, AEC, as attachments to letters NS-SL-507 (12/8/72), NS-SL-518 (12/22/72), NS-SL-521 (12/29/72), NS-SL-524 (1/4/73) and NS-SL-543 (1/12/73), (Westinghouse Proprietary); and supplemental information on fuel design transmitted from R. Salvatori, Westinghouse NES, to D. Knuth, AEC, as attachments to letters NS-SL-527 (1/2/73) and NS-SL-544 (1/12/73).

10. Persson, R., E. Blomsjo, M. Edenius, "High Temperature Critical Experiments with H_2O moderated Fuel Assemblies in KRITZ," in Technical Meeting No. 2/11, NUCLEX72 (1972).

11. CARLVIK, I., "A method for calculating collision probabilities in general cylindrical geometry and applications to flux distributions and Dancoff factors," U.N. International Conference on the Peaceful Uses of Atomic Energy, Geneva, 2, UN, New York (1965)225-231.

12. CARLVIK, I., "Integral transport theory in one-dimensional geometries," Nukleonik, 10(1967)104-119.

13. CARLVIK, I., "Collision probabilities for finite cylinders and cuboids," Nuclear Science and Engineering, 30(1967a)150-151.

14. CASE, K. M., de HOFFMANN, F. and PLACZEK, G., "Introduction to the Theory of Neutron Diffusion," Government Printing Office, Washington, D.C. (1953).

REFERENCES

15. C. A. Olson, "CONDOR, A Thermal Hydraulic Performance Code for Boiling Water Reactors," WCAP 10107, Rev. 1. December 1983.

16. S. Levy, "Forced Convection Subcooled Boiling: Prediction of Vapor Volumetric Fraction," GEAP-5157, April 1966.

17. N. Zuber, et al, "Steady State and Transient Void Fraction in Two Phase Flow Systems," Final Report, Vol. I, GEAP-5417, January 1967.

18. R. W. Dittus, L. M. K. Boelter, Univ. Calif. Publs. Engng. 2, p. 443, 1930.

19. J. R. S. Thom, et al., "Boiling in Subcooled Water during Flow up Heated Tubes or Annuli," Proc. Instn. Mech. Engrs., Vol. 180, Pt3C, p. 226.

20. Stamm'ler, R. J. J., Abbate, M. J., "Methods of Steady-State Reactor Physics in Nuclear Design," Academic Press (London), 1983.

21. Goldstein, R., and Cohen, E. R., "Theory of Resonance Absorption of Neutrons, "Nuclear Science and Engineering 13 pp. 132-140 (1962).

22. Nordheim, L. W., "The Theory of Resonance Absorption," Proceedings of Symposia Applied Mathematics, Vol. II: "Nuclear Reactor Theory," Edited by G. Birkhoff and E. P. Wigner - American Nuclear Society (1961) p. 58-88.

APPENDIX - DICUSSION OF RESONANCE INTERACTION TREATMENT

For slightly-enriched uranium fuel typical of LWR lattices, the interaction between the resonances of U-235 and U-238 results in only a small adjustment to the effective group cross-sections. Consequently, a first-order correction is sufficient to include the interaction effect. In addition to U-235, small resonance interaction effects arise during fuel depletion from such burnup products as Pu-239, Xe-131, Pm-147, and Sm-152. To illustrate how the resonance interaction is accounted for, the discussion below first describes how the group cross-sections are obtained when a single resonance isotope only, is present and then describes the modification made to include the interaction between resonance absorbers when several are present.

Part I - Group Cross-Sections for Single Resonance Isotope

The effective group cross-section for absorption, for example, is given by:

$$\overline{\Sigma}_a = N\frac{\int \sigma_a(\mu)\,\phi(\mu)\,d\mu}{\int \phi(\mu)\,d\mu} \qquad \text{Eq. (1)}$$

The flux $\phi(\mu)$ for a heterogeneous system is given as a function of lethargy, μ, by the following equation:

$$\phi(\mu) = P(\mu) \cdot \sum_n \beta_n \left(\frac{\lambda\Sigma_p + \Sigma_{en}}{\Sigma_a(\mu) + \lambda\Sigma_s(\mu) + \Sigma_{en}} \right) \qquad \text{Eq. (2)}$$

Σp denotes the total background scattering cross-section for the fuel mixture; Σa and Σs are the absorption and scattering cross-sections for the mixture, including resonance contribution. A derivation for this

expression of the flux may be found in Chapter IX, pp. 308-318 of Reference 20. The expression for the flux above is based on a rational approximation for the fuel collision probability P_{FF} of the type:

$$P_{FF} = x \cdot \sum_n \left(\frac{\beta n}{x+\alpha_n} \right) \qquad \text{Eq. (3)}$$

where $x = \Sigma t/\Sigma e$; Σe is the escape cross-section and is given by $\Sigma e = \frac{S_F}{4V_F}$. The parameters Σt, S_F, and V_F denote the total cross-section, surface area and volume of the fuel mixture, respectively. Σ_{en} in Equation (2) is equal to $\alpha_n \cdot \Sigma_e$. Equation (2) also makes use of the Intermediate Resonance (IR) treatment of Goldstein and Cohen (21). The effect of the flux depletion due to the reduced slowing down density with increasing lethargy is accounted for through the $P(\mu)$ term in Equation (2) which denotes the resonance escape probability to lethargy μ. A two-term rational approximation is used in PHOENIX for the fuel collision probability which leads to a two-term equivalence relation to evaluate the resonance integral (Equation 2.3-10 of topical). However, a single term approximation for P_{FF} is also needed to derive the expression for the group cross-section. An equivalent single-term rational approximation is used for P_{FF}:

$$P_{FF} = \frac{\Sigma_t}{\Sigma_t + \Sigma_e^*} \qquad \text{Eq. (4)}$$

with $\Sigma_e^* = \alpha^* \cdot \Sigma_e$

An α^* is found which produces the same RI as the two term equivalence relation of Equation (3) with α_1 and α_2. Finding α^* is made easier by the fact that, in both the narrow resonance and wide resonance

approximations, the RI is, to a good approximation, proportional to the square root of the background cross-section (Reference 22). Hence, a good first approximation to α^* can be found from:

$$\beta_1\sqrt{\lambda\Sigma_p + \alpha_1\Sigma_e} + \beta_2\sqrt{\lambda\Sigma_p + \alpha_2\Sigma_e} = \sqrt{\lambda\Sigma_p + \alpha^*\Sigma_e}$$

Using Equation (2) for the flux and using the single rational approximation of Equation (4) leads to the following expression for the group absorption cross-section:

$$\bar{\Sigma}_a = N \frac{\int P(\mu)\left[\frac{\Sigma_b^*}{\Sigma'(\mu) + \Sigma_b^*}\right]\sigma_a(\mu)\,d\mu}{\int P(\mu)\left[\frac{\Sigma^*_b}{\Sigma'(\mu) + \Sigma_b^*}\right]d\mu} \qquad \text{Eq. (5)}$$

where $\Sigma_b^* = \lambda\Sigma_p + \Sigma_e^*$ and $\Sigma'(\mu) = \Sigma_a(\mu) + \lambda\Sigma_{RS}(\mu)$.
Σ_{RS} denotes the resonance-only scattering cross-section of the fuel.

The macroscopic resonance integral at a background cross-section of $\sigma_b^* = \Sigma_b^*/N$ (N is number density of resonance absorber) is given by:

$$R(\sigma_b^*) = N\int \sigma_a(\mu)\left[\frac{\Sigma_b^*}{\Sigma'(\mu) + \Sigma_b^*}\right]d\mu \qquad \text{Eq. (6)}$$

Before proceeding further, two group averages for the resonance escape probability will be defined.

$$\bar{P} = \frac{\int P(\mu)\, dR}{R} \qquad \text{and} \qquad \tilde{P} = \frac{\int P(\mu)\, d\mu}{\Delta\mu} \qquad \text{Eq. (7)}$$

with R defined by Equation (6) and $\Delta\mu$ denoting the lethargy width of the energy group.

Using Equations (6) ands (7) into Equation (5) yields the following for the group average absorption cross-section:

$$\bar{\Sigma}_a = \frac{\bar{P} R\,(\sigma_b^*)}{\tilde{P}\,\Delta\mu - \dfrac{\bar{P}\,R\,(\sigma_b^*)}{\Sigma_b^*}} \qquad \text{Eq. (8)}$$

To obtain the denominator in Equation (8), the term Σ_b^* was replaced by $\Sigma_b^* + \Sigma' - \Sigma'$ which was then approximated as $\Sigma_b^* + \Sigma' - \Sigma_a$. That is, the resonance scattering integral $\int \Sigma_{RS}(\mu)\, \phi(\mu) d\mu$ was neglected. This is a good approximation for predominately absorbing resonances and for wide resonances. However, whether the approximation is good or not is irrelevant since the resonance integral tables in WIMS have been adjusted to give correct Σ_a values at the tabulated background cross-sections when Equation (8) or equivalently when Equation (9) below is used.

Finally, letting I denote the macroscopic RI divided by the group lethargy width $\Delta\mu$, $I = R/\Delta\mu$, and making the approximation that $\tilde{P} = \bar{P}$ yields the final expression for the group absorption cross-section, $\bar{\Sigma}_a$:

$$\overline{\Sigma}_a = \frac{I(\sigma_b^*)}{1 - \frac{I(\sigma_b^*)}{\Sigma_b^*}} \qquad \text{Eq. (9)}$$

It may be shown that as long as the resonances are centered in the lethargy group, the ratio $\widetilde{P}/\overline{P}$ is given by:

$$\widetilde{P}/\overline{P} = 1 + \frac{1}{12}\ (1-P)^2 + O[(1-P)^3] \qquad \text{Eq. (10)}$$

where P is in the total resonance escape probability to lethargy μ. Thus, the approximation $\widetilde{P} = \overline{P}$ in Equation (9) only introduces an error of $(1-P)^2$ as long as the resonances are well centered in the group structure. The WIMS resonance groups have been chosen to provide a uniform distribution of resonances as far as possible and in cases of only a single resonance within the group, then this resonance has been placed close to the lethargy center of the group.

Part II - Resonance Interactive Correction

Equation (9) defines how the group cross-section for a single resonance isotope is obtained in terms of its RI evaluated at the background cross-section σ_b^*. This section describes how the interaction between resonances is accounted for when there are several resonance isotopes present. The average absorption cross-section for all resonance isotopes combined is given by an expression that is analogous to Equation (9):

$$\bar{\Sigma}_a = \sum_J \bar{\Sigma}_{aJ} = \frac{\sum_J I_J}{1 - \sum_i \left(I_i / \Sigma_b^* \right)} \qquad \text{Eq. (11)}$$

The contribution from resonance isotope J is given by:

$$\bar{\Sigma}_{aJ} = \frac{I_J}{1 - \sum_i Ii/\Sigma_b^*} \qquad \text{Eq. (12)}$$

The resonance integral $I_J = R_J/\Delta\mu$ for isotope J in the presence of other resonance absorbers is given in analogous fashion to Equation (6) by the following:

$$I_J = \frac{N_J}{\Delta\mu} \int \frac{\Sigma_b^*}{\Sigma_J^{'}(\mu) + (\Sigma_b^* + \Sigma_J^X)} \sigma_{aJ}(\mu)\, d\mu \qquad \text{Eq. (13)}$$

where Σ_J^X represents an average value of the resonance absorption and scattering of all isotopes with the exception of isotope J in question:

$$\Sigma_J^X = \frac{\sum_{i \neq J} I_i}{1 - \sum_i I_i/\Sigma_b} \qquad \text{Eq. (14)}$$

where the I_i are the lethargy-averaged RI defined by Equation 6 for single resonance isotopes (e.g., without resonance interaction included) with $I_i = Ri/\Delta\mu$.

To summarize, the interaction effect is accounted for by first evaluating the single element lethargy-averaged resonance integrals I_J according to Equation (6) with $I_J = R_J/\Delta\mu$. These are then used to determine an average background cross-section Σ_J^X according to Equation (14) which is added to the background cross-section Σ_b^* in order to re-evaluate the RI for each resonance isotope with the interaction effect included, using Equation (13). The RI terms with resonance interaction included, I_J are then summmed according to Equation (11) to arrive at the group average absorption (or in similar fashion, fission) cross-section.

An example of the accuracy of the resonance interaction treatment is given in Table A-1. This example, taken from Reference 1 compares the interaction treatment described above with direct numerical calculations using the SDR code (Reference 3) for a pin cell problem containing 3 w/o enriched UO_2 in a 1:1 volume ratio with H_2O. The results in Table A-1 demonstrate that the interaction treatment in WIMS/PHOENIX gives a good first-order correction for resonance interaction.

TABLE A-1

EFFECTS OF U^{235} NUCLIDE INTERACTION FOR 3% ENRICHMENT

AVERAGE CROSS-SECTIONS IN RANGE 9.118 KeV to 4.0 eV

(From Reference 1)

U-238 σ_a			U-235 σ_a			U-235 $\nu\sigma_f$		
WIMS without inter-action	WIMS with inter-action	SDR	WIMS without inter-action	WIMS with inter-action	SDR	WIMS without inter-action	WIMS with inter-action	SDR
2.4762	2.4460	2.4368	30.96	29.26	29.36	38.64	36.52	37.26